Exploring downstream pathways of aberrantly activated kinases for targeted leukemia therapy

Inauguraldissertation

zur
Erlangung der Würde eines Doktors der Philosophie
vorgelegt der
Philosophisch-Naturwissenschaftlichen Fakultät
der Universität Basel

Von

Christelle Gasser
aus Nunningen, SO

Basel, 2008

Genehmigt von der Philosophisch-Naturwissenschaftlichen Fakultät auf Antrag von

Prof. Dr. Jürg Schwaller

Prof. Dr. Nancy E. Hynes

Prof. Dr. Jan Cools

Basel, den 25. November 2008

Prof. Dr. Eberhard Parlow
Dekan

Abstract

Genetic alterations resulting in uncontrolled protein tyrosine kinases (PTKs) activity are frequently found in leukemia and in human solid cancers. Although the development of small molecule kinase inhibitors has revolutionized therapy for PTK-induced chronic myeloid leukemia, their effect is limited in cancers with several genetic alterations and increased multi-factorial drug resistance is hampering therapies. To overcome these limitations, it is indispensable to identify essential targets acting *downstream* of an oncogenic PTK.

FLT3-ITD mediated leukemogenesis is associated with increased expression of oncogenic PIM serine/threonine kinases. To dissect their role in FLT3-ITD-mediated transformation, we performed bone marrow reconstitution assays. Unexpectedly, FLT3-ITD cells deficient for PIM1 failed to reconstitute lethally irradiated recipients whereas lack of PIM2 induction did not interfere with FLT3-ITD-induced disease. PIM1-deficient bone marrow showed defects in homing and migration and displayed decreased surface CXCR4 expression and impaired CXCL12/CXCR4 signaling. Through siRNA-mediated knockdown, chemical inhibition, expression of a dominant negative mutant or and re-expression in knockout cells we found PIM1 activity to be essential for proper CXCR4 surface expression and migration of cells towards a CXCL12 gradient. PIM1 directly phosphorylated Serine 339, a residue in the CXCR4 intracellular domain essential for normal receptor recycling. In primary leukemic blasts high levels of surface CXCR4 were associated with increased PIM1 expression, and could be significantly reduced by a small molecule PIM inhibitor in some patients. Our data suggest that PIM1 activity is essential for homing and migration of hematopoietic cells through direct modification of CXCR4. Since CXCR4 is also important for homing and maintenance of cancer stem cells, PIM1 inhibitors may exert their anti-tumor effects in part by interfering with interactions with the microenvironment. We extensively tested different classes of PIM inhibitors and could show that some of these compounds could impair survival and growth of different hematopoietic cellular systems, including blasts from AML patients.

The second goal of my thesis was to create a mouse model for a PTK-fusion gene, NUP214/ABL1, associated with human T-cell acute leukemia. We generated two transgenic lines expressing the NUP214/ABL1 fusion from a T-cell linked (lck) promoter. However, no phenotype was observed after more than one year. Further experiments are ongoing to analyze whether co-expression of putative collaborating oncogenes, associated in human T-cell leukemia, such as HOX11/HX11L2 is able toinduce or respectively accelerate leukemogenesis.

Contributions to this thesis

Without the help of following people, this work would not have been possible!

M. Nawijn & A. Berns sent us the PIM1$^{-/-}$, PIM2$^{-/-}$ and FVB/N mice (Chapter II).

R. Grundler & J. Duyster performed the *in vivo* mouse work, as well as some FACS experiments (Chapter II).

A. Spoo & C. Dierks sent us some AML patient cDNA (Chapter II).

A. Bullock and S. Knapp performed the MALDI-TOF experiment (Chapter II); identified and sent us the imidazo[1,2-*b*]pyridazines compounds as well as the beta-carboline compounds (Chapter III).

V. Pogacic performed the *in vitro* kinase assay and the Western Blot with K00135 (Chapter III).

L. Brault performed the *in vitro* kinase assay and the Western Blot with Carb13 (Chapter III); as well as migration assays, the calcium flux experiment, the phospho-Western Blots and helped at the confocal microscope (Chapter II).

A. Biondi and S. Meyer-Monard provided us with frozen AML patient samples (Chapter III).

J. Cools sent us the NUP214/ABL1 plasmid (Chapter IV).

The transgenic mouse core facility (Biozentrum, Basel) performed the oocyte injections (Chapter IV).

Table of contents

I. Introduction

1. Cancer

Research of the last century has generated a rich and complex body of knowledge, revealing cancer to be a disease involving dynamic changes in the genome. The foundation has been set by the discovery of mutations producing oncogenes with dominant *gain of function* alterations and tumor suppressor genes with recessive *loss of function* alterations. Both classes of cancer genes have been identified through their alterations in human and animal cancer cells and by their elicitation of cancer phenotypes in experimental models. Several lines of evidence indicate that tumorigenesis in human is a multi-step process and that these steps reflect genetic alterations that drive a progressive transformation of normal human cells into highly malignant derivatives (*Hanahan, 2000*).

These observations became more concrete by extensive experimental work indicating that the genomes of tumor cells are invariably altered at multiple sites, having suffered disruption through lesions as subtle as point mutations and as obvious as changes in chromosome complement. Transgenic models of tumorigenesis have repeatedly supported the conclusion that tumorigenesis in mice involves multiple rate-limiting steps (*Bergers, 1998*). Taken together, observations of human cancers and animal models argue that tumor development proceeds via a process formally analogous to Darwinian evolution, in which a succession of genetic changes, each conferring one or another types of selective advantage, leads to the progressive conversion of normal into cancer cells (*Foulds, 1954*; *Nowell, 1976*).

There are more than 100 distinct types of cancer, and subtypes of tumors can be found within specific organs. My thesis focused on the molecular genetics of human leukemia.

2. Leukemia

Leukemia is defined as a cancer of the hematopoietic system and is characterized by an abnormal proliferation of white blood cells. Leukemia significantly contributes to the overall cancer burden: worldwide, over 200'000 people are confronted with the disease every year and for more than 80%, the disease ends tragically (*WHO, 2002*).

Leukemia can clinically and biologically be divided in *acute* and *chronic* forms: Acute leukemia is characterized by the rapid accumulation of immature blood cells, resulting from a differentiation block. This crowding makes the bone marrow unable to produce healthy blood cells. Acute forms of leukemia peak in childhood and elderly people. Chronic leukemia is distinguished by excessive build up of more mature and differentiated, but still abnormal, blood cells. Typically taking months to years to progress, the cells are produced at a much higher rate than normal cells, resulting in a large number of abnormal white blood cells in the blood. Chronic leukemia mostly occurs in older people, but can theoretically occur in any age group. Biologically, leukemias are classified into lymphocytic or myeloid, dependent on which cell population of the blood-forming system is affected and based on the molecular genetic lesions.

3. Molecular genetics of leukemia

There is abundant evidence that most hematological malignacies includes clonal disorders characterized by acquired somatic genetic alterations in hematopoietic progenitors.

Non-random chromosome aberrations (inversions, reciprocal translocations, insertions, deletions, trisomies and monosomies) are found at diagnosis in leukemic blasts of approximately 55% of adults with acute myeloid leukemia (AML) and the pre-treatment karyotype has long been recognized as the most important independent predictor of clinical outcome in this disease. As a consequence, chromosome-banding analysis has become a part of routine diagnostics and several cytogenetic abnormalities are considered in the recent WHO classification of AML.

However, approximately 45% of AML patients lack any major chromosomal abnormalities and the identification of pathogenetically relevant genetic lesions as well as the discrimination between prognostically different subsets of patients within this group remains a major challenge (*Frohling, 2005*). New methods like comparative genomic hybridization (CGH) arrays or genome wide sequencing will identify genome-wide disease-related genetic aberrations that have not yet been detected by existing technologies (*Inazawa, 2004; Mullighan, 2007; Ley, 2008*).

Clinical and experimental research suggests that the molecular pathogenesis of acute leukemia falls into two broadly defined functional complementation groups. One group, often referred as class I mutations, comprises mutations that activate distinct signal transduction pathways that enhance cellular proliferation and/or survival of hematopoietic progenitors. Another group, class II mutations, comprises mutations that affect transcription factors or components of the transcriptional co-activation complex resulting in impaired hematopoietic differentiation and/or aberrant acquisition of self-renewal properties by hematopoietic progenitors at a particular step of differentiation (*Frohling, 2005; Kelly, 2002*) (**Figure 1**). In general, mutations conferring proliferative and/or survival advantage to hematopoietic progenitors are consequences of aberrant activation of signal transduction pathway components such as protein tyrosine kinases (PTK) (JAK2, FLT3, KIT, ABL1, PDGFR). By itself, over-expression of several activated PTKs has been shown to be sufficient to transform cells *in vitro* and to induce myelo- and/or lymphoproliferative disorders mimicking chronic leukemia in animal models ranging from zebrafish to mice.

Mutations impairing differentiation of hematopoietic cells are targeting transcriptional regulators essential for normal hematopoietic development, like CBF, RARα or MLL. Although they have oncogenic potential, these mutations are generally not sufficient to induce a malignant phenotype *in vivo*. Several mutations within each of these groups rarely occur in the same AML patient whereas mutations between complementation groups often occur together in the same AML, indicating functional cooperation between these two groups, and thus the multi-step pathogenesis in the induction of the leukemic phenotype (*Frohling, 2005; Gilliland, 2004*). Cooperativity between different mutations has been validated in several mouse leukemia models (*Grisolano, 2003; Kelly, 2002)*.

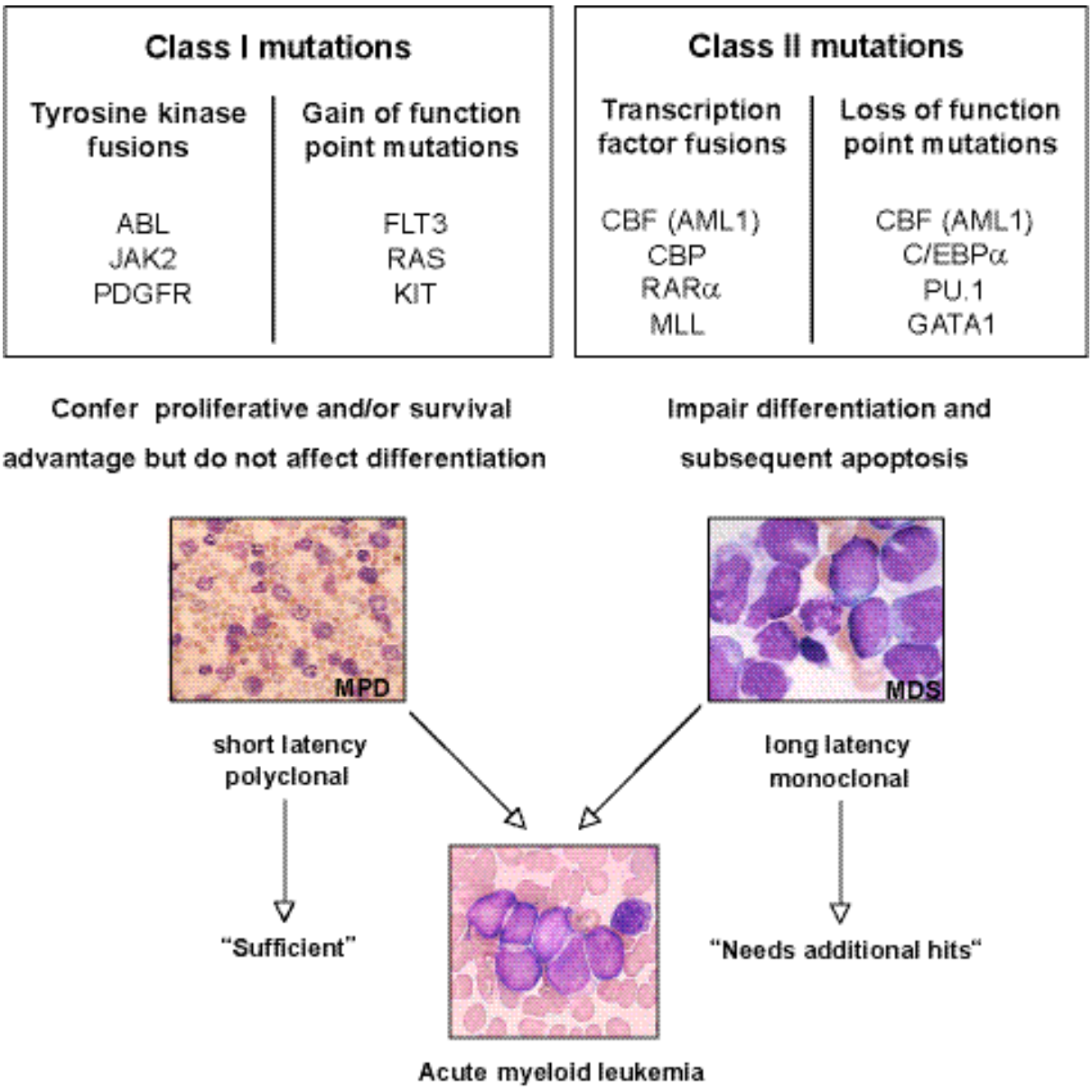

<u>Figure 1:</u> A two-hit model for acute leukemia.

In leukemias, two types of genetic alterations are distinguished and referred to as class I and class II mutations. Class I mutations provide proliferative and/or survival advantage and are sufficient to induce a myeloproliferative disease (MPD) in mouse models. Class II mutations impair differentiation and result in a myelodysplastic syndrome-like disease (MDS) in mouse models. Cooperation of class I mutations with class II mutations is necessary to induce a leukemia phenotype.

3.1 Class I mutations

Class I mutations include different protein tyrosine kinases that become constitutively activated by either fusion to a N-terminal partner protein (often providing an oligomerization domain) or by distinct point mutations in the kinase domain or internal tandem repeats in the juxtamembrane domain (*Chalandon, 2005; Steffen, 2005*). Two important examples are further mentioned here:

FLT3*.* The FMS-like PTK 3 (FLT3) gene, encoding a transmembrane class III receptor PTK, plays a crucial role in normal hematopoiesis. In normal bone marrow, FLT3 is expressed at high levels in early progenitor cells but is also expressed at abundant levels in a high proportion of cases of acute leukemia, suggesting a role in survival or proliferation of leukemic blasts. Over a decade ago, the FLT3 internal tandem duplication (ITD) in the juxtamembrane domain were discovered and more than 20% of adult and 10% of pediatric AML patients harbour this mutation (*Nakao, 1996*). Kinase domain FLT3 mutations have also be found to be present in leukemic blasts of about 7% of AML and in less than 5% of ALL patients. Both mutation types lead to deregulated kinase activity. *In vitro* studies have suggested that FLT3 mediates its proliferative and anti-apoptotic effects through several signalling pathways including STAT5, RAS/MAPK and PI3K/AKT (*Chalandon, 2005; Steffen, 2005, Choudhary, 2005*). Several studies have shown that expression of mutated FLT3 induces a lethal myelo-lymphoproliferative disease in mice (*Kelly, 2002; Grundler, 2003*).

ABL1*.* Almost half a century ago, Nowell and Hungerford described a distinct cytogenetic abnormality in cells from patients with chronic myeloid leukemia (CML) as the Philadelphia chromosome (*Nowell, 1960*). It took more than two decades to characterize the Philadelphia chromosome as the consequence of a translocation between chromosome 9 and 22 leading to a fusion of the BCR gene to the ABL1 PTK gene. This translocation is found in more than 90% of patients with CML (*Sherbenou, 2007*). Although the BCR/ABL1 fusion is exceptionally rare in T-cell acute lymphoblastic leukemia (ALL), recent findings suggest that ABL1 fusions also play a role in the pathogenesis of T-ALL (*Graux, 2004*). A fluorescent *in situ* hybridization-based screen detected marked extra-chromosomal episomal amplification of ABL1 in more than 5% of the patients. Further mapping of the episome showed a fusion of ABL including the kinase domain to the nucleoporin 214 (NUP214) gene. In the tumor cells this translocation is often associated with other

genetic lesion such as deregulated expression of the homeobox genes HOX11 (TLX1) or HOX11L2 (TLX3) or deletion of the cell cycle inhibitor CDKN2A (*Graux, 2004*). Apart from the NUP214/ABL1 fusion, variant ABL1 fusions such as ETV6-ABL1 or EML1-ABL1 have also been reported in T-ALL with a lower incidence (*De Keersmaecker, 2005; Van Limbergen, 2001*).

4. Therapeutic targeting of oncogenic PTK activity

The entire set of genes encoding for protein kinases (also referred as the human kinome) encompasses more than 500 members and of these, more than a third have been associated so far with cancer (*Manning, 2002*). The development of small molecule inhibitors targeting aberrant PTK activity represents a milestone in cancer research. The most prominent example is imatinib mesylate (also known as Gleevec, Novartis), blocking ABL, KIT and PDGFR. It has become first-line therapy of newly diagnosed Philadelphia-chromosome positive CML in chronic phase reaching hematologic and cytogenetic response rates of >80-90% (*Deininger, 2005*). However, the development of resistance to imatinib remains a major challenge to be overcome. Imatinib resistance of BCR/ABL-positive leukemia has been attributed to at least four different molecular mechanisms: emergence of point mutations in the BCR/ABL kinase domain, over-expression of the BCR/ABL fusion gene, compensatory switch to another kinase pathway, extra-cellular sequestration of imatinib by p-glycoprotein–mediated active drug efflux from the target cell. Second generation related small molecule PTK inhibitors such as Nilotinib or Dasitinib are able to block some but not all imatinib-resistant ABL mutations (*Hantschel, 2008*). Another important therapeutic target is FLT3 receptor tyrosine kinase. FLT3 is constitutively active in 30% of adult AML cases by either internal tandem duplications (ITDs) or kinase domain mutations. Several small-molecule FLT3 inhibitors (such as PKC-412, CEP701, SU11248, MLN518) have been identified and are currently undergoing clinical trials (*Knapper, 2006*). Similar to ABL, acquired additional mutations can result in resistance against FLT3 inhibitors and prompted the search for novel, structurally diverse FLT3 inhibitors that could be alternatively used to override drug resistance (*Heidel, 2006*, *Weisberg, 2008*).

The number of newly developed compounds with inhibitory activity against PTKs is growing fast and it is foreseeable that we will soon have at hand a large number of potent small molecule inhibitors that target different oncogenic kinases involved in various hematologic malignancies and other cancers. However, mutations of the targets as a consequence of adaptive resistance will always be a threat to this approach, and therefore the underlying molecular mechanisms need to be investigated to identify critical downstream signalling pathways that could be efficiently targeted (*Pear, 2000; Chalandon, 2005*).

5. Therapeutic targeting of critical downstream messengers

The transforming activity of oncogenic PTKs is mediated by parallel activation of several downstream signalling pathways. In general, multiple constitutively auto-phosphorylated tyrosine residues of an oncogenic PTK can serve as a docking site for multiple adapters or signalling mediators to become themselves activated through a chain of consecutive phosphorylation events. Final downstream mediators of this complex signalling network are mostly phospho-proteins that translocate from the cytoplasm to the nucleus of the cells to act as transcriptional regulators activating a distinct group of target genes. Signalling pathways that act as mediators of leukemic PTKs include PI3K/AKT, RAS/MAPK, JAK/STAT, SHH or NFκB (*Chalandon, 2005*; *Steelman, 2008*) (**Figure 2**). A major effector of leukemogenic PTK activity is the JAK/STAT signal transduction pathway.

5.1 The JAK/STAT pathway

The JAK/STAT pathway is a key signalling pathway activated by ligation of a large number of different cytokine receptors. It consists of three families of genes: the JAKs, or Janus family of protein tyrosine kinases, the signal transducers and activators of transcription (STAT) family, encompassing seven proteins, and the suppressors of cytokine signalling/cytokine-induced SH2-containing (SOCS/CIS) family, which serves as endogenous inhibitors. The JAK/STAT pathway generally mediates signals from a cytokine receptor to the nucleus.

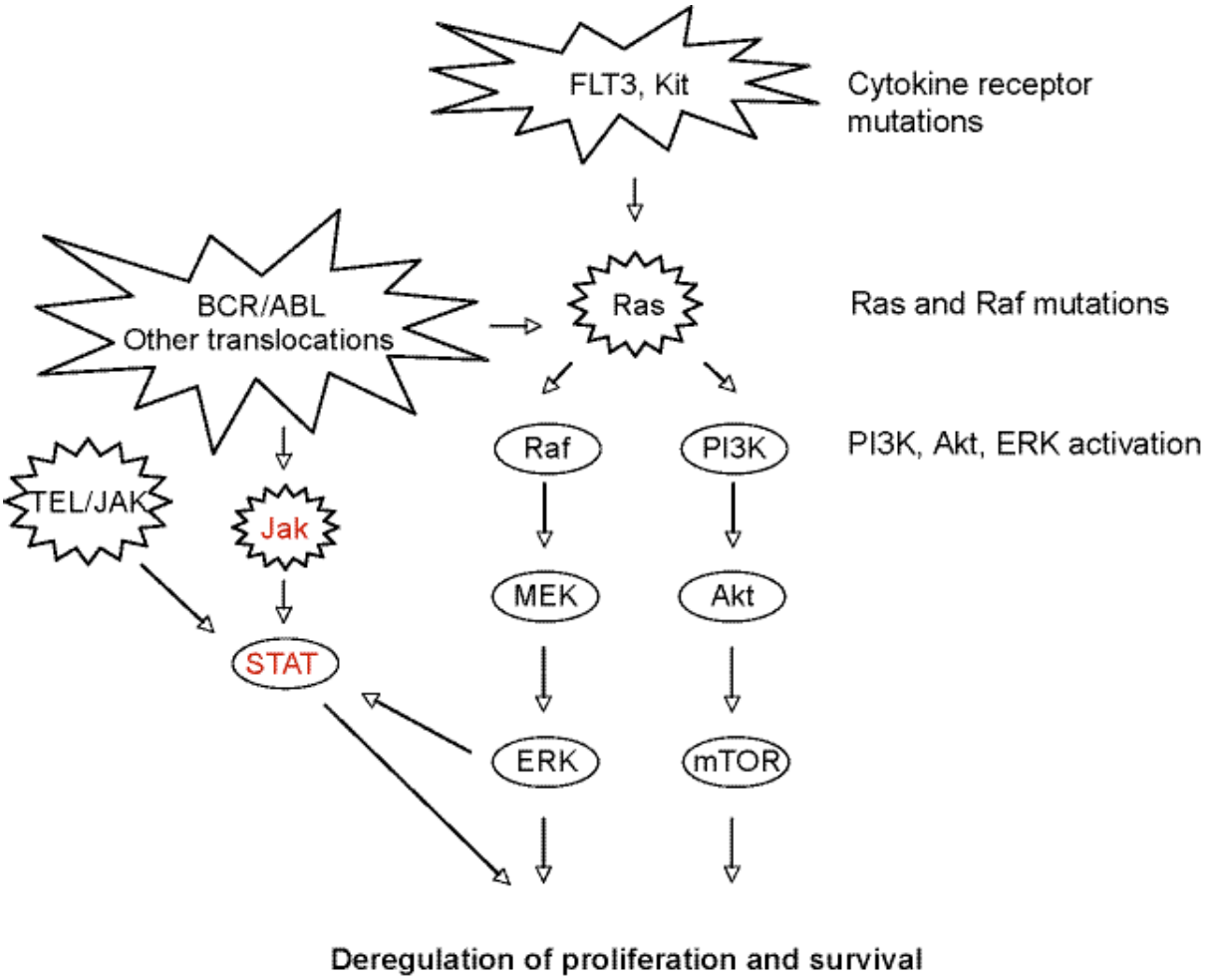

<u>Figure 2:</u> Sites of mutation that can result in activation of the Raf/MEK/ERK, PI3K/PTEN/Akt/mTOR and Jak/STAT pathways in hematopoietic cells.

Mutations have been detected in *FLT3*, *KIT*, *RAS* and *JAK*. The *BCR/ABL* chromosomal translocation is present in virtually all chronic myeloid leukemias (CMLs) and some acute lymphocytic leukemias (ALLs). Many of these mutations and chromosomal translocations result in activation of the Raf/MEK/ERK and PI3K/PTEN/Akt/mTOR cascades. The frequently mutated genes are indicated by a jagged symbol (adapted from Steelman, 2008).

JAK proteins associate with cytokine receptors, and ligand-stimulation of the cytokine receptor and activation of associated JAKs lead to phosphorylation of specific tyrosine residues on the receptor. This allows (SH2-containing) signalling proteins, including STATs, to bind. JAKs will then phosphorylate STATs leading to hetero-and homodimer formation and translocation to the nucleus, where the complexes can bind to specific DNA response elements and activate gene transcription (*Kisseleva, 2002*) (**Figure 3**). The JAK/STAT pathway is negatively regulated mainly by the SOCS and CIS families of proteins or alternatively by protein-tyrosine phosphatases (such as PTP and SHP2) as well as by ubiquitinylation and degradation (*Steelman, 2008*).

Constitutive activation of the JAK/STAT pathway occurs in a broad spectrum of human cancers, including solid tumors and hematological malignancies. Constitutive PTK activity, resulting from fusion proteins or point mutations, is a hallmark of many hematological malignancies such as myeloproliferative diseases (MPD), AML, ALL and CML. These constitutive active PTKs abrogate the cytokine dependence of certain hematopoietic cell lines and are not dependent on ligand binding (*Levine, 2007; Stirewalt, 2003)*.

Constitutive STAT activation has been found in many human cancers. Constitutive STAT activation has been generally linked to transformation by specific mutated constitutive active PTKs, such as BCR/ABL, TEL/PDGFRβ, TEL/JAK2 or FLT3 mutations. Of these fusion proteins, BCR/ABL interacts with STAT5 and can activate STAT5 independently of JAK2, suggesting that STAT5 may be directly phosphorylated and activated by the fusion protein. Activation of STAT5 has been found to be essential for efficient transformation of hematopoietic cells by BCR/ABL or TEL/JAK2 (*Steelman, 2008; Schwaller, 2000*). STAT5, with its two isoforms, STAT5a and STAT5b, is an important regulator of proliferation of hematopoietic cells in response to cytokines, growth factors and growth hormones (*Mui, 1995*). In hematopoietic cells, STAT5 regulates the expression of several PTK-inducible genes such as Bcl-XL or A1, Oncostatin M (OSM), cyclin D1 or PIM1 (*Socolovsky, 1999; Yoshimura, 1996; Matsumura, 1999; Lilly, 1992*).

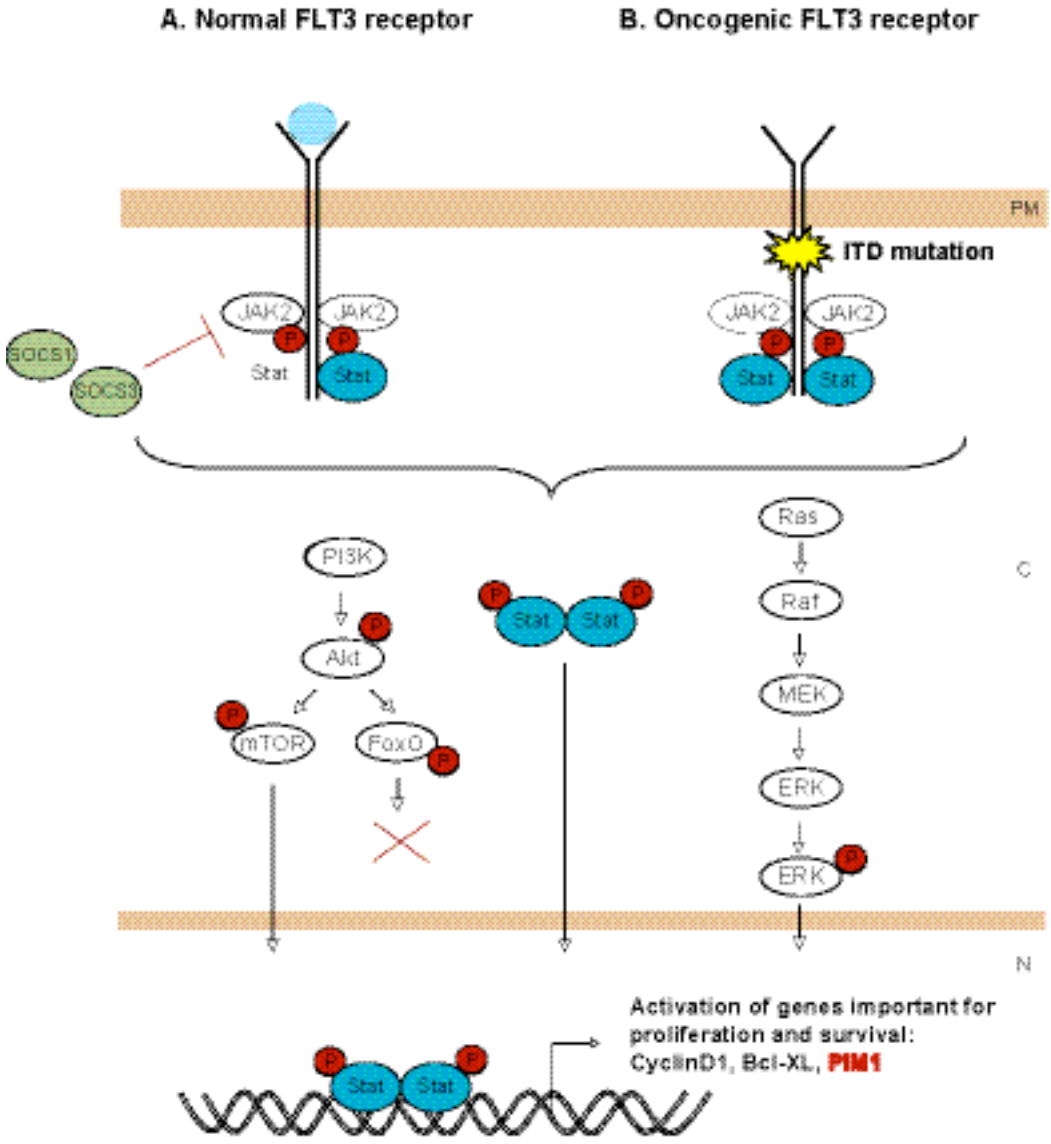

Figure 3: Mechanisms of activation of JAK2 kinase activity by mutations in the *FLT3* signalling pathway.

A. FLT3 ligand binds the FLT3 receptor, which results in JAK2 phosphorylation, recruitment of STAT signalling proteins, phosphorylation and activation of downstream signalling pathways including STAT transcription factors, MAPK signalling proteins and the PI3K-AKT pathway. Negative regulation of JAK2 is mediated by SOCS proteins

B. The oncogenic FLT3 receptor harbouring an internal tandem duplication (ITD) mutation in the juxtamemebrane domain undergoes ligand-independent activation, which also results in JAK2 phosphorylation, recruitment of STAT proteins and activation of downstream signalling pathways.

6. The PIM family of serine/threonine kinases

Cloning of retroviral murine leukemia virus (MLV) integration sites in c-myc-induced malignant murine lymphomas led to the identification of the PIM (Proviral Integration Moloney leukemia virus) genes (*Cuypers, 1984*). There are three different PIM genes, located on chromosomes 6, X and 22, encoding three serine/threonine kinases: PIM1, PIM2 and PIM3. At the amino acid level, PIM2 and PIM3 show 61% and 71% identity to PIM1, respectively (*van der Lugt, 1995; Baytel, 1998; Allen, 1996*). PIM1 and PIM2 genes are characterized by alternative transcriptional start sites that allow the expression of several isoforms, all containing the entire kinase domain. PIM1 and PIM2 are ubiquitously expressed at low levels in many tissues and are strongly induced in leukocytes in response to a large number of cytokines including IL2, IL3, IL4, IL5, IL6, IL7, IL9, IL12, IL15, GM-CSF, G-CSF, interferon α, interferon γ, EPO, TPO, prolactin, concanavalin A, lipopolysaccharide or phorbol myristate acetate (*Allen, 1997; Dautry, 1988; Lilly, 1992; Temple, 2001; Domen, 1993; Matikainen, 1999; Yip-Schneider, 1995; Miura, 1994; Borg, 1999; Wingett, 1996; Bachmann, 2005, Wang, 2001*). In normal animals, highest PIM1 mRNA levels were found in thymus and testis, whereas highest PIM2 mRNA levels were seen in the brain and thymus and PIM3 mRNA is most abundant in the kidney, breast and brain (*Selten, 1985; Allen, 1997; Feldman, 1998*). PIM kinases seem to be constitutive active molecules with a short half-life (of minutes) and their regulation appear to be largely at the level of transcription and degradation by the proteosome (*Mikkers, 2002; Fox, 2003*). There seem to be a certain degree of functional redundancy among the PIM kinase family: retroviral infection of myc-induced lymphomas in $PIM1^{-/-}$ mice resulted in tagging and up-regulation of PIM2 and infection of lymphomas lacking both PIM1 and PIM2 resulted in tagging PIM3 (*Mikkers, 2002; Bachmann, 2005*). Mice lacking PIM1 or PIM2 are viable and fertile with only mild defects in the hematopoietic system. Surviving mice lacking all three PIM kinases display reduced body size owing to decreased cell number in virtually all tissues but have a normal lifespan (*Mikkers, 2004*). Colony forming assays with bone marrow from $PIM1^{-/-}$ $PIM2^{-/-}$ $PIM3^{-/-}$ mice demonstrated that PIMs act redundantly in clonogenic growth in response to IL3, IL6, SCF and TPO; however, PIM1 seems to be the most crucial PIM for these responses (*Mikkers, 2004*). As PIM

kinases contribute to both cell proliferation and survival, they could provide a selective advantage in tumorigenesis.

The best-studied PIM kinase is PIM1. Examination of the substrate sequence specificity of PIM1 revealed strong preference for the peptide K-R-R-A-**S/T**-G-P with the presence of basic amino acid residues at the N terminal side being essential for substrate recognition. This suggests that under *in vitro* conditions, (K/R)3-X-**S/T**-X (X being neither basic nor large hydrophobic residue) might be the optimized PIM1 recognition site (*Friedmann, 1992*). Stepwise replacement experiments allowed further refinement of the consensus sequence for PIM1 phosphorylation to K/R-K/R-K-R/K-L-**S/T**-X where X is an amino acid residue with a small side chain (*Palaty, 1997*). In addition to phosphorylation of cellular substrates, these *in vitro* experiments also revealed auto-phosphorylating activity of PIM1 (*Hoover, 1991; Padma, 1991*). Mass-spectrometric analysis of GST-fusions of *Xenopus laevi* PIM1 identified potential auto-phosphorylation sites including S190 and T205, both conserved between species (*Palaty, 1997*). Negative regulation of the stability of PIM1 by the protein phosphatase 2A (PP2A) suggests that auto-phosphorylation and/or phosphorylation by so far unknown regulatory kinases are important determinants of PIM1 function (*Losman, 2003; Ma, 2007*). PIM1 has been implicated in signal transduction and transcriptional regulation, as well as cell cycle regulation and cell survival (*Bachmann, 2005; Wang, 2001*). The effect of PIM1 in signal transduction seems to be mediated by several substrates such as SOCS1 and SOCS3, that are involved in negative regulation of cytokine-induced JAK/STAT signaling (*Chen, 2002*), or the nuclear adapter protein p100 (a PIM1 binding partner), that is an activation factor of transcription factor c-Myb (*Leverson, 1998*). Other potential PIM1 substrates suggest that PIM1 can regulate nuclear transcription. Indeed, HP1 (heterochromatin-associated protein 1) and PAP1 (PIM1 associated protein) function in transcriptional repression by the silencing of chromatin and regulation of mRNA splicing, respectively (*Koike, 2000; Maita, 2000*). PIM1-mediated cell cycle regulation is driven by active phosphorylation, which enhances the activity of cell cycle promoters like Cdc25A (a G1 regulator) and Cdc25C (a G2/M regulator) as well as the inactivation of cell cycle inhibitors such as $p21^{Cip1/Waf1}$ and C-TAK1. PIM1 also binds and directly phosphorylates p27/KIP1 (CDKN1B) at residues T157 and T198 that allow binding of p27/KIP1 to 14-3-3 proteins resulting in its nuclear export and proteosome-dependent degradation

(*Mochizuki, 1999, Bachmann, 2004; Wang, 2002, Liu 2008*). Moreover, Zippo et al. showed that PIM1 acts a a cofactor of myc, phosphorylating chromatine at myc-target loci and contributes to a myc-dependent transformation (*Zippo, 2007*).

Further associations of PIM1 with the nuclear mitotic apparatus protein complexes seem to facilitate the progression through mitosis (*Bhattacharya, 2002*). As a whole, deregulated PIM1 activity would result in acceleration of the passage of cells from G2 into M-phase of the cycle. The role of PIM1 in apoptosis and survival is exercised by direct linking with proteins of the Bcl2 family: PIM1 phosphorylates and inhibits the pro-apoptotic protein BAD (*Aho, 2004; Kim, 2006; Macdonald, 2006*) (**Figure 4)**. Taken together, deregulated constitutive active PIM kinases enhancing cellular proliferation and survival could play a role in oncogenesis.

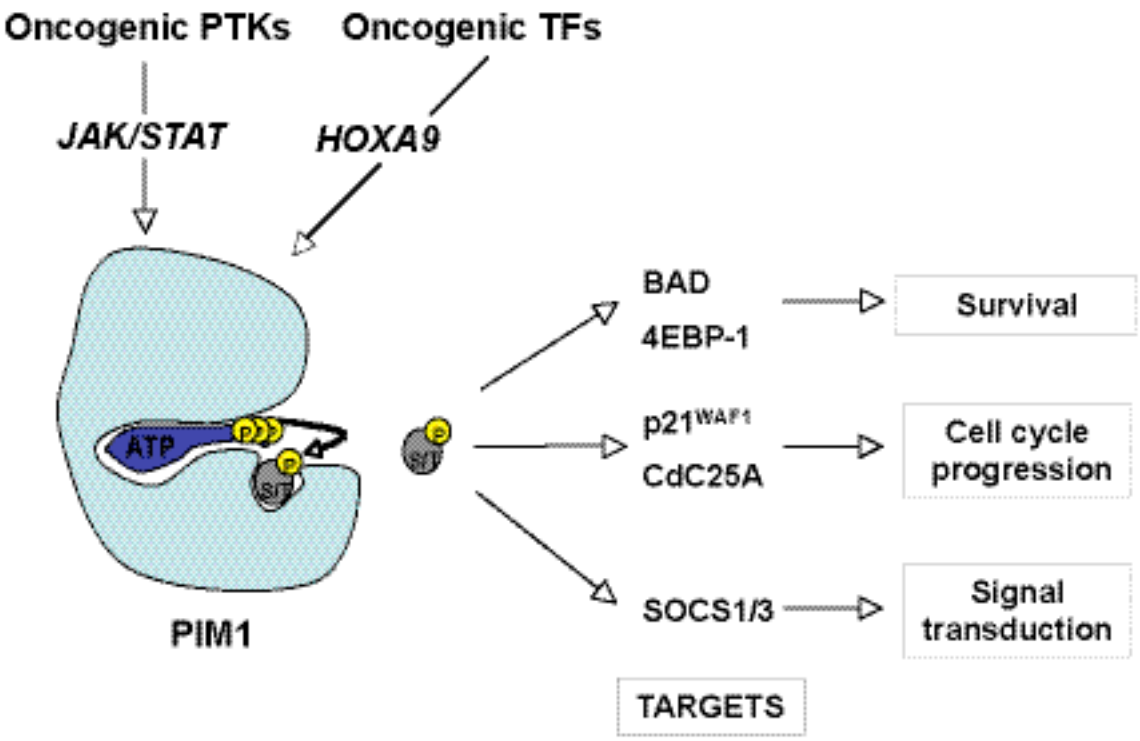

Figure 4: PIM kinases.

PIM kinases are downstream targets of oncogenic protein tyrosine kinases (PTKs) such as BCR/ABL or FLT3/ITD and mutated transcription factors (TFs) like MLL-X fusions. Phosphorylation of various targets supports cellular growth and survival.

6.1 Role of PIM kinases in cancer

Identification of PIM1 as being deregulated through recurrent proviral integration sites in murine lymphomas suggested early on that it might play a role in cancer pathogenesis (*Cuypers, 1984; Mikkers, 2002*). The tumorigenic activity of PIM1 and PIM2 kinases as cooperating oncogenes has been demonstrated in various transgenic mouse models. Early studies found PIM1 being over-expressed in 30% of human myeloid and lymphoid leukemias in absence of any PIM1 gene rearrangements or amplifications (*Amson, 1989; Selten, 1986*). In several cellular models of malignant myeloproliferative disorders, PIM1 expression was found to be up-regulated and proposed to be a mediator of cell proliferation and survival of oncogenic protein tyrosine kinases such as BCR/ABL or FLT3-ITD (*Nieborowska-Skorska, 2002; Kim, 2005; Liang, 1996; Adam, 2006*). Elevated levels of PIM1 found in a large fraction of human AML are most probably the consequence of the presence of activated FLT3 mutations in conjunction with class II mutation-mediated aberrant activation of transcriptional regulators of PIM1 (*Hu, 2007*). PIM1 over-expression alone is sufficient to induce cytokine independence in murine hematopoietic cells (*Nosaka, 2002; Pogacic, 2007*). Apart from leukemia, PIM1 seem to play an important role in the biology of malignant B cell lymphomas and prostate cancer.

In diffuse large B-cell lymphomas (DLBCL) and less frequently in other B-cell malignancies, PIM1 is targeted by aberrant somatic hypermutation (ASHM). ASHM-mediated PIM1 mutations have been detected in up to 50% of DLBCL cases, mostly affecting the coding sequence or the 5' untranslated region of PIM1 (*Pasqualucci, 2001*). Although those mutations involving the coding exons are predictive of change in the structure and in some cases, the function of the PIM1 protein, their role for the pathogenesis of B-cell lymphomas remained unclear. These lymphomas are characterized by chromosomal translocations leading to deregulation of several proto-oncogenes controlled by the immunoglobulin gene promotor and enhancer elements. It has been demonstrated that BCL6 translocations involve immunogloblulin (Ig) genes but also a number of non-Ig loci as partners including PIM1 in some rare cases (*Akasaka, 2000*).

Several studies have proposed that PIM1 over-expression can be used as a biomarker to distinguish between benign lesions and malignant glands in prostate cancer samples (*Dhanasekaran, 2001*). Gene expression profiling in human and

mouse prostate cancer tissues found co-transcriptional regulation of PIM1 and c-myc, possibly mediating a synergistic oncogenic effect in prostate cancer (*Dhanasekaran, 2001; Ellwood-Yen, 2003; Zippo, 2007*). Generally, decreased or absent PIM1 expression significantly correlated with measures of poor outcome. *In vitro* studies found that PIM1 induced genetic instability in human prostate epithelial cells as cells over-expressing PIM1 showed abnormal mitotic spindles, centrosome amplification and chromosome mis-aggregations (*Valdman, 2004*).

However, PIM1 is not the only PIM kinase involved in B cell lymphomas, solid cancers and leukemia. PIM2 was reported being over-expressed and associated with several malignancies originating from the B-cell lineage, including CLL and DLBCL as well as in prostate cancer (*Yoshida, 1999; Cohen, 2004; Dai, 2005*). In contrast, PIM3 has so far only been found in solid cancer but not in leukemia (*Fujii, 2005; Li, 2006*).

Taken together, increased expression of one or several PIM kinases are found in human hematological malignancies as well as solid cancers. By using siRNA-mediated strategies, PIM knockdown significantly impaired growth and/or survival of leukemia, prostate and liver cancer cells (*Li, 2006; Fujii, 2005; Dai, 2005; Adam, 2006*). Interestingly, whereas certain tumor cells (e.g. prostate and liver cell lines) were severely affected by knockdown of a single PIM kinase, others (some but not all leukemia cell lines) needed more than the knockdown of one single PIM to be significantly affected. These studies all suggest that inhibition of aberrant PIM activity by small molecules could open a new avenue for cancer therapy.

6.2 Small molecule inhibitors of PIM kinases

As outlined above, there is increasing evidence that PIM1 might be an important downstream player in cancer development and progression. The nature of PIM1 as constitutive active serine/threonine kinase and its deregulated expression in various cancers have made it a promising new drug target. An increasing number of ATP-competitive small molecule inhibitors of protein kinases have been successfully developed as new therapeutic option for cancer. However, owing to the similarity of the ATP binding sites between kinases, it has been challenging to identify specific inhibitors. PIM1 is unique among protein kinases due to the absence of the canonical hydrogen bond donor in the hinge region (the region deep in the ATP binding pocket linking the upper and lower lobe) that is a key element for the binding

of many ATP-mimetic kinase inhibitors. Due to this structural peculiarity, classical ATP-competitive kinase inhibitors may only weakly bind to the PIM family of kinases (*Kumar, 2005*). The earliest reported inhibitor of PIM1 function is LY294002, which was initially identified as a specific PI3K inhibitor (*Jacobs, 2005*). Seventy co-crystal structures of low molecular mass, low-affinity compounds with PIM1 have been solved in order to identify novel chemical classes as potential PIM1 inhibitors (*Kumar, 2005*). Recently, Ruboxistaurin, a PKCβ inhibitor being previously used in trials to treat diabetic complications, has been found to efficiently inhibit PIM1 and *in vivo* experiments suggest its potential use in acute myeloid leukemia with FLT3 mutations (*Fedorov, 2007*). Quercetagetin has also been reported to be a moderately potent and selective cell permeable inhibitor of PIM1 kinase that is able to inhibit PIM1 activity in prostate cancer cells in a dose-dependent manner (*Holder, 2007*). A series of substituted pyridone molecules was recently identified from a high throughput screen as potent inhibitors of PIM1 kinase; they may serve as useful starting scaffolds for the development of other improved and selective PIM1 inhibitors (*Cheney, 2007; Tong, 2008*).

During my PhD, I have investigated the role of PIM kinases in the pathogenesis of hematological malignancies induced by oncogenic PTKs and I have tested several types of potential small molecule inhibitors targeting PIM kinases.

II. Role of PIM kinases in the pathogenesis of FLT3-ITD induced myeloproliferations

1. Results

Increasing clinical and experimental evidence suggested that aberrant expression of PIM kinases might play an important role in the pathogenesis of leukemic disorders that are induced by constitutive activation of PTKs such as ABL, JAK2 or FLT3. Multiple studies have reported PIM1 and/or PIM2 being up-regulated in hematological malignancies harbouring mutated activated PTKs (*Adam, 2006; Kim, 2005; Amson, 1989; Nieborowska-Skorska, 2002*). Deregulated PIM kinase activity seem to be important for maintenance of a transformed hematopoietic cell as functional interference by expression of dominant-negative acting PIM mutants or PIM-isoforme specific siRNA significantly impaired growth and proliferation of human and mouse hematopoietic cells that where transformed by BCR/ABL or FLT3-ITD (*Adam, 2006*). Over-expression of PIM1 is able to transform growth-factor-dependent hematopoietic cells and to induce a lethal leukemia-like disease in mice after a long latency (*Nosaka, 2002; Grundler, unpublished observation*). However, it is not known whether PIM kinases are essential for the induction of PTK-mediated leukemic disorders.

Expression of FLT3-ITD induces MPD in transgenic mice, as well as in bone marrow transplantation models (*Kelly, 2002; Gilliland, 2003, Grundler, 2005*). By using a genetic approach, we investigated the role of PIM kinases for the development of malignant myeloproliferation mediated by FLT3-ITD.

1.1 *In vitro* and *in vivo* leukemogenic activity of FLT3-ITD is independent of PIM2

To investigate the role of PIM kinases in hematological diseases induced by oncogenic protein tyrosine kinases, we expressed the constitutively active FLT3-ITD mutant in primary murine bone marrow cells. Retroviral expression of FLT3-ITD in wild type bone marrow cells induced growth factor-independent growth as shown in colony forming assays as well as in liquid culture (**Figure 5A**). Expression of FLT3-ITD in PIM1$^{-/-}$ bone marrow cells resulted in a significant lower number of colonies growing with and without IL3. No differences in colony formation and growth properties were observed in WT (FVB/N) and PIM2$^{-/-}$ bone marrow cells expressing FLT3-ITD when grown in presence or absence of IL3 (**Figure 5B**). Liquid culture of the cells over five days revealed no difference in viability but a general reduced growth rate of bone marrow cells originating from PIM1$^{-/-}$ animals compared to PIM2$^{-/-}$ or wild type mice (**Figure 5C**). These *in vitro* results suggest that PIM1 and not PIM2 is involved in signalling events that are essential for IL3 and/or FLT3-ITD regulated proliferation.

To study the role of PIMs in FLT3-ITD mediated leukemogenesis *in vivo*, we performed bone marrow transplantations with cells from WT, PIM1$^{-/-}$ or PIM2$^{-/-}$ donor mice. Cells were infected with *MSCV-FLT3-ITD-EGFP* or control EGFP retrovirus and transplanted into sub-lethally (750rad) irradiated synergic (FVB/N) recipient mice. Mice that were transplanted with cells lacking PIM1 developed no hematological disorder during one year of post-transplant observation (**Figure 6A**). Histological analysis of the normal sized spleens of FLT3-ITD-transplanted animals revealed no pathological changes six months after transplantation (**Figure 6C**). In contrast, animals that received a transplant of FLT3-ITD-tranduced bone marrow cells from WT or PIM2$^{-/-}$ mice developed a myeloproliferative disorder characterized by a massive expansion of EGFP-positive myeloid (CD11b^{+}) cells in the peripheral blood characterized by FACS analysis 26 days post transplantation (not shown). There was no significant difference in survival between recipients of WT versus PIM2$^{-/-}$ bone marrow transduced with FLT3-ITD. Both mice groups succumbed to disease with a median survival time of 108 and 138 days, respectively (**Figure 6A**).

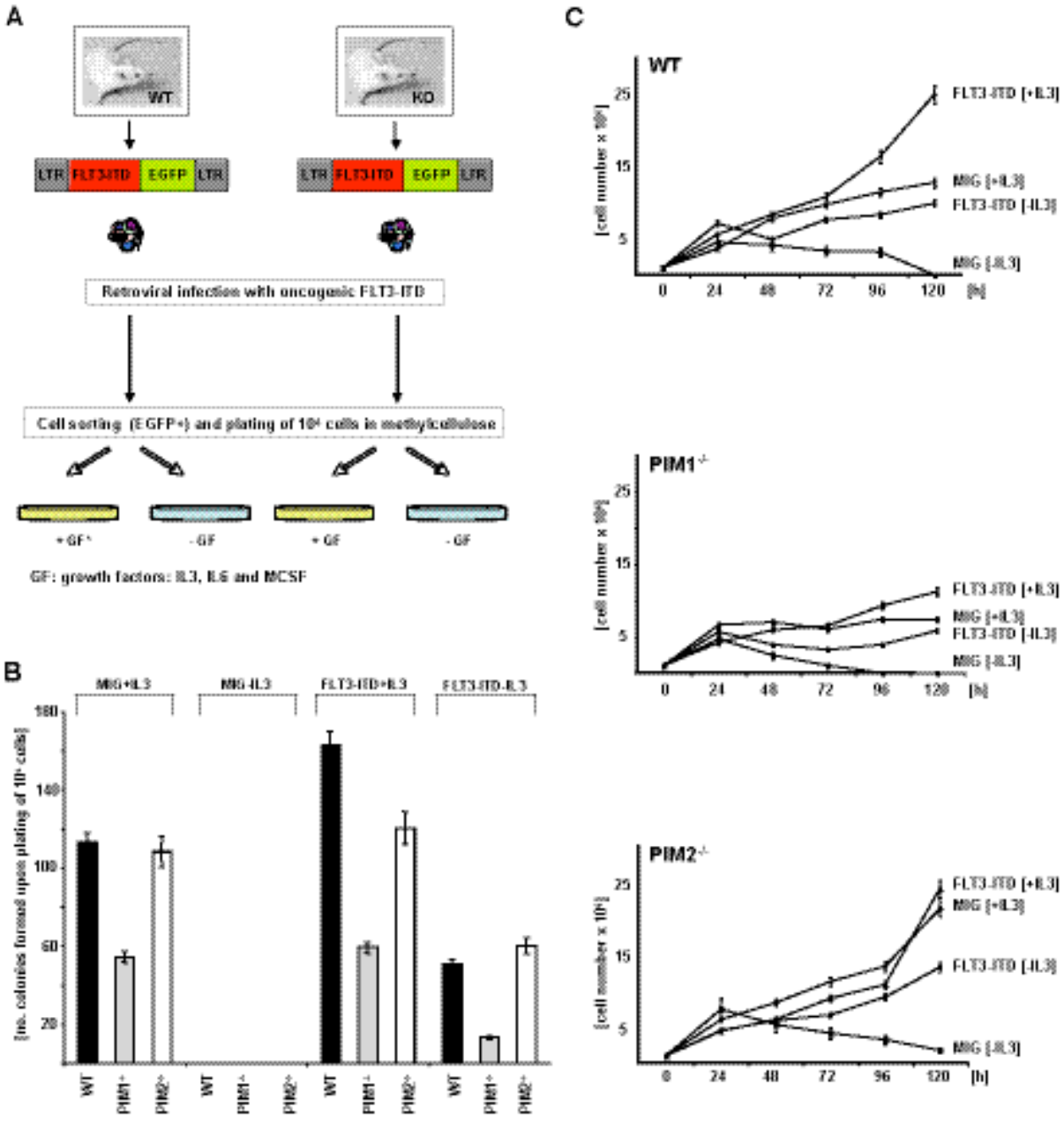

<u>Figure 5:</u> In vitro and in vivo FLT3-ITD mediated transformation in presence and absence of PIM serine/threonine kinases.

A. Schematic representation of the experimental settings.

B. Comparative analysis of clonogenic growth of FLT3-ITD expressing bone marrow cells from wildtype and PIM1$^{-/-}$, or PIM2$^{-/-}$ mice: 10^4 EGFP$^+$ cells were sorted 48h after infection and plated in methylcellulose in presence of absence of IL3.

C. Comparative analysis of liquid culture growth of FLT3-ITD expressing bone marrow cells from wildtype and PIM1$^{-/-}$, or PIM2$^{-/-}$ mice: 1-5.10^5 cells were plated 48h after infection in presence or absence of IL3 and counted each day in triplicates.

Macroscopically, diseased mice of both groups showed enlarged spleens and thymi. Histopathological examinations of the spleens revealed extensive infiltrations with neoplastic myeloid cells (**Figure 6C**). All mice receiving a transplant of FLT3-ITD transduced bone marrow developed exactly the same mixed myeloid/T-lymphoid phenotype, as published before (*Grundler, 2005*). Following the EGFP+ reconstituted cells by flow cytometry revealed significant expansion of FLT3-ITD expressing WT or PIM2$^{-/-}$ cells within the first month post transplantation. In contrast, although detectable over several weeks, FLT3-ITD expressing PIM1$^{-/-}$ cells underwent no significant expansion (**Figure 6B**).

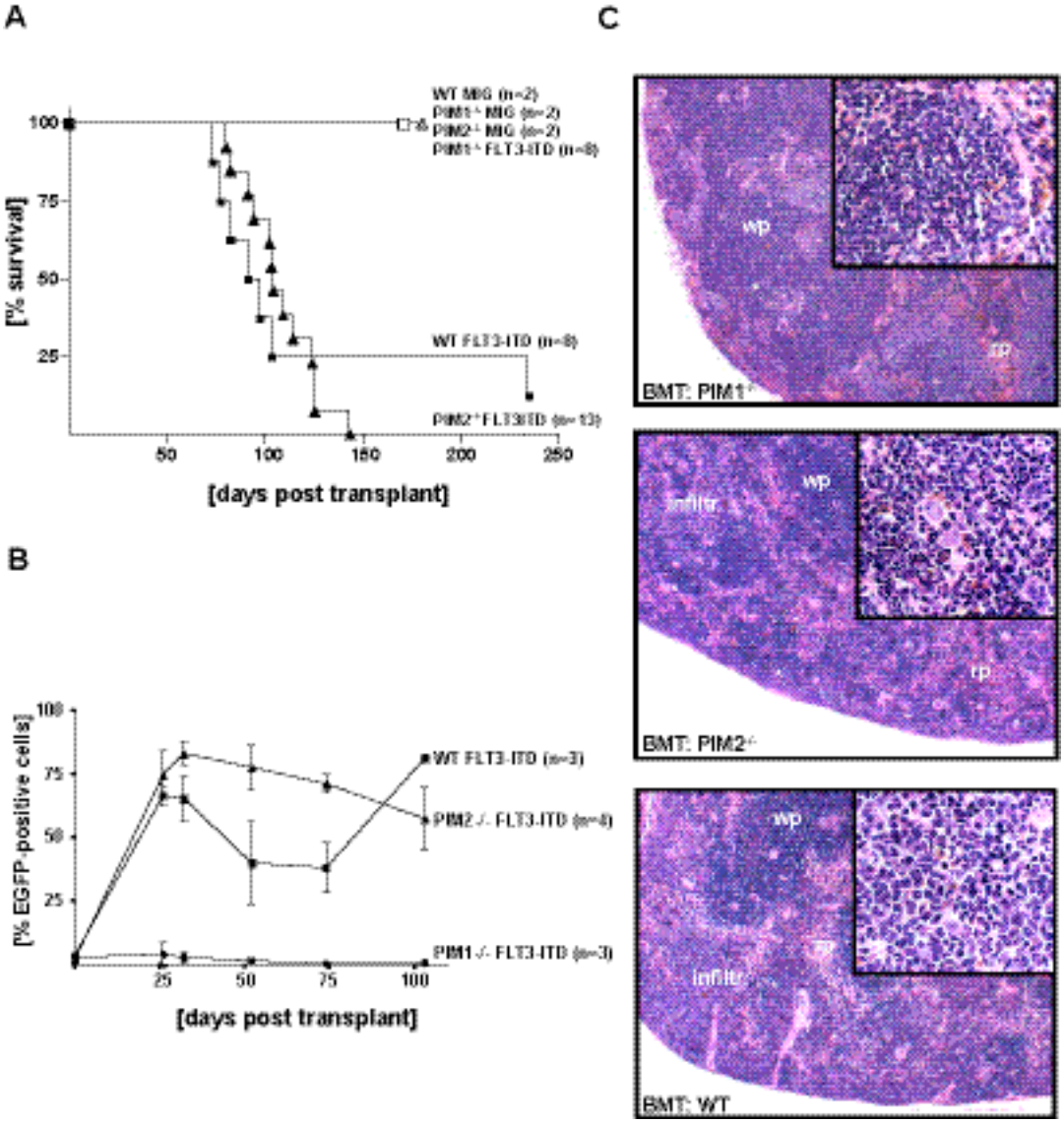

Figure 6: Transplantation of wildtype (WT) or PIM2$^{-/-}$, but not PIM1$^{-/-}$ leads to FLT3-ITD induced myeloproliferative disorder.

A. Kaplan Meier survival plot: WT, PIM1$^{-/-}$ or PIM2$^{-/-}$ bone marrow was transduced with FLT3-ITD or empty vector (*MigRI*) as indicated and transplanted into sub-lethally irradiated (750rad) recipient mice. All mice that underwent transplantation with FLT3-ITD transduced WT or PIM2$^{-/-}$ bone marrow died, or were sacrificed because of disease conditions

B. Flow cytometric analysis of EGFP^{+} cells in peripheral blood samples post transplant.

C. Histopathological analysis of spleen biopsies from animals transplanted with FLT3-ITD expressing bone marrow cells. Extensive splenic myeloid infiltrations in animals that received wild-type or PIM2^{-7-} FLT3-ITD^{+} cells were shown (rp= red pulp, wp= white pulp, infiltr= infiltration).

Although the experiments were performed in the same way for all conditions, we could not exclude that the absence of FLT3-ITD-mediated disease could result from the inability of PIM1$^{-/-}$ cells to reconstitute irradiated mice. During the first series of experiments, a non-lethal irradiation dose was applied to the recipient mice (750rad). To further exclude the possibility of a homing failure in PIM1$^{-/-}$ cells, we increased the irradiation to a lethal dose of 900rad and repeated the experiments. Again, animals receiving FLT3-ITD expressing cells from WT and PIM2$^{-/-}$ donors did develop an identical MPD phenotype as described above. In contrast, all recipients transplanted with PIM1$^{-/-}$ bone marrow expressing either the control vector or *MSCV-FLT3-ITD-EGFP* died within three weeks most probably from a lack of bone marrow reconstitution (**Figure 7A**). A rapid decline of all hematopoietic cell lineages was observed in the first two weeks after transplantation (**Figure 7B**). To exclude the possibility of a quantitative difference in transplanted hematopoietic stem cells, we compared the number of lin^{-}, Sca1^{+} and c-kit^{+} cells but no difference was found (**Figure 7C**)**.** Taken together, these unexpected results suggested that PIM1 could play an essential role in early bone marrow reconstitution.

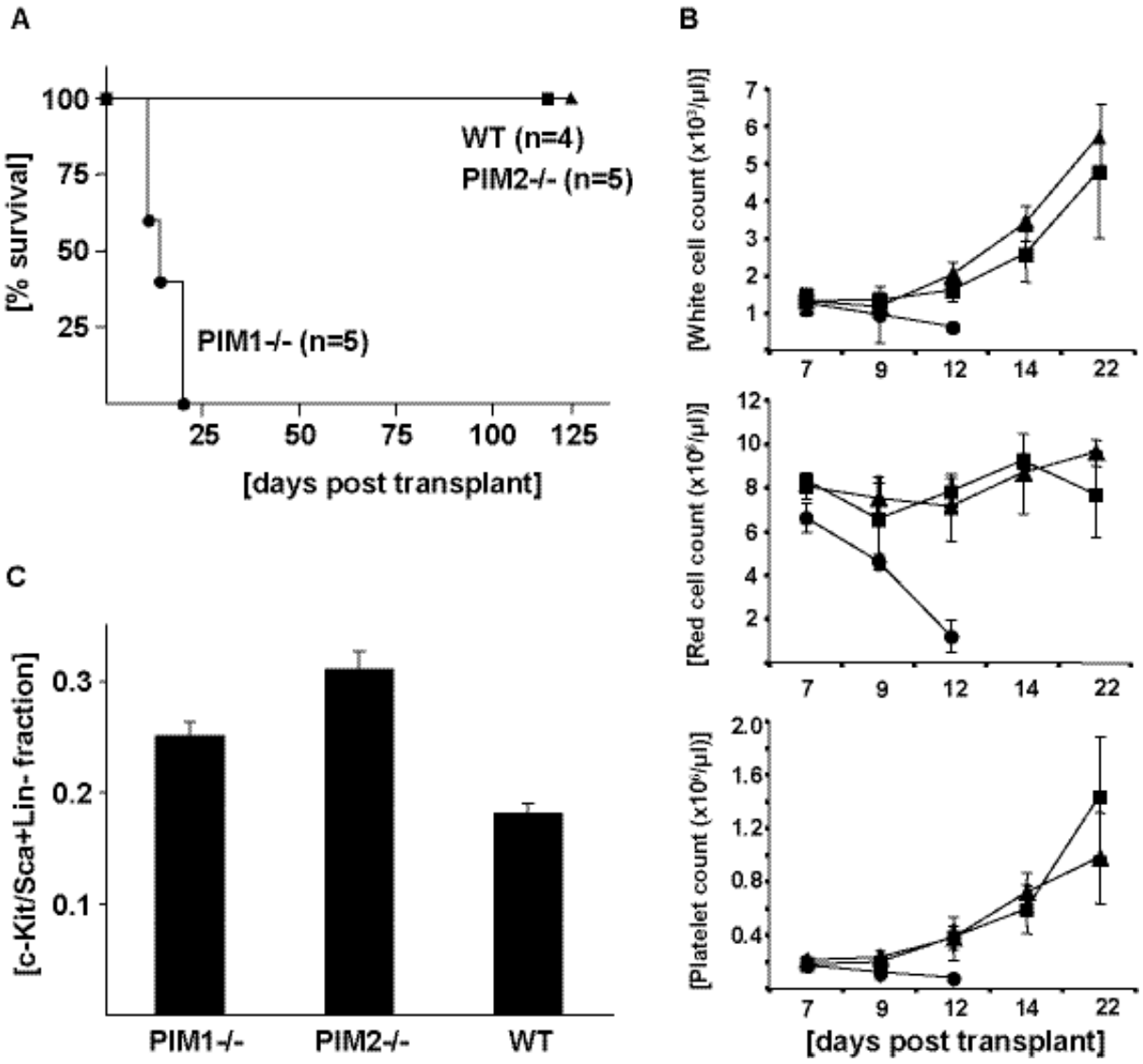

Figure 7: PIM1$^{-/-}$ bone marrow cells do not reconstitute lethally irradiated recipient animals.

A. Overall survival of lethally irradiated (950rad) recipients receiving WT, PIM1$^{-/-}$ or PIM2$^{-/-}$ bone marrow cells.

B. Hematopoietic reconstitution following transplantation of 3.10^6 WT (n=4), PIM1$^{-/-}$ (n=5) or PIM2$^{-/-}$ (n=5) bone marrow cells into lethally irradiated mice. Data represent mean ± SD. (WBC= peripheral blood leukocyte count, RBC= peripheral blood erythrocyte count, PTK= peripheral blood platelet count).

C. Analysis of Lin$^-$ Sca1$^+$ c-kit$^+$ cells in the bone marrow of 6-8 weeks old WT, PIM1$^{-/-}$ and PIM2$^{-/-}$ female mice.

1.2 Role of PIM1 in early homing and migration of HSCs

The observed lack of early bone marrow reconstitution could be theoretically based on a defect of hematopoietic stem cell homing and migration towards their niches or on insufficient expansion due to limited self-renewal. Previous studies suggested that engraftment of HSCs could be divided into three phases: homing, trans-marrow migration and lodgement in the niche (Nilsson, 2006). The rapid decline (<2 weeks) of all hematopoietic lineages shortly after transplantation suggests that PIM1$^{-/-}$ hematopoietic stem cells are impaired in their homing and/or migration capacities.

In order to understand the role PIM1 plays in homing, we labelled bone marrow from WT and PIM1$^{-/-}$ mice with the vital dye CFSE (Carboxyfluorescein succinimidyl ester) and injected equal numbers of viable, positively labelled cells into lethally irradiated recipients and determined the amount of cells that homed to the bone marrow and to the spleen 4 and 20 hours post-transplant (**Figure 8A & B**). A significant time-independent decrease in CFSE-labelled cells was observed in the spleen and the bone marrow of mice injected with PIM1$^{-/-}$ cells compared to mice receiving labelled cells from WT animals. No significant difference in viability of CFSE-labelled cells was observed between the genotypes, as determined by PI staining (**Figure 8C**). As PIM1$^{-/-}$ cells were not able to home to hematopoietic organs such as the bone marrow or the spleen, this finding suggested that PIM1 could play an important role in homing of hematopoietic stem cells.

Figure 8: PIM1$^{-/-}$ bone marrow cells do not reconstitute lethally irradiated recipient animals and have an impaired homing capacity.

A. Schematic representation of the experimental settings.

B. Homing of CFSE-labelled bone marrow cells from PIM1$^{-/-}$ and wild-type FVB/NJ mice to the bone marrow (upper panel) and the spleen (lower panel) of wild-type recipients. Data represent the mean ± SD of duplicates.

C. Viability of bone marrow cells from PIM1$^{-/-}$ and wild-type FVB/NJ mice 4 and 20 hours post CFSE stain was detected by PI staining. Data represent the mean ± SD of duplicates.

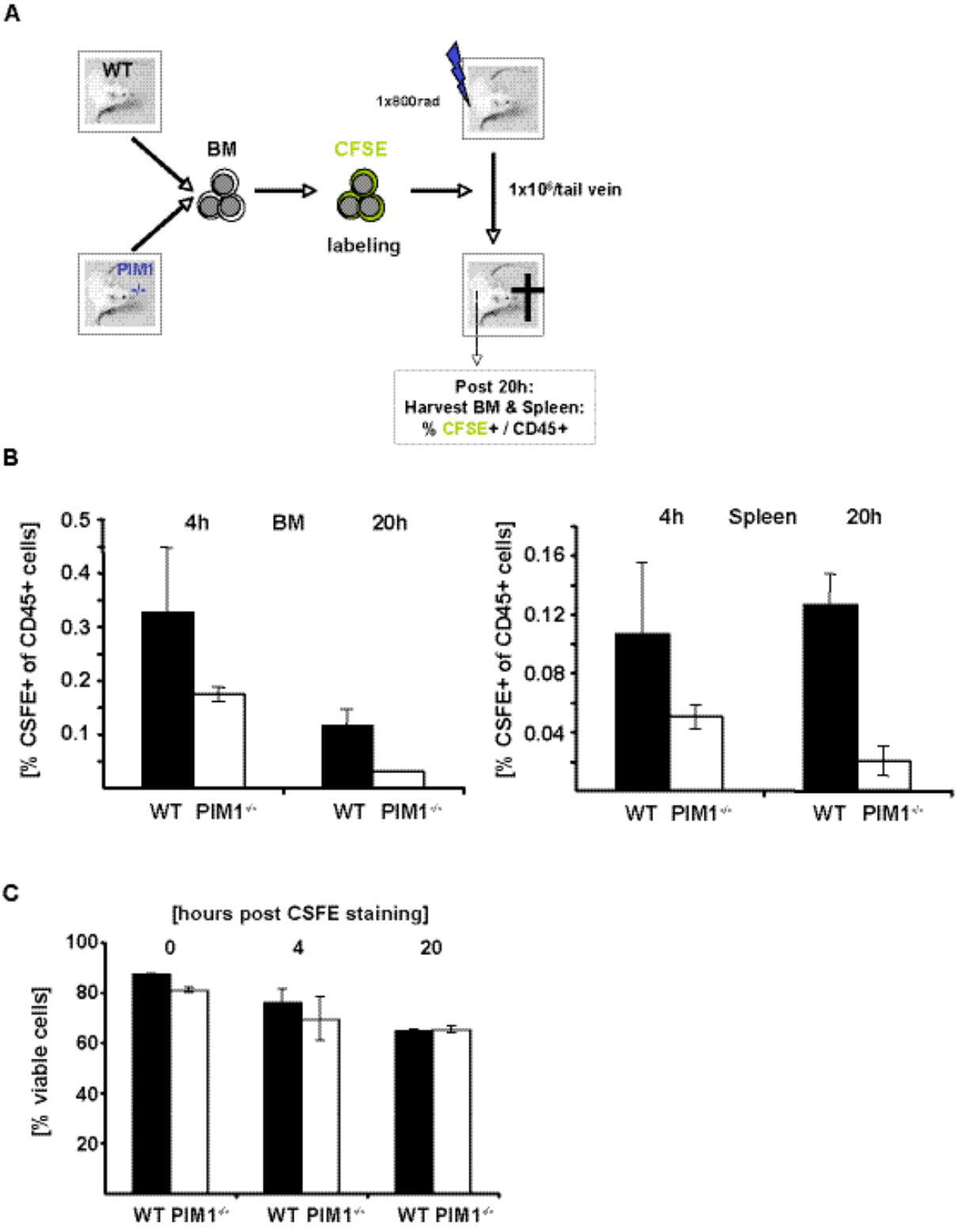
A
WT
PIM1 -/-
BM
CFSE
labeling
1x800rad
1x10⁶/tail vein
Post 20h:
Harvest BM & Spleen:
% CFSE+ / CD45+
B
[% CSFE+ of CD45+ cells]
4h
BM
20h
WT PIM1-/-
WT PIM1-/-
4h
Spleen
20h
WT PIM1-/-
WT PIM1-/-
C
[hours post CSFE staining]
[% viable cells]
0
4
20
WT PIM1-/-
WT PIM1-/-
WT PIM1-/-

1.3 PIM1 is a functional regulator of the CXCR4 chemokine receptor

Previous studies have shown that interaction of the chemokine receptor CXCR4 with its ligand CXCL12/SDF1α is essential for homing and trans-marrow migration of HSCs (*Lapidot, 2005; Burger, 2006*). In order to find out whether CXCR4 signalling could be involved in the grafting defect of PIM1$^{-/-}$ bone marrow, we first compared *in vitro* migration of PIM1$^{-/-}$ and WT bone marrow cells towards a CXCL12 gradient. Cells lacking PIM1 showed impaired migration, even in the presence of hematopoietic growth factors like IL3, IL6 and SCF **(Figure 9A**). Flow cytometric analysis of the same cells revealed that PIM1$^{-/-}$ cells expressed lower levels of surface CXCR4, but not of other surface molecules also involved in homing like integrins α4 and α5 (**Figure 9B & D**). Cellular response to CXCL12 is characterized by a rapid Ca^{2+} flux. Interestingly, almost no Ca^{2+} flux was observed in bone marrow cells lacking PIM1 when compared to wild type cells (**Figure 9C**). Furthermore, CXCL12 induced activation of CXCR4 downstream signals such as phosphorylation of AKT and ERK was impaired in PIM1$^{-/-}$ cells (not shown). These observations suggested that PIM1 might be a functional regulator of the CXCL12/CXCR4 signalling axis.

Figure 9: Decreased steady-state CXCR4 surface expression of PIM1$^{-/-}$ bone marrow cells is associated with impaired migration and CXCL12-induced signalling.

A. Bone marrow cells from PIM1$^{-/-}$ and FVB/NJ mice were allowed to migrate toward a CXCL12 gradient (300ng/mL) along with background migration as indicated. The migration index was calculated as a percentage of input cells. Data represent the mean ± SD of triplicates.

B. Cell surface expression of CXCR4 on bone marrow cells from PIM1$^{-/-}$ and wild-type mice was analyzed by staining with PE-conjugated anti-mouse CD184 antibody (open histogram). Non-specific binding was assessed by using a PE-conjugated rat-IgG2b antibody (grey histogram).

C. Calcium flux was monitored in freshly isolated WT and PIM1$^{-/-}$ bone marrow cells after stimulation with CXCL12 (300ng/mL).

D. Cell surface expression of integrin α_4 (CD49d) and integrin α_5 (CD49e) was analyzed by staining with PE-conjugated anti-mouse CD49d and CD49e antibodies, respectively (open histograms). Non-specific binding was assessed with a PE-conjugated rat IgG2b and IgG2a antibody, respectively (grey histograms).

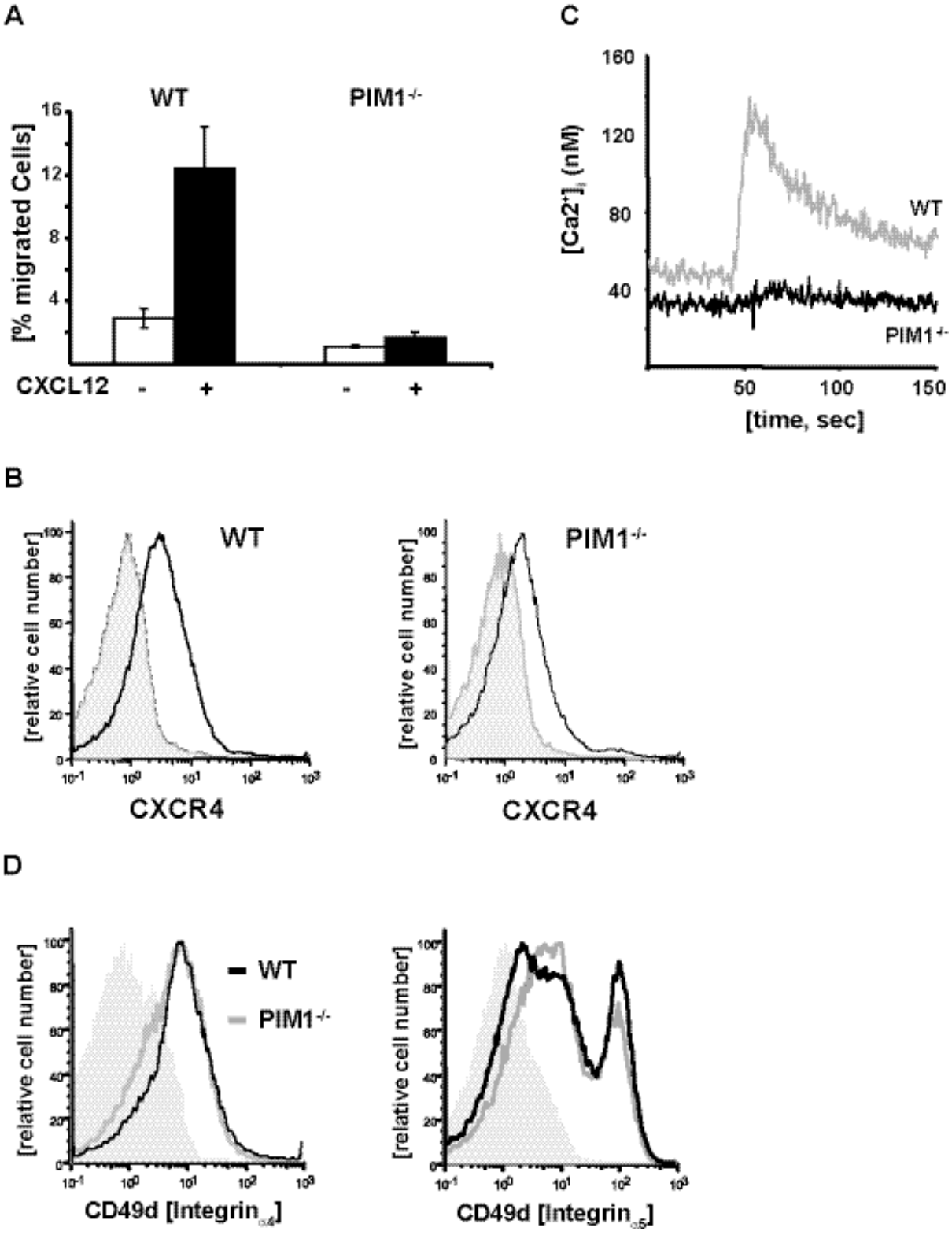
A
WT
PIM1-/-
[% migrated Cells]
16
12
8
4
CXCL12 - + - +
C
160
120
80
40
[Ca2+]i (nM)
WT
PIM1-/-
50
100
150
[time, sec]
B
WT
PIM1-/-
[relative cell number]
CXCR4
CXCR4
D
WT
PIM1-/-
[relative cell number]
CD49d [Integrin α4]
CD49d [Integrin α5]

To further investigate this possibility, endogenous PIM expression was down-regulated by virally expressed PIM-specific siRNA in BaF/3 cells. Knockdown of PIM1 resulted in a significant decrease of CXCR4 surface expression whereas PIM2 siRNA showed no effect (**Figure 10A**). Interestingly, Western Blot analysis revealed no change in total CXCR4 protein expression suggesting that PIM1 selectively regulates surface CXCR4 expression (**Figure 10B**).

Likewise, expression of a dominant-negative acting PIM1 mutant (PIM1-KD, kinase-dead) also down-regulated surface CXCR4 level suggesting that PIM1 kinase activity is indeed required (**Figure 10C**). Taken together, these results suggested that PIM1 could selectively control the surface presentation of CXCR4. We therefore tested whether re-expression of PIM1 in $PIM1^{-/-}$ bone marrow cells could rescue surface CXCR4 expression and migration towards a CXCL12 gradient. For this, $PIM1^{-/-}$ bone marrow cells were retrovirally infected with PIM1 and CXCR4 surface expression was analyzed. Infected cells showed CXCR4 surface levels comparable with wild type cells (**Figure 11A**). In addition, expression of PIM1 restored the capability of the cells to efficiently migrate towards CXCL12 (**Figure 11B**). It has to be noted that prolonged *in vitro* culture of bone marrow cells (that is necessary for viral transduction) also affects cellular migration and might be responsible for increased migration observed in cells transduced with the control vector. Taken together, our results suggested that PIM1 is a critical regulator of CXCR4 surface expression and function in hematopoietic cells.

To further test the hypothesis that PIM1 kinase activity is required for the regulation of CXCR4 surface expression, I used a small molecule inhibitor against PIM1 (K00486) that we recently characterized (see part III). As the efficacy of this compound is limited to human PIM1, we treated human JURKAT T-cell leukemia cells, expressing high levels of PIM1 and surface CXCR4, for 2h with 10µM K00486. A transient but significant decrease of surface CXCR4 was observed by flow cytometry as well as significantly reduced migration of the cells towards a CXCL12 gradient without affecting the viability (**Figure 11C & D**). These data further support a functional link between PIM1 kinase activity and surface expression and function of CXCR4.

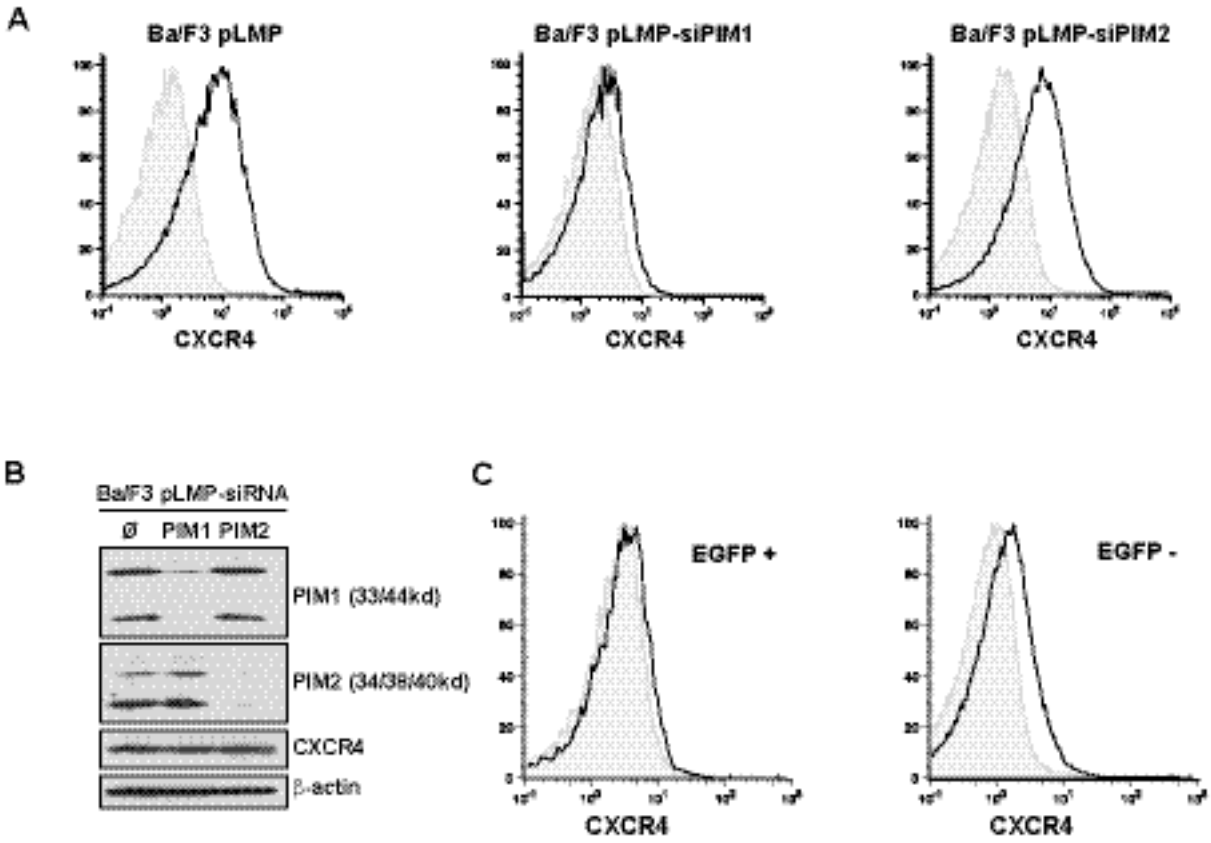

Figure 10: PIM1 activity regulates CXCR4 surface expression in hematopoietic cells.

A. Down-regulation of PIM1 but not PIM2 resulted in reduced surface expression of CXCR4 in BaF/3 cells. BaF/3 cells were retrovirally transduced with *pLMP*, *pLMP-siPIM1* or *pLMP-siPIM2*, expressing siRNAs. Cell surface expression of CXCR4 was analyzed by staining with PE-conjugated anti-mouse CD184 antibody (open histogram). The level of non-specific binding was assessed by using a PE-conjugated rat-IgG2b as isotype control (grey histogram).

B. Down-regulation of PIM1 and PIM2 protein expression was confirmed by Western Blot analysis. No change in total CXCR4 expression was observed.

C Wildtype bone marrow cells were transduced with *MSCV-PIM1-KD-IRES/GFP* and 48h later surface CXCR4 was compared on EGFP+ vs. EGFP- cells. Cell surface expression of CXCR4 was analyzed by staining with PE conjugated anti-mouse CD184 antibody (open histogram). Non-specific binding was assessed as described above.

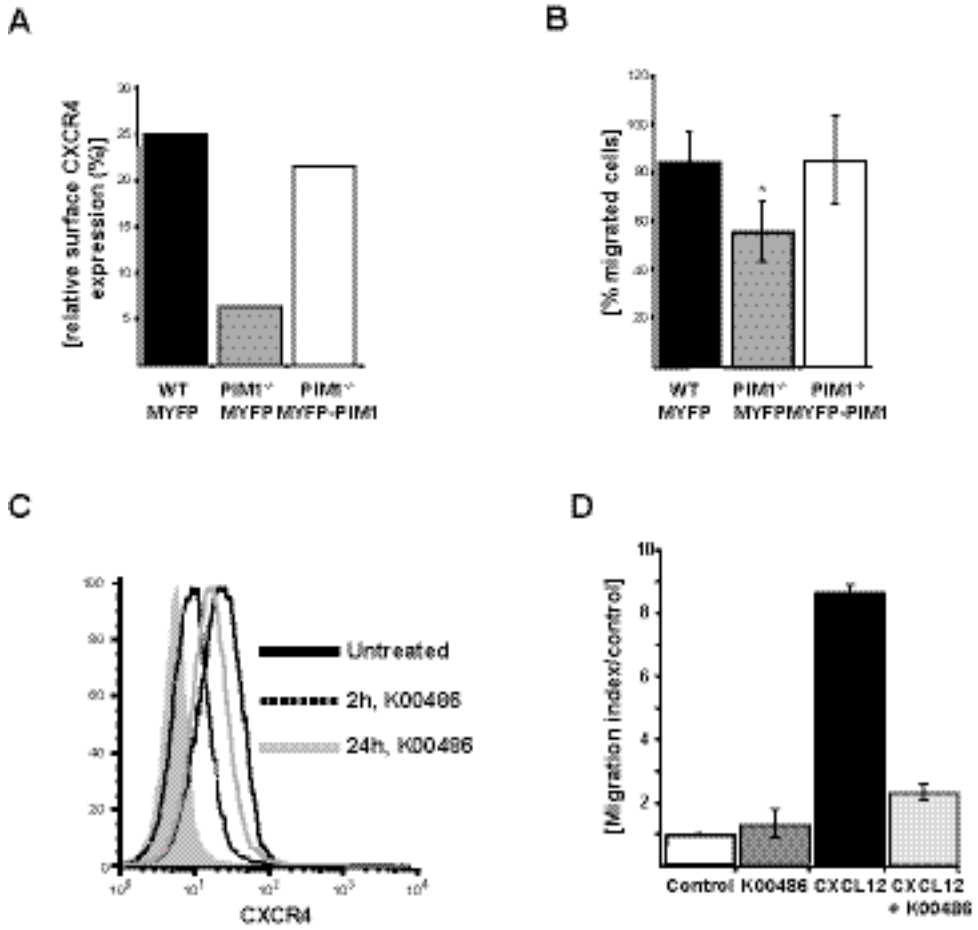

Figure 11: PIM1 activity regulates CXCR4 surface expression in hematopoietic cells.

A. WT and PIM1$^{-/-}$ bone marrow was transduced with *pMSCV mPIM1-YFP* or empty vector (*MYFP*) as indicated. Cell surface expression of CXCR4 was analyzed by staining with PE-conjugated anti-mouse CD184 antibody.

B. Bone marrow cells from wild-type and PIM1$^{-/-}$ mice, transduced with *pMSCV mPIM1-YFP* or empty vector (*MYFP*) as indicated, were allowed to migrate toward a CXCL12 gradient (300ng/mL). The migration index was calculated as a percentage of input cells. Data represent the mean ± SD of triplicates.

C. Treatment of human Jurkat leukemia cells with a small molecule PIM1 inhibitor (K00486, 10µM) leads to a transient but significant reduction of surface CXCR4 expression after 2h (strong dotted line) and 24h (fine dotted line). Viability of the cells was not significantly changed within the time of the experiment determined by 7-AAD staining (not shown).

D. Jurkat cells were allowed to migrate towards a CXCXL12 gradient (100ng/mL) with or without pre-treatment with the K00486 PIM1 inhibitor (2h, 10µM). Data represent the mean ± SD of triplicates.

1.4 PIM1 as mediator of elevated surface CXCR4 in human leukemic blasts

Several studies have previously demonstrated that elevated surface CXCR4 expression is an adverse prognostic marker in patients with acute myeloid leukemia (AML) (*Rombouts, 2004; Spoo, 2007*). Since our results suggested that PIM1 might be a regulator of surface CXCR4 expression, we compared the PIM1 expression levels in leukemic samples that have previously been analyzed for surface CXCR4 expression (*Spoo, 2007*). Interestingly, although we were limited to a small number of samples we observed a tendency for higher PIM1 expression in AML samples with high CXCR4 surface expression ($p<0.05$) (**Figure 12A**). In contrast, we found no significant correlation between surface CXCR4 and CXCR4 mRNA levels (**Figure 12A**). These data suggested that PIM1 signalling might be necessary for increased CXCR4 surface expression on AML blasts.

In order to address this possibility we freshly isolated leukemic blasts from patients with newly diagnosed AML expressing high surface CXCR4. Cells were treated with 10µM of the PIM1 inhibitor K00486 for 30min (collaboration with C. Dierks and A. Spoo, Freiburg). A significant decrease in CXCR4 surface expression was observed in two out of 3 patient samples without impaired viability (**Figure 12B**). These observations further supported the hypothesis that PIM1 can act as an important regulator of surface CXCR4 expression in primary human leukemic cells.

As several studies have shown over-expression of PIM1 in many hematologic malignancies as well as solid tumors, we determined whether elevated PIM1 levels might also affect CXCR4 function by using Ba/F3 hematopoietic cells stably over-expressing human PIM1 (*Adam, 2006*). Interestingly, transmigration towards a gradient of 10nM CXCL12 was significantly enhanced for PIM1 over-expressing cells and could be significantly impaired in the presence of the K00486 inhibitor (**Figure 12C**). These results suggested that deregulated PIM1 might exert its oncogenic activity also through increase of CXCR4 surface expression and function.

CXCR4 surface expression is regulated by ligand (CXCL12)-induced internalization and surface re-expression or degradation (*Busillo, 2007*). In order to find a mechanistic link between CXCR4 and PIM1, we monitored CXCR4 surface expression on JURKAT cells upon stimulation with CXCL12 and in presence or absence of the PIM1 inhibitor K00486.

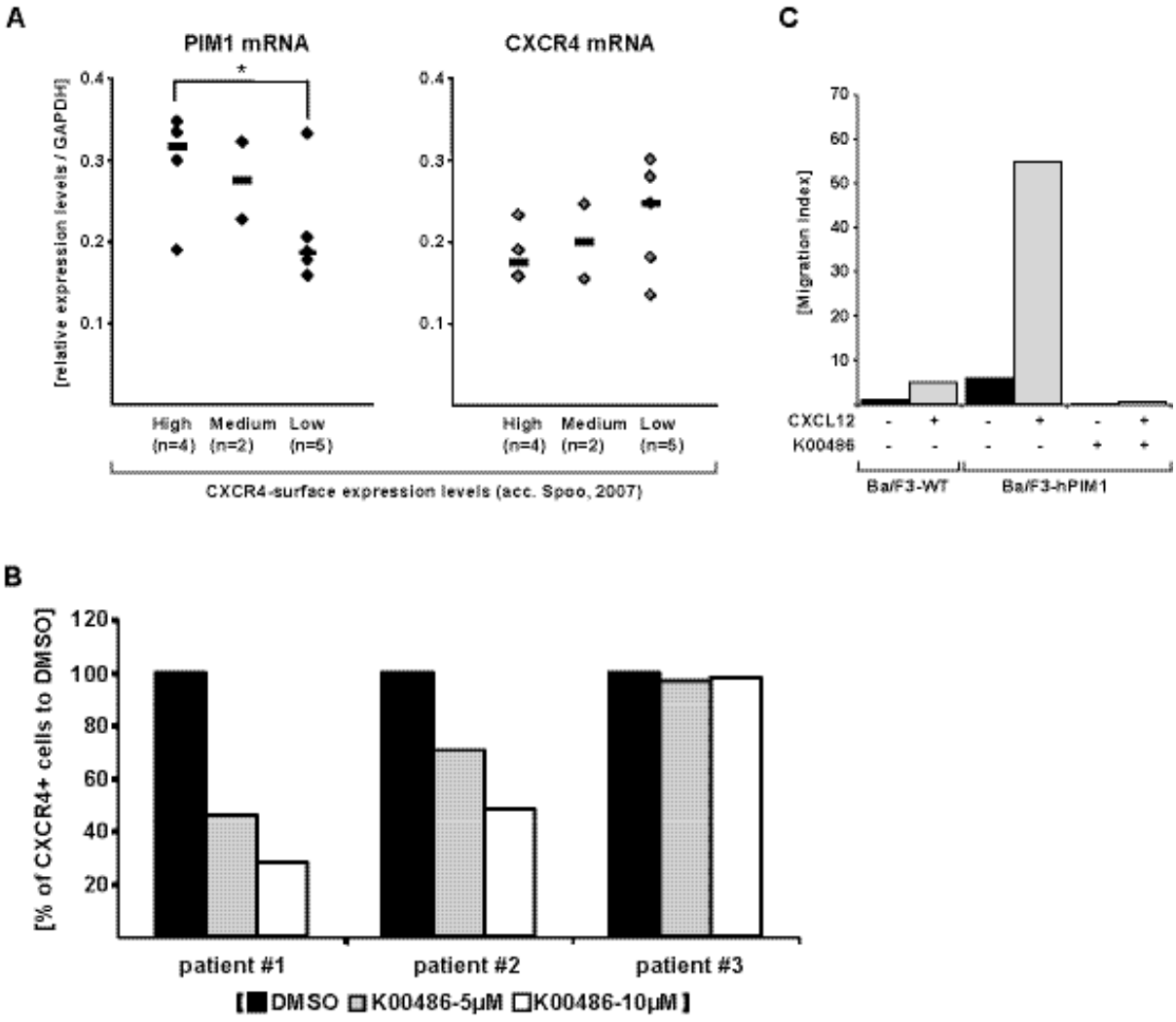

<u>Figure 12:</u> Expression and regulation of PIM1 and CXCR4 in primary acute myeloid leukemia blasts.

A. Expression of PIM1 and CXCR4 mRNA in leukemic cells from AML patients with high vs. Low surface CXCR4 expression (as described in Spoo, 2007) by Q-PCR analysis. The values are normalized to GAPDH levels and represent median values of two independent experiments performed in triplicates (one-way ANOVA: p-values ≤ 0.05).

B. Regulation of CXCR4 surface expression in primary blasts from three AML patients upon treatment with the K00486 PIM1 inhibitor (30min, DMSO, 5µM or 10µM K00486).

C. BaF/3 cells stably over-expressing human PIM1 as well as WT BaF/3 cells were allowed to migrate toward a CXCL12 gradient (10nM) in presence or absence of the K00486 inhibitor (10µM, 2h). The migration index was calculated as a percentage of input cells.

After 90min of a 10nM CXCL12 exposure, most of the surface CXCR4 was internalized, as shown previously (*Ding, 2003*). Exposition of the cells for 30min to 10nM CXCL12 followed by an extensive washing of the cells resulted in a rapid surface re-exposure of CXCR4 to about 80% of the starting level. Pre-treatment of the cells for 1h with 10µM K00486 increased the internalization of CXCR4 to more than 90% after 90min. Interestingly, surface re-expression after washing out K00486 and CXCL12 was significantly impaired, reading only 40% of the starting level (**Figure 13A**). To visualize the observed effects, CXCR4 expression was analyzed by immunofluorescent staining at the end of the experiment (t=3.5h). CXCL12 treatment resulted in the internalization of a significant fraction of CXCR4 and washing out in almost complete restoration of the CXCR4 surface level. In presence of the PIM1 inhibitor, CXCL12 also led to CXCR4 internalization; however after washing out, an important fraction of the receptor remained in the cytoplasm (**Figure 13B**). To exclude unspecific effects mediated by the PIM1 inhibitor, this experiment was also performed with cells retrovirally expressing PIM1-specific siRNA, leading to significant down-regulation of PIM1 protein expression. Again, the CXCR4 surface re-expression after CXCL12 exposure was impaired to about 50% compared to wild type cells (not shown). Taken together, these experiments strongly suggested that PIM1 can act as regulator of CXCR4 surface expression.

Figure 13: Functional inhibition of PIM1 impairs surface (re)-expression of CXCR4.

A. Delayed ligand-induced surface (re)-expression of CXCR4 in the presence of PIM1 inhibitor shown by flow-cytometric evaluation in Jurkat cells. 30min treatment with CXCL12 (10nM) before washing (indicated as W) allows induction of recycling of CXCR4 on the cell surface evaluated 1, 2 and 3 hours after washing compared to non-washed cells. Recycling is delayed when cells are pre-treated for 1h with K00486 (10µM).

B. Confocal immunofluorescence analysis of distribution of CXCR4 in Jurkat cells after 3.5 hours treatment as mentioned in **A**. The left column of the panel shows CXCR4 distribution without PIM inhibitor, the right column of the panel with PIM1 inhibitor treatment. Propidium iodide was used for nuclei staining.

A

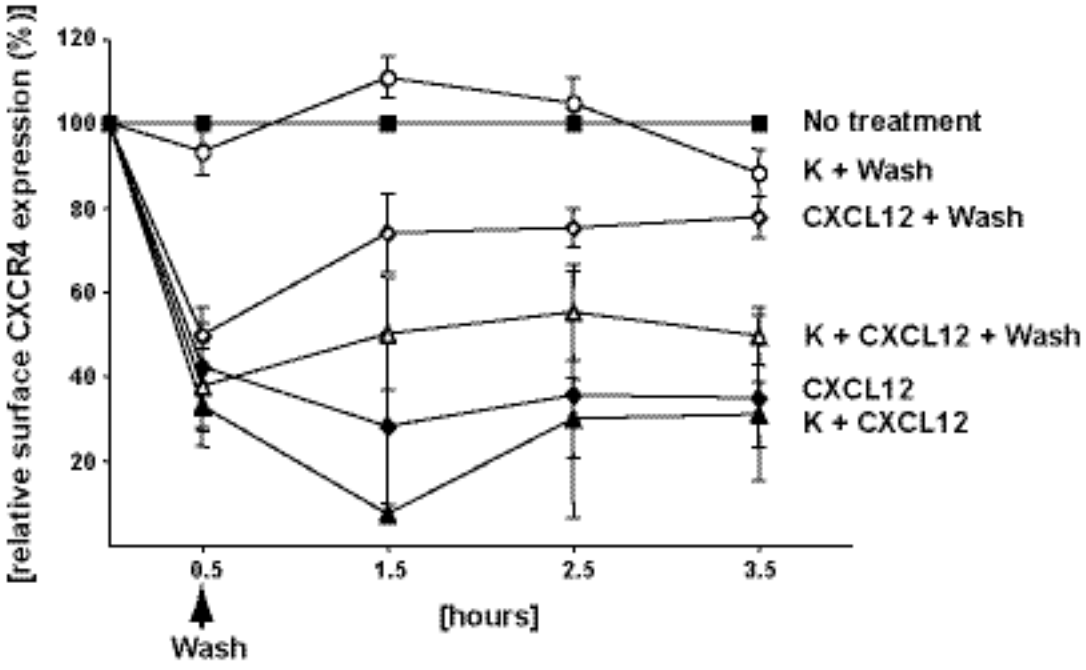
[relative surface CXCR4 expression (%)]
120
100
80
60
40
20
0.5
1.5
2.5
3.5
[hours]
Wash
No treatment
K + Wash
CXCL12 + Wash
K + CXCL12 + Wash
CXCL12
K + CXCL12

B

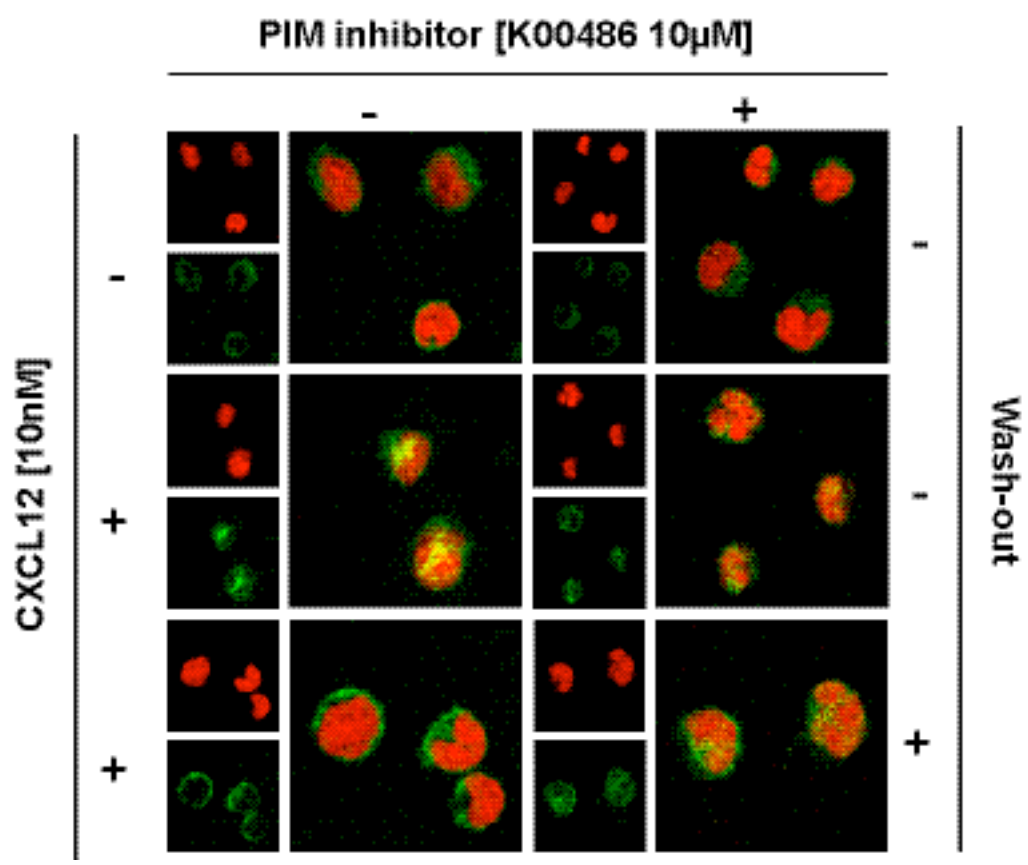
PIM inhibitor [K00486 10µM]
-
+
CXCL12 [10nM]
-
+
-
+
Wash-out
-
-
+

1.5 PIM1 directly phosphorylates CXCR4 at S339 on C-terminus

Functional regulation of CXCR4 by PIM1 activity raised the question whether PIM1 kinase could directly interact and modify the CXCR4 receptor. Immunolocalization experiments in Jurkat cells supported this possibility, showing partial overlapping signals for CXCR4 and PIM1, predominantly located in the cytoplasm of the cells (**Figure 14A**).

Previous studies have shown that CXCR4 undergoes ligand dependent and independent endocytosis and surface re-expression depending on the integrity of the intracellular C-terminal domain, rich in serine and threonine residues (*Busillo, 2007*). We identified three putative PIM1 recognition sites in this region: S325, S330 and S 339, each containing the preferred -5 or -3 arginine relative to the target serine (**Figure 14B**). To assess their potential as PIM1 phosphorylation sites, 46 C-terminal residues of CXCR4 were expressed as a GST fusion protein and treated *in vitro* with purified PIM1 protein. Only one single PIM1-dependent phosphorylation was detected by mass spectrometry (all mass spectrometry analysis were performed by Stefan Knapp and co-workers, SGC, Oxford, UK) as a shift of 80 Da in the intact protein mass. No phosphorylation was detected on GST alone.

To further define the phosphorylation site, we prepared a series of C-terminal deletion mutants and treated them with PIM1 and analyzed changes in phosphorylation by mass spectrometry. Phosphorylation was observed for short deletions including the C46Δ13 construct but was lost upon further truncations, locating the likely substrate site to the C-terminal residue S339 (**Figure 14C**). To confirm S339 as PIM1 phosphorylation site on the CXCR4 intracellular C-terminal, the phosphorylation reaction was repeated using a similar peptide harbouring a S339A mutation (**Figure 14C**). MALDI-TOF experiments revealed only phosphorylation of the wild type peptide but not of the S339A mutant. These results strongly suggested that PIM1 regulation of CXCR4 could result from direct phosphorylation of the C-terminal domain at S339. A CXCR4 phospho-specific antibody has previously allowed the demonstration that phosphorylation of S339 occurs upon stimulation by CXCl12 by phorbol ester or by EGF (*Woerner, 2005*). This antibody was used in a series of *in vitro* kinase assays to confirm that PIM1-dependent phosphorylation of CXCR4 was lost specifically in the S339A mutant but not in other mutants (S325A and S330A) corresponding to other putative PIM1 recognition sites (**Figure 14D**). To further confirm this finding, we analyzed the effect

of the PIM1 inhibitor on CXCL12-mediated phosphorylation of CXCR4 in Jurkat cells. K00486 treatment resulted in a decreased phosphorylation of S339 comforting our finding that PIM1 is a CXCR4-modyfing kinase *in vivo* (**Figure 14E**).

Taken together, in a collaborative effort with several groups, we were able to demonstrate that *in vitro* and *in vivo* transformation of hematopoietic cells is independent of PIM2, that PIM1$^{-/-}$ bone marrow cells have an early grafting defect, that PIM1 can regulate surface expression and function of the CXCR4 chemokine receptor, that PIM1 can modify the intracellular domain of CXCR4, that elevated PIM1 levels correlate with surface CXCR4 levels on human AML blasts and that blocking PIM reduces surface CXCR4 expression and migration towards a CXCL12 gradient.

Figure 14: PIM1 phosphorylates the CXCR4 C-terminus at Serine 339.

A. Confocal immunofluorescence analysis of CXCR4 and PIM1 distribution in Jurkat cells: panel D shows a partial co-localization of PIM1 and CXCR4. TOTO-3 was used for nuclei staining.

B. Deletion series defining the CXCR4 C-terminal region phosphorylated by PIM1. Schematic representation of human CXCR4 showing the C-terminal 46 amino acids expressed as a GST fusion. Three putative PIM1 recognition sites are shown in red. A series of C-terminal truncations map PIM1 phosphorylation to a peptide region including S339 (indicated by the shaded area).

C. Identification of S339 as a PIM1 phosphorylation site. MALDI TOF spectra of an 11-mer CXCR4 peptide (shaded sequence from **B**) shows PIM1 phosphorylation of the wild-type (WT) sequence but not of a mutant S339A peptide. Box shows detail of the WT phosphorylation +/- PIM1 treatment.

D. *In vitro* kinase assay performed with different CXCR4 C-terminal mutants confirms that CXCR4 is phosphorylated by PIM1 on S339. Protein is detected by anti-PIM1 or anti-phospho-CXCR4 (Ser339) antibody.

E. Determination of CXCR4-S339 phosphorylation state in Jurkat cells incubated for 2.5 hours with CXCL12 (10nM) with or without 1h pre-treatment with the PIM1 inhibitor (10µM). S339 phosphorylation is inhibited in presence of K00486

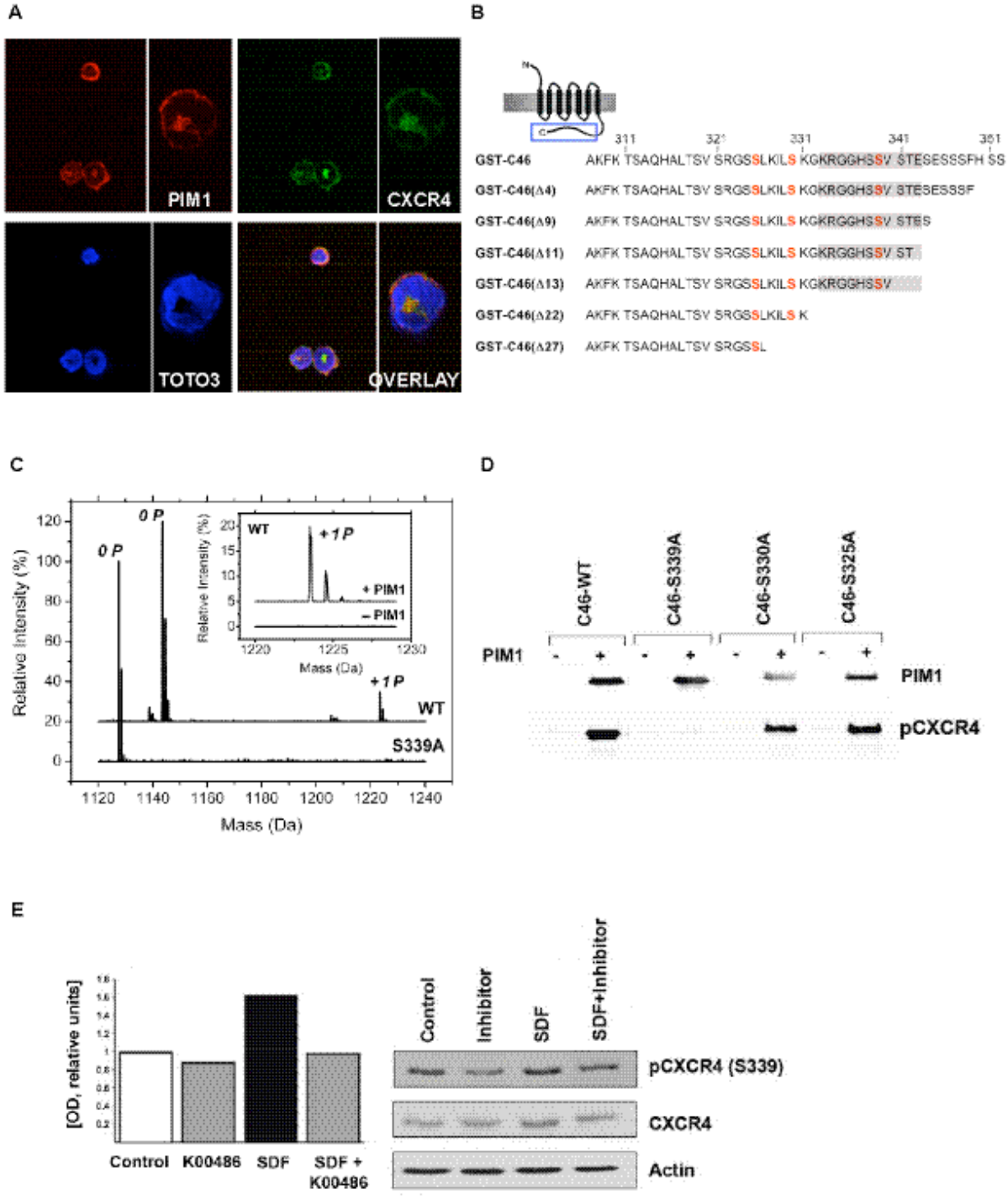
A
PIM1
CXCR4
TOTO3
OVERLAY
B
311
321
331
341
351
GST-C46 AKFK TSAQHALTSV SRGSSLKILS KGKRGGHSSV STESESSSFH SS
GST-C46(Δ4) AKFK TSAQHALTSV SRGSSLKILS KGKRGGHSSV STESESSSF
GST-C46(Δ9) AKFK TSAQHALTSV SRGSSLKILS KGKRGGHSSV STES
GST-C46(Δ11) AKFK TSAQHALTSV SRGSSLKILS KGKRGGHSSV ST
GST-C46(Δ13) AKFK TSAQHALTSV SRGSSLKILS KGKRGGHSSV
GST-C46(Δ22) AKFK TSAQHALTSV SRGSSLKILS K
GST-C46(Δ27) AKFK TSAQHALTSV SRGSSL
C
Relative Intensity (%)
0 P
+1 P
WT
S339A
Mass (Da)
+ PIM1
– PIM1
D
C46-WT
C46-S339A
C46-S330A
C46-S325A
PIM1
PIM1
pCXCR4
E
[OD, relative units]
Control
K00486
SDF
SDF + K00486
Control
Inhibitor
SDF
SDF+Inhibitor
pCXCR4 (S339)
CXCR4
Actin

2. Discussion

Several lines of evidence suggest that the family of PIM serine/threonine kinases plays an important role in the pathogenesis of hematological malignancies. PIM kinases have been reported as being deregulated by oncogenic protein tyrosine kinases (PTK), such as the FLT3-ITD mutant found in up to a third of human AMLs. Functional *in vitro* studies using various cell lines have produced partly conflicting results regarding the role of PIM1 or PIM2 (that are both expressed in the hematopoietic system) in the pathogenesis of PTK-mediated leukemogenesis (*Mizuki, 2003; Adam, 2006; Kim, 2005*). Our study addressed the role of PIM kinases in primary cells and the results showed that transformation of hematopoietic cells by FLT3-ITD *in vitro* and *in vivo* is independent of PIM2 **(Figures 5, 6 & 7A**). This finding is unexpected, as previous work demonstrated that knockdown of PIM2 by siRNA, or by expressing dominant-negative "kinase dead" mutants (PIM-KD), significantly impaired growth and survival or FLT3-ITD expressing hematopoietic cells (*Adam, 2006*). However, the previous experiments were performed in immortalized cell lines that stably express FLT3-ITD, whereas in the present work primary mouse bone marrow cells were used. The PIM kinases have been identified through serial retroviral gene tagging in *c-myc* induced lymphomas in wild type as well as in PIM knockout mice suggesting that the loss of one PIM can be compensated by deregulation of the others (*Mikkers, 2002*). However, there are reports suggesting that in some situations, the loss of a particular PIM kinase may not be compensated by the presence of other PIMs. For example, the growth of bone marrow derived mast cells from PIM1 knockout animals is significantly reduced despite induction of PIM2 by IL-3 (*Domen, 1993, Didichenko 2008*). Our present work clearly demonstrated that in primary murine bone marrow cells expressing FLT3- ITD, the lack of PIM1 cannot be compensated by the presence of PIM2. Using bone marrow reconstitution assays, we showed that FLT3-ITD induced a lethal myelo- and lymphoproliferative disorder *in vivo* in absence of PIM2. Interestingly, $PIM1^{-/-}$ cells expressing an empty retrovirus (*MigRI*) or FLT3-ITD transplanted in a sub-lethally irradiated host, were detectable but gradually declined over several weeks post-transplant (**Figure 6C**). Transplantation of an identical number of $PIM1^{-/-}$ cells into lethally irradiated hosts resulted in early death (2-4 weeks) of all recipients suggesting that cells lacking PIM1 have an inherent homing defect which was further

confirmed in a series of experiments measuring homing to the bone marrow and the spleen 4 and 20 hours after transplantation (**Figure 8**). However, expression of FLT3-ITD in bone marrow cells from PIM1$^{-/-}$ mice resulted in generally impaired growth *in vitro* (**Figures 5 & 6**) indicating that these cells do not only display a homing defect but in addition also have a growth disadvantage compared to WT or PIM2$^{-/-}$ bone marrow cells. Homing of hematopoietic stem cells (HSCs) to the bone marrow niche is a complex and still not well-understood process involving several signalling pathways. There is strong evidence that interaction of the chemokine CXCL12 expressed on stroma cells with its receptor CXCR4 expressed on HSCs plays an essential role in this process (*Lapidot, 2005; Juarez, 2004; Burger, 2006*). Proper functioning of the CXCL12/CXCR4 axis seems to be crucial for directing homing/engraftment of normal as well as leukemic HSCs into bone marrow after transplantation (*Peled, 1999; Tavor, 2004*). Our results provide strong evidence that PIM1 can functionally regulate CXCR4. Absence of PIM1 is associated with impaired CXCL12-induced Ca^{2+} flux and activation of downstream effectors (**Figure 9**). In addition, functional down-regulation by siRNAs or expression of a dominant-negative acting kinase-dead mutant, or treatment with a small molecule PIM kinase inhibitor leads to down-regulation of CXCR4 expression at the surface of hematopoietic cells (**Figures 10-13**). In addition, co-localization studies, as assessed by immunofluorescence, as well as *in vitro* kinase assays suggested that PIM1 could directly modify the intracellular C-terminal domain of CXCR4 (**Figure 14**).

Our results showed that PIM1 regulates surface expression of CXCR4. PIM1$^{-/-}$ hematopoietic cells have a subtle but measurable defect in cytokine-mediated growth and survival (*Domen, 1993*, **Figure 5**). Therefore is very likely that impaired *in vivo* homing of PIM1$^{-/-}$ marrow cells might be the result of inappropriate function of several PIM targets including CXCR4. Interestingly, PIM1$^{-/-}$ marrow cells do not completely lack CXCR4: in fact, they express less surface CXCR4 most probably as a consequence of inappropriate re-expression. As PIM1$^{-/-}$ mice are viable and have a normal lifespan, a lower amount of surface CXCR4 seems to be sufficient to regulate steady-state hematopoiesis. G protein-coupled receptors like CXCR4 are regulated by desensitization, internalization and degradation (*Busillo, 2007*). CXCR4 seems to undergo ligand-dependent but also independent internalization and surface re-exposure in hematopoietic cells. In both internalization and re-exposure of CXCR4, the serine/threonine-rich intracellular C-terminus seems to play a key role

(*Orsini, 1999; Pelchen-Matthews, 1999*). Natural mutants in patients with WHIM syndrome as well as artificial truncation and alanine scanning mutagenesis have suggested multiple regions in the CXCR4 C-tail as potential phospho-acceptor sites (*Hernandez, 2003*). However, although multiple protein kinases have been proposed (PKC, GRK3, GRK6), no specific kinase has yet been found to be clearly implicated (*Busillo, 2007*).

Here, we observed that functional interference of PIM1 led to a decrease in CXCR4 surface expression whereas the total amount of the CXCR4 protein remains unchanged (**Figure 10B**). In addition, our work demonstrated that PIM1 regulates surface re-expression whereas internalization of the receptor seems not to be affected (**Figure 13**). A similar phenotype has been previously observed in T-cells deficient in synaptotagmin 3 (SYT3), although the underlying mechanism remained unclear (*Masztalerz, 2007*). Our experiments using mass spectrometry and *in vitro* kinase assays showed that PIM1 directly phosphorylates Ser339 in the CXCR4 C-terminal domain (**Figure 14**). It is worth noting that this site is in a motif that closely resembles the consensus PIM recognition motif with -5 arginine and -2 histidine although the preferred -3 arginine is absent (*Bullock, 2005*). The CXCR4 Ser339 is known being phosphorylated in brain cancer cells upon stimulation with CXCL12, phorbol-ester (PMA) or EGF (*Woerner, 2005*). Interestingly, both CXCL12/CXCR4 and EGF/EGFR lead to activation of the JAK/STAT signalling pathway that regulates PIM1 expression (*Soriano, 2003*) while PMA treatment is also known to produce a rapid induction of PIM1 expression (*Wingett, 1996*). As some of the PIM1 target sites like the apoptosis regulator BAD (Ser112) or the cell cycle regulator p21 (WAF1) (Thr145/Ser146), are also phosphorylated by other protein kinases such as RAF1, PAK5, RSK2/5 for the former, and PKC-δ, or AKT for the latter (*Aho, 2004; Kim, 2006; Zhang, 2007*), it remains unlikely that PIM1 is the only kinase that phosphorylates CXCR4-Ser339. Interaction of CXCL12 with CXCR4 does not only provide signals for efficient migration and homing, but seems also to support survival of hematopoietic progenitor cells (*Lataillade, 2002*). There is increasing evidence that CXCR4 is a key regulator of homing and retention of leukemic stem cells within the marrow niche allowing these cells to escape spontaneous and chemotherapy-induced cell death (*Juarez, 2004; Burger, 2006*). These findings are supported by the negative prognostic impact of high CXCR4 expression levels in patients with acute myeloid leukemia (*Spoo, 2007; Rombouts, 2004*).

Consequently, targeting leukemic stem cells within the bone marrow by disruption of the CXCL12/CXCR4 interaction by small molecule inhibitors has been recently proposed (*Juarez, 2007*). The association of elevated PIM1 expression with expression of high levels of surface CXCR4 in leukemic blasts from AML patients (**Figure 12A**) suggests that targeting aberrant PIM activity by small molecules would be rather promising by its effects on interfering not only with self-renewal but also with migration and homing of leukemic cells. Indeed, structural analysis of PIM1 has allowed us to identify a group of selective small molecule inhibitors with potent anti-leukemic activity *in vitro* (see part III). Short-term treatment of leukemic blasts from 3 AML patients with the PIM inhibitor (K00486) resulted in a significant decrease of steady-state surface CXCR4 expression in two samples (**Figure 12B**). Ongoing experiments aim to understand why some AML blasts are resistant to CXCR4 regulation after treatment with the PIM inhibitors. Taken together, we have dissected the role of PIM serine/threonine kinases for FLT3-ITD leukemogenesis *in vitro* and *in vivo*. Our work demonstrated that PIM2 is dispensable for transformation by FLT3-ITD and cells lacking PIM1 are impaired for growth and survival that cannot be overridden by FLT3-ITD. Most importantly, our work demonstrated that PIM1 activity directs cellular homing and migration by regulation of surface CXCR4. Moreover, CXCR4 is also important for homing and maintenance of cancer stem cells, meaning that PIM1 inhibitors may exert their anti-tumor effects in part by interfering with interactions within the microenvironment.

3. Outlook

High levels of surface CXCR4 expression have been proposed to be an adverse prognostic factor in acute myeloid leukemia (Rombouts, 2004; Spoo, 2007). In addition, migration and homing of precursor B-cell acute lymphoblastic leukemia (pre-B ALL) cells have been shown to depend on CXCL12/CXCR4 interactions (*Spiegel, 2004*). Interestingly, in this study, pre-B ALL cells express high levels of surface CXCR4, yet only low levels of intracellular CXCR4 could be found. In contrast, in normal cord blood cells or $CD34^+$ bone marrow cells, most of the CXCR4 molecules were localized within the cells and only a small fraction was constitutively expressed at the surface. In collaboration with Andrea Biondi (Monza), we have previously analyzed the expression of PIM kinases in childhood acute leukemia and found significant elevated PIM1 levels in over 50% of a panel of more than fifty patients (unpublished). These observations raise the possibility that PIM1 expression might be generally linked to elevated surface CXCR4 expression. In order to analyze this possibility, we will compare PIM levels with surface and intracellular CXCR4 levels in a larger cohort of human acute leukemia samples by flow cytometry and Western blotting in a prospective manner.

The CXCL12/CXCR4 signalling axis is not only important for homing and migration of hematopoietic stem cells but is a key pathway involved in progression and metastasis of several human cancers. Deregulated expression of PIM1 was also observed upon progression of a similar spectrum of malignancies including carcinomas from prostate, breast or the head and neck region. In order to further analyze the link between PIM kinases and the CXCL12/CXCR4 signalling axis, we will examine the regulation of surface CXCR4 in prostate cancer in which up-regulation of PIM1 upon progression has been validated in several studies (*Dhanasekaran, 2001*). We will use four human prostate cancer cell lines (PC3, DU145, LNCaP, BHP1, kindly provided by Lukas Bubendorf, Institute for Pathology, University Hospital Basel). Previous studies have shown that PC3, LNCaP and DU145 express high levels of CXCR4 (*Mochizuki, 2004*). Interestingly, in preliminary experiments, we have observed dose-dependent cytotoxic effects after treatment with a PIM1 inhibitor (see below) in PC3, LNCaP and DU145 (derived from advanced cancer lesions) but not in BPH1 cells derived from hyperplasia. We will first determine steady-state PIM and CXCR4 expression levels by Q-PCR and

Western blotting, as well as surface and intracellular CXCR4 expression by flow cytometry. Second, CXCR4 levels as well as migration towards a CXCL12 gradient will be determined upon blocking PIM function by specific siRNAs, expression of PIM-KD mutants or short-term treatment with a PIM inhibitor. These data will provide evidence that regulation of migration through modification of the CXCL12/CXCR4 signalling axis is not limited to leukemic cells but also occurs in solid cancer cells expressing PIMs.

III. Targeting PIM kinases with small molecule inhibitors: a new avenue for anti-leukemic therapy?

1. Results

Several groups have solved the x-ray crystal structure of PIM1 in complex with nucleotid analogs and a number of small molecule ATP-competitive inhibitors (*Kumar, 2005; Jacobs, 2005; Qian, 2005*). Their studies revealed a constitutively active kinase conformation of PIM1 in the absence of phosphorylated residues in the activation loop. Interestingly, PIM kinases have an atypical hinge region characterized by an insertion of one additional residue and the presence of a proline that allows formation of only one hydrogen bond with ATP or ATP-mimetic inhibitors (*Bullock, 2005a; Bullock, 2005b*). Probably due to this unique structural feature, all potent PIM inhibitors published to date interact with the kinase in an ATP competitive but not ATP mimetic binding mode. In close collaboration with two structural biology labs (Prof. Stefan Knapp, SGC, Oxford and Prof. Nathanael Gray, DFCI, Boston), we have tested several molecular scaffolds that interacted and inhibited PIM kinases in cell-free experimental assays (**Figure 15**). In order to screen for cellular activity of a new compound, we used stably transduced murine IL-3 dependent Ba/F3 lympho-myeloid cells with retrovirus expressing human PIM1, PIM2 or PIM1 and PIM2. As PIM over-expression renders these cells growth-factor independent we expected that blocking of human PIMs by any inhibitor would impair growth and survival of these cells. In case we observed a cellular effect of compound X in these cells, we applied these compounds to human leukemia cell lines over-expressing endogenous PIMs (e.g. MV4;11, AML with FLT3-ITD and MLL/AF4; or K562, BCR/ABL+, CML in blast crisis). We have collected a panel of 15 different human leukemia cell lines (K562, MV4;11, RS4;11, MOLM13, PL21, SEM, KOPN8, KCL22, KOCL33, KOCL44, KOCL45, JURKAT, THP1, HL60, AML1-USD) that can be tested. In case significant cytostatic and/or cytotoxic effects were observed, selected compounds were tested for their effects on primary human leukemic blasts. One has to note that freshly isolated (or reconstituted frozen) samples of human acute leukemia cells can generally only be grown *in vitro* for a limited period of time in liquid as well as in

semi-solid medium (methylcellulose) cultures. In order to obtain any insights about general toxicity, we also applied given compounds to human umbilical cord blood mononuclear cells or CD34+ cells isolated from healthy donors (kindly provided by Prof. Andrea Biondi, Monza, Italy).

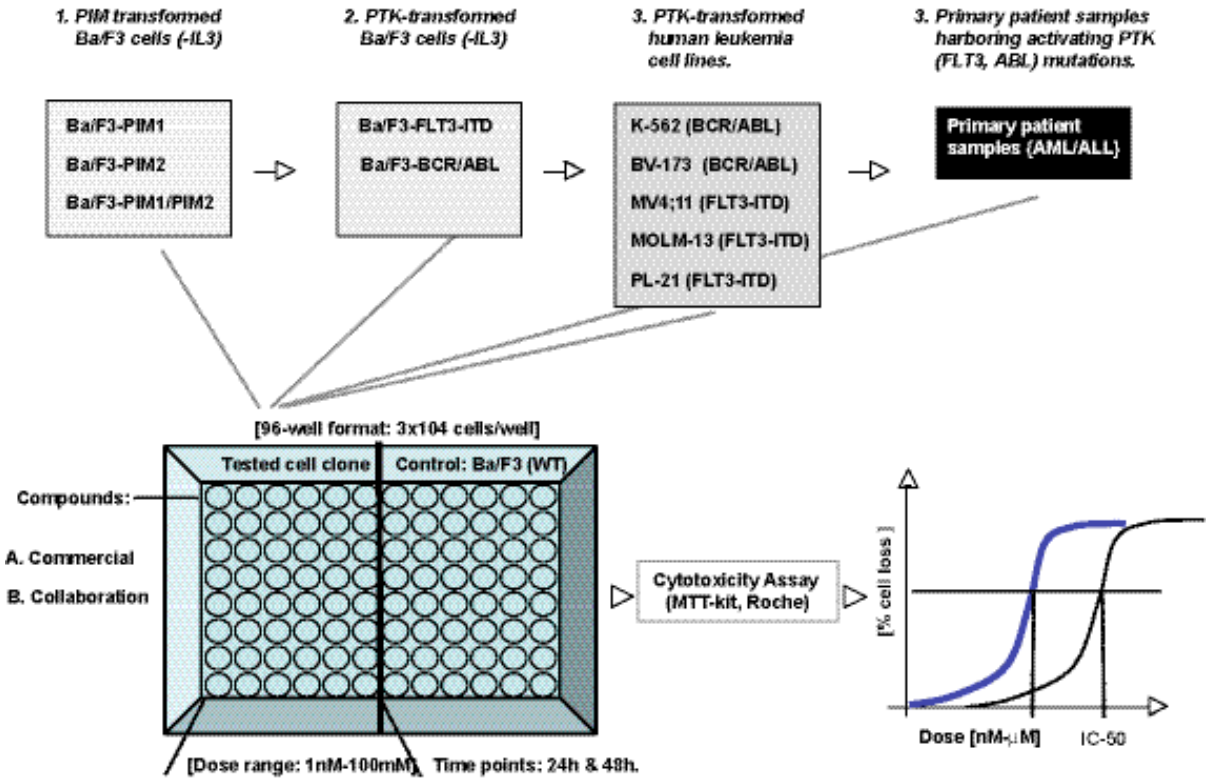

Figure 15: Validation of novel PIM1 inhibitors in cellular leukemia models *in vitro*.
Work-flow for testing cellular efficacy on putative small molecule PIM kinase inhibitors in PIM-transformed BaF/3 cells, human leukemia cell lines and primary patient samples. Cytotoxic effects on leukemic cells are determined by MTT-analysis.

1.1 Imidazo[1,2-*b*]pyridazines

In 2004, a structure activity relationship (SAR) analysis and optimizations of imidazo[1,2-*a*]pyridines as potential cyclin-dependent kinases (CDK) inhibitors were described (*Byth, 2004*). Such inhibitors were expected to be useful as anti-tumor agents due to the key role that the CDK enzymes play in controlling the cell cycle.

These compounds were further modified to reduce the lipophilicity of the core structure: additional heteroatoms were added into the pyridine ring of the imidazo[1,2-*a*]pyridine and this lead to the identification of imidazo[1,2-*b*]pyridazines (*Byth, 2004*). Using a structural approach, Prof. Stefan Knapp and co-workers reported imidazo[1,2-*b*]pyridazine to potentially inhibit PIM kinases and showed that these compound were around 100-fold more selective for PIM1 over PIM2 (in cell free assays), independent of the high sequence homology and conservation of the active site. Several imidazo[1,2-*b*]pyridazines were included in a small kinase-targeted compound collection obtained from BioFocus (Cambridge, U.K.) biased toward simple scaffolds that are prospective low affinity compounds for lead development (*Bullock, 2005*).

To understand the structural basis for substrate selectivity by PIM kinases, Prof. Stefan Knapp and co-workers resolved the x-ray crystal structure of PIM1 in complex with a consensus substrate peptide and the inhibitor K00135 at 1.9Å resolution, revealing the kinase with typical bi-lobal architecture and catalytic domains positioned in a constitutively closed conformation. The overall structure of the protein was found to be similar to structures that have previously been described (*Kumar, 2005; Bullock, 2005*) (**Figure 16**, kindly provided by S. Knapp). The serine/threonine PIM1 kinase has been shown to have a strong preference for substrates with basic residues, particularly arginine, at positions -5 and -3 and a small side chain at +1. Peptide library screening could define additional selectivity for histidine at position -2, proline at -1 and glycine at +1, facilitating the design of a high-affinity consensus peptide, pimtide (ARKRRRHPS*GPPTA). As in the case of the PIM1-BIM1 peptide complex, the substrate peptide was well defined between residues Lys^{6} and Gly^{1}, whereas the termini were not visible in the electron density and assumed to be disordered. Novel kinase inhibitor scaffolds as PIM1 inhibitors were established. (*Bullock, 2005a; Bullock, 2005b*).

Although the imidazo[1,2-*b*]pyridazine inhibitors, such as K00135, bind to the ATP-binding site of PIM1, they do not mimic binding of ATP by forming hydrogen bonds with the kinase hinge region (shown in pink in **Figure 16B**) but rather bind to the opposite side of the pocket, participating in a hydrogen bond network formed by the conserved active site Lys^{67}, a structural water molecule, the αC residue of Glu^{89} and the activation loop residue Phe^{187} (**Figure 16**). In addition, a number of hydrophobic contacts, particularly with PIM1 residues Leu^{44}, Phe^{49}, Ile^{104}, and

Leu^{120}, stabilize this interaction. The unusual hinge architecture of PIM1, which has a proline at the hinge position 123 allows the formation of only one hydrogen bond to ATP or ATP-mimetic inhibitors. Stefan Knapp and co-workers suggested that this active site architecture, together with the unexpected binding mode of the studied imidazo[1,2-*b*]pyridazine, could result in surprisingly specific PIM inhibitors. Initial screening of a panel of more than 50 diverse serine/threonine kinase catalytic domains showed that this scaffold only interacts with another kinase (Cdc-like kinase 1). A small library of inhibitors based on the imidazo[1,2-*b*]pyridazine scaffold targeting PIM1 kinase was generated and temperature-shift assays were used to identify ligands interacting with PIM kinases. This assay monitors the linear affinity-dependent stability increase of proteins and has been shown to correlate well with binding constants and IC_{50} values (*Bullock, 2005*). In the study done here, we also observed an excellent correlation of temperature shift data (T_m) with *in vitro* kinase assay IC_{50} values and identified three inhibitors with high potency: K00135, K0486 and K00152 (**Figure 16D**). The structure-activity relationship of the library was established with two varying positions, R1 and R2. Their crystal structures suggest that a large trifluoro-methoxy moiety might favourably interact with the side chain of Arg^{122}.

K00135 impairs growth and survival of Ba/F3 cells stably expressing human PIMs and human leukemia cell lines. As outlined above, stable over-expression of human PIMs renders murine BaF/3 cells growth factor independent. PIM kinases have a short cellular half-life, reflected by high levels of human PIM mRNA detected (not shown) but only moderate levels of steady-state human PIM proteins could be seen. Treatment of the cells with the proteosomal inhibitor MG-132 lead to a substantial increase in PIM protein levels **(Figure 17A)**. To address the cellular effects of imidazo[1,2-*b*]pyridazines, we treated BaF/3 cells over-expressing human PIMs with different concentrations of the inhibitor, ranging from nanomolar to low micromolar levels. Cell survival was determined 24h after treatment by trypan blue exclusion. As shown in **Figure 17B,** for the K00135 compound, a dose dependent decrease in viability was observed after 24h in BaF/3-hPIM1 cells growing in absence of IL3 whereas BaF/3-hPIM2 cells were less sensitive as expected from the higher IC_{50} values for PIM2 determined for this compound (not shown).

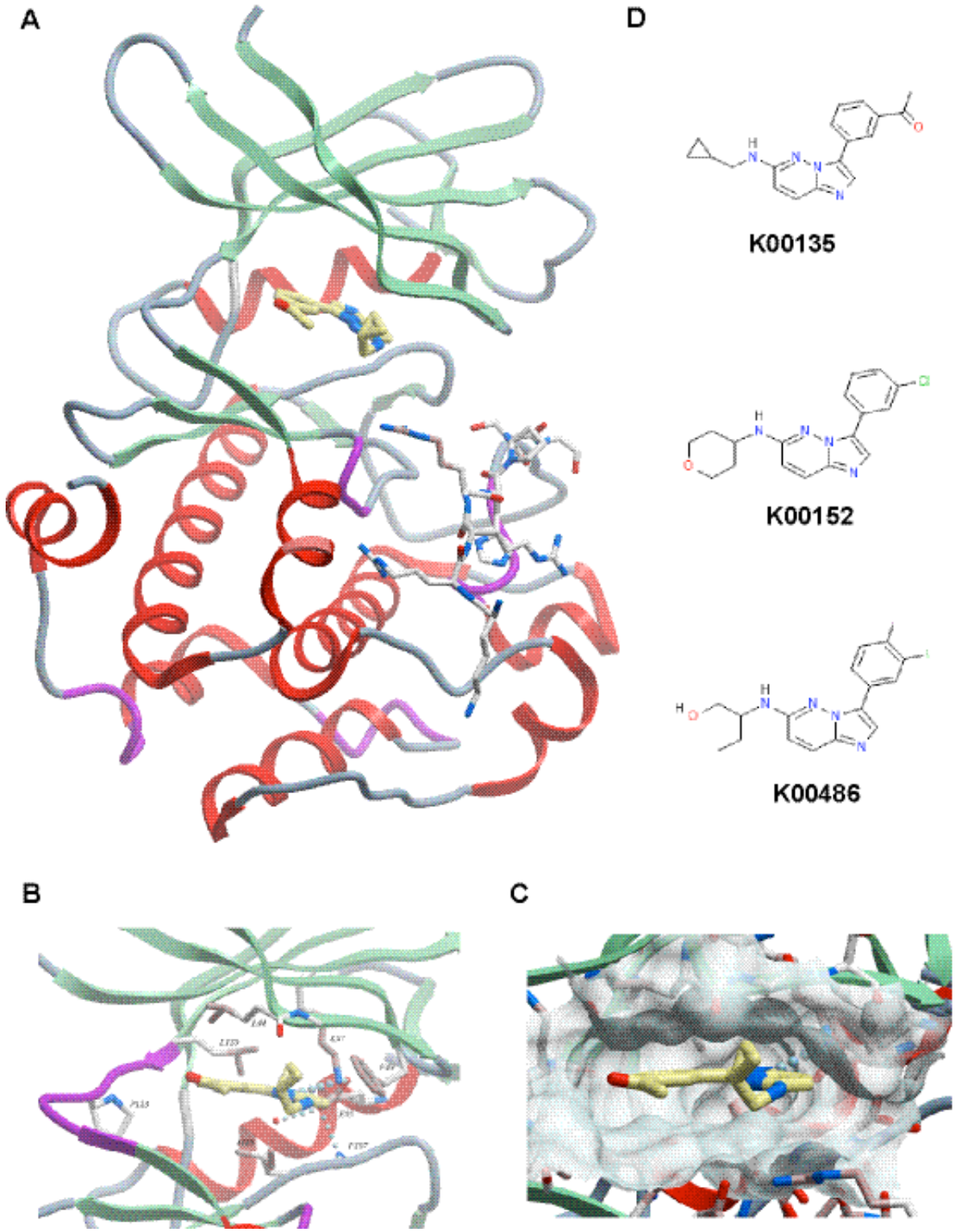

Figure 16: Structure of PIM1 in complex with the imidazopyridazine K00135 inhibitor.

A. Structural overview. The inhibitor and the substrate peptide are shown in ball-and-stick representation. (**A**-**C**, kindly provided by S. Knapp, SGC, Oxford, UK)

B. View from the hinge region, highlighted in magenta. (Dotted lines= hydrogen bonds).

C. Surface representation showing shape complementarity with the active site.

D. Structure of K00135, K00152 and K00486.

Despite better potency in *in-vitro* kinase assays, effects on cell survival using K00486 and K00152 were similar. Seven other imidazo[1,2-*b*]pyridazines showed no cellular effects most probably due to a high polarity limiting cellular penetration and/or limited solubility (not shown). Importantly, no significant decrease in viability was observed in wildtype BaF/3 cells growing in IL3 in the presence of all three effective inhibitors tested. In addition, these compounds did not seem to significantly interfere with molecules of murine origin that are critical for IL3-mediated cell growth.

Cytotoxic effects of K00135, as well as effects on clonogenic growth were tested in a panel of human leukemia cells lines: MV4;11, RS4;11, MOLM13, KOCL45, SEM, KOP8N and K562. Cytotoxic effects of K00135 were observed in all cell lines tested **(Figure 18).** We also assessed the effect of K00135 on clonogenic growth of leukemia cells. Among the tested cell lines, only MV4;11, MOLM13 and K562 were able to form distinct colonies (as defined to be composed of >50 cells) when plated in methylcellulose. A significant reduction of clonogenic growth was observed in MV4;11 and MOLM13 even at inhibitor concentrations lower than 1μM whereas colony formation of K562 was no affected even at higher doses as expected from the relative resistance of this cell line to this class of inhibitors **(Figure 19, top)**. To determine the mechanism of K00135-mediated cell death, the induction of apoptosis was measured by flow cytometry on MV4;11 cells treated with 1μM K00135 using PO-PRO-1, which is a sensitive indicator of apoptotic cells, and 7-AAD, recognizing dead cells. The percentage of apoptotic MV4;11 cells increased in a time-dependent manner, with 2.8% of cells undergoing apoptosis and 15.3% dead after 12h and 8.5% apoptotic and 40.5% dead cells after 36h of treatment **(Figure 19, bottom)**.

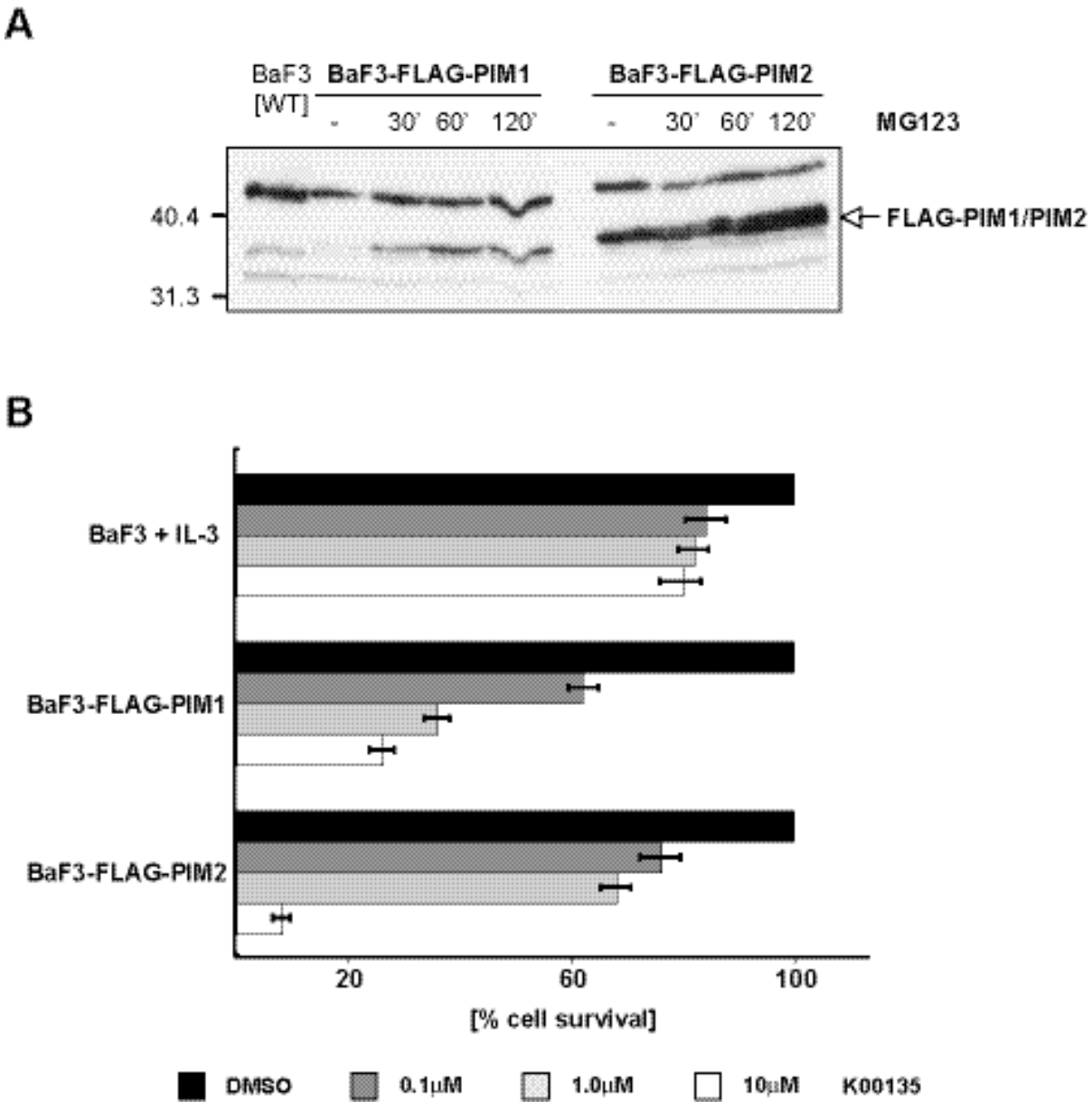

<u>Figure 17:</u> Effect of K00135 on BaF/3 cells stabely expressing human PIMs.

Increasing amounts of K00135 were added to MV4;11 and RS4;11 and other cell lines and cell viability, as well as IC_{50} values were determined 24h and 48h later (IC_{50} values were determined using the Cell Proliferation Reagent WST-1 from Roche).

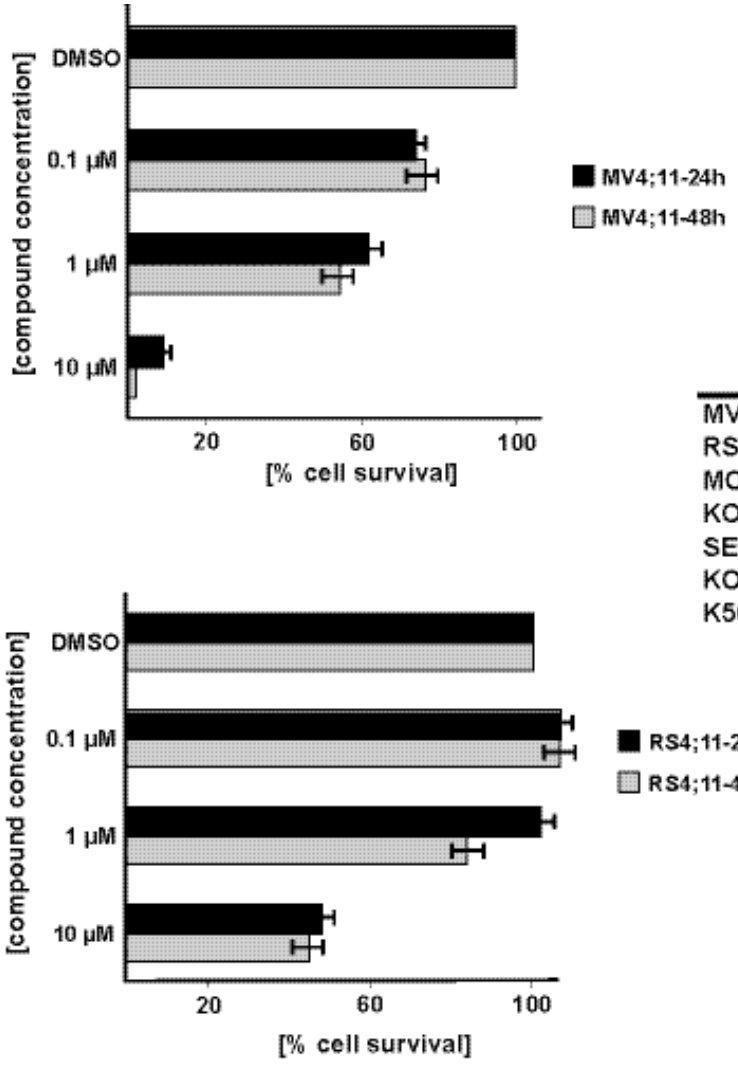

	IC-50 in µM (48h)
MV4;11	0.4
RS4;11	8.8
MOLM13	0.3
KOCL45	8.2
SEM	6
KOPN8	6.1
K562	8

<u>Figure 18:</u> Effect of K00135 on human leukemia cell lines.

Increasing amounts of K00135 were added to MV4;11 and RS4;11 and other cell lines and cell viability, as well as IC_{50} values were determined 24h and 48h later (IC_{50} values were determined using the Cell Proliferation Reagent WST-1 from Roche).

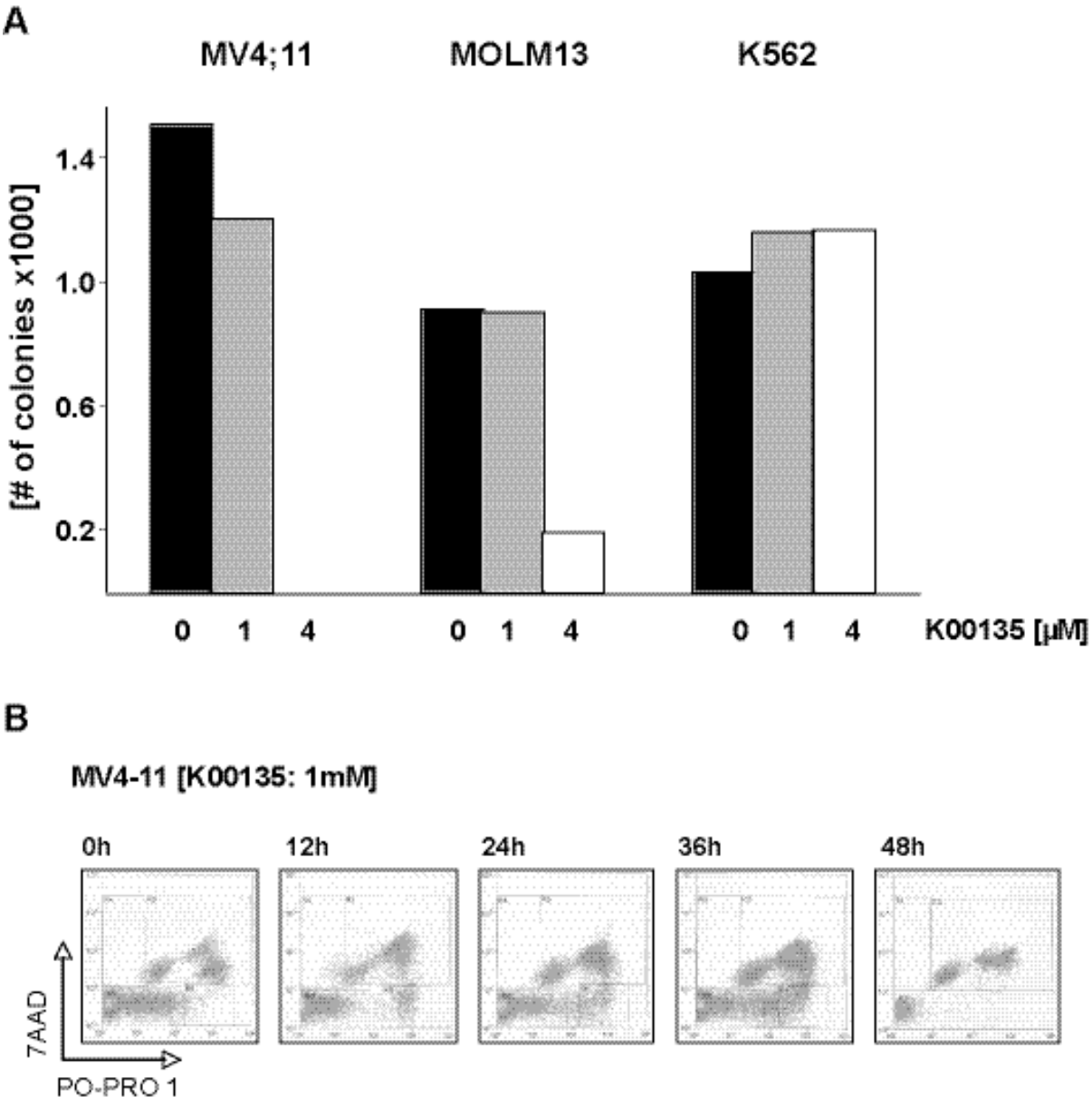

Figure 19: Effect of K00135 on leukemic cells.

A. Effect of K00135 on clonogenic growth of leukemia cell lines in methylcellulose.

B: MV4;11 cells were grown in the presence of 1µM K00135 for indicated amount of time. Apoptosis was analyzed with 7-AAD (indicator of dead cells) and PO-PRO-1 (sensitive indicator of apoptotic cells) followed by flow cytometric analysis. Representative quadrants from analysis are shown.

In vitro effect of K00135 on primary human leukemic blasts. When leukemic blasts from five patients with newly diagnosed AML (kindly provided by Dr. Sandrine Meyer, Department of Hematology, University Hospital Basel) were cultured in methylcellulose, formation of typical small leukemic cell clusters (<50 cells) was observed (**Figure 20B**). These could not be analyzed by classic quantitative colony forming assays. However, exposure of leukemic blasts to K00135 in a short-term culture resulted in a significant decrease in survival for all patient samples. Although K00135 showed an effect on colony formation of all primary cells analyzed, no significant difference in survival was observed between the patients harbouring FLT3-ITD mutation (patients 1 and 2) and those without (patients 3-5) (**Figure 20A**). Cytotoxic effects of K00135 were also tested on normal human cord blood cells at anti-leukemic doses. In this experiment, only a minor effect on the survival of normal umbilical mononuclear cells was noticed (**Figure 20C**).

Effect of K00486 on prostate cancer cells. Several previous reports showed elevated expression of PIM1 in biopsies of prostate tumours related to the grade and neoplastic transformation of the prostate carcinomas (*Xu, 2005; Dhanasekaran, 2001; Chen, 2005*). In order to test cellular effects of imidazo[1,2-*b*]pyridazines on prostate cells, we applied these compounds to four different human prostate carcinoma cell lines (PC3, LNCAP, DU145 and BPH1). In contrast to Ba/F3 cells, these cells grow as single adherent layers in Petri dishes. We treated the cells with different concentrations of K00486 for 48h. A dose-dependent decrease in viability was observed in all cell lines. Interestingly, BPH1 cells originating from a prostate hyperplasia were less sensitive to K00486 than LNCaP or PC3 cells, originally isolated from bone marrow metastasis of a high-grade adeno-carcinoma (**Figure 21**). It is of interest to note that optimized cellular effects could only be obtained when the cells were plated at low to mediated density (22'500 cells/cm^2). These results showed that imidazo[1,2-*b*]pyridazine inhibitors have *in vitro* cytotoxic activity not only in leukemia but also in prostate cancer.

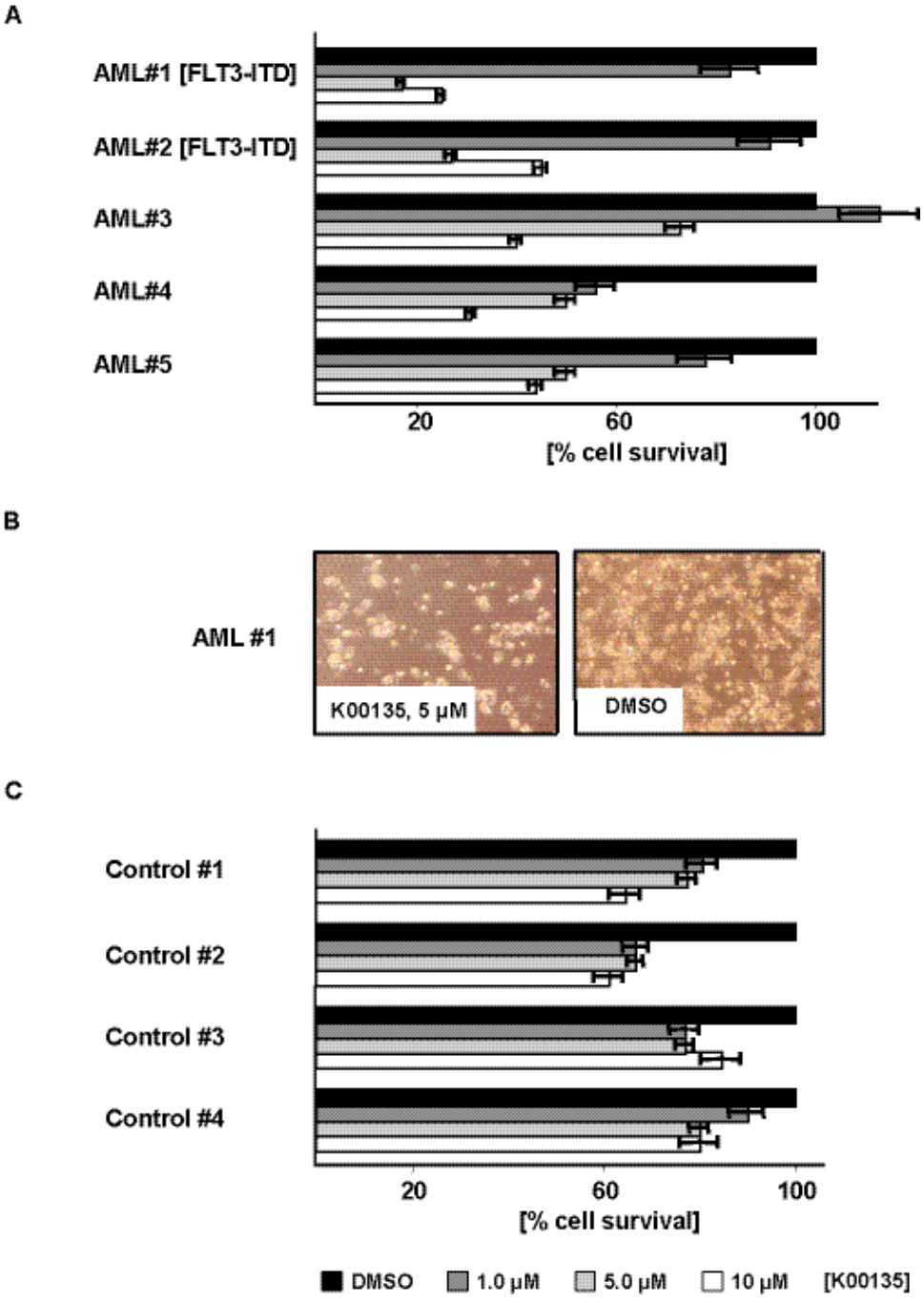

Figure 20: K00135 impairs in vitro survival of primary leukemic blasts.

A. Leukemic blasts from five patients were grown in liquid cultures with or without increasing amounts of K00135 and cell viability was determined 24h later (expressed as a percentage and normalized to the viability of cells treated with 0.1% DMSO only).

B. When cultured in methylcellulose in the presence of K00135, significantly lower density of characteristic small leukemic clusters were observed, compared to control cultures.

C. Cytotoxic effects of K00135 were analyzed in liquid cultures of umbilical vein-derived mononuclear cells from four healthy donors and cell viability was determined as a percentage compared with the viability of cells treated with 0.1% DMSO only.

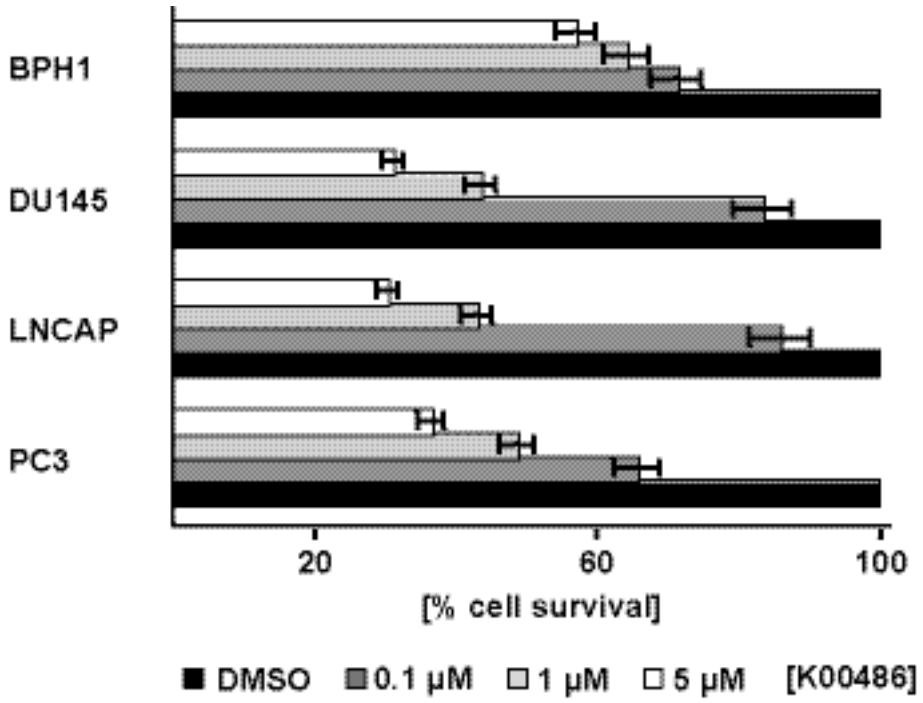

Figure 21: Effect of K00486 on prostate cancer cell lines.
Increasing amounts of K00486 were added to four prostate cancer cell lines 24h after plating and the viability was determined as percentage compared to the viability of cells treated with DMSO only (trypan blue exclusion).

Effect of imidazo[1,2-b]pyridazine inhibitors (K00135) on phosphorylation of PIM1 substrates. To show that PIM1 kinase activity is indeed affected by K00135 in leukemic cells, we monitored the phosphorylation status of its downstream targets by immunoblotting using phospho-specific antibodies. The anti-apoptotic protein BAD has been shown to be serine phosphorylated by both PIM1 and PIM2 (Kim, 2006; Macdonald, 2006). To show inhibition of PIM1 activity in MV4;11 cells, PIM protein was immunoprecipitated and analyzed for its ability to phosphorylate BAD on Ser^{112} and Ser^{136} *in vitro* in the presence (1h) or absence of 2µM K00135. As shown in **Figure 22B**, phosphorylation of BAD by PIM1 and PIM2 was abrogated in the presence of K00135. To further analyze the effects of K00135 on PIM function, phosphorylation of two known direct PIM targets (BAD and 4E-BP1) was followed by immunoblotting. Short-term exposure of the cells to 1µM K00135 led to a significant decrease of BAD and 4E-BP1 phosphorylation **(Figure 22C)**. In contrast, no changes were observed in phosphorylation of AKT (not shown). These results

suggested that K00135 indeed blocks PIM kinases in MV4;11 cells, however off-target effects on currently unknown proteins cannot be excluded.

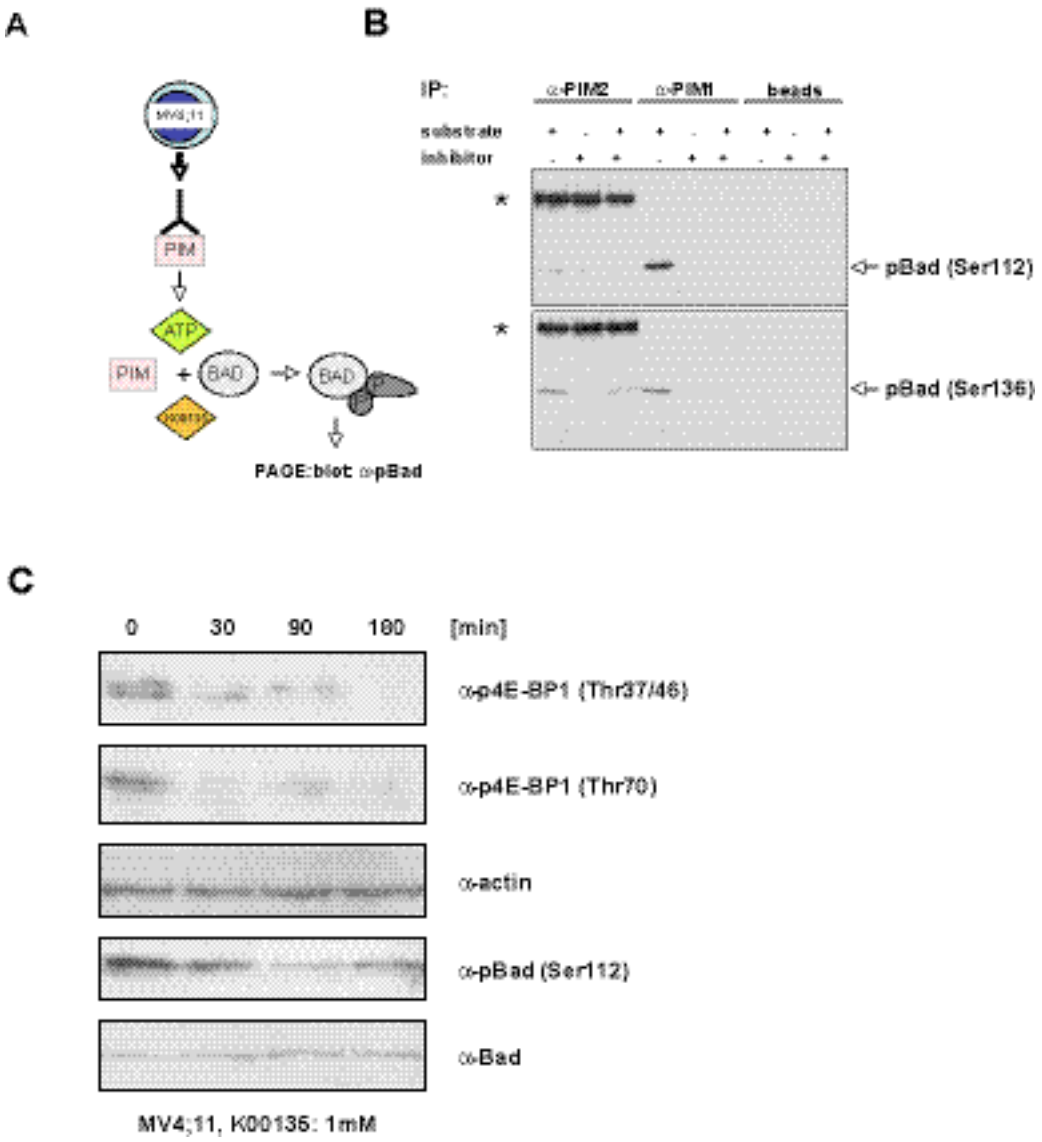

Figure 22: K00135 impairs phosphorylation of known downstream PIM targets.

A. Schematic representation of the *in vitro* kinase assay.

B. PIM proteins were immuno-precipitated from MV4;11 cells and the agarose-protein A-immuno-precipitate complex was tested for its ability to phosphorylate BAD *in vitro* in the presence or absence of K00135. (*Asterisks* = heavy chain of the anti-PIM2 rabbit antibody recognized by the anti-rabbit IgG secondary antibody)

C. MV4;11 cells were incubated with 1 µM K00135 for indicated times, harvested and protein extracts separated by SDS-PAGE. The effect of K00135 on PIM endogenous targets was followed by Western Blotting with indicated phospho.specific antibodies

1.2 Beta-carbolines

β-Carboline alkaloids are a large group of natural and synthetic indole alkaloids with different degrees of aromaticity, some of which are widely distributed in nature, and found in various plants, foodstuffs, marine creatures, insects, mammalians as well as human tissues and body fluids. These compounds are of great interest due to their diverse biological activities. Particularly, some of these compounds have been shown to intercalate into DNA, to inhibit CDK, Topoisomerase, and monoamine oxidase, and to interact with benzodiazepine receptors and 5-hydroxy serotonin receptors. Furthermore, some of these chemicals also demonstrated a broad spectrum of pharmacological properties including sedative, anxiolytic, hypnotic, anti-convulsant, anti-tumor, anti-viral, anti-parasitic as well as anti-microbial activities (Cao, 2007).

By using temperature-shift screening, where ligand binding is simply detected as a relative increase in the protein's melting temperature, and cell-free *in vitro* kinase assays, Prof. Stefan Knapp and co-workers identified several β-carboline derivates (named as AMTC, Carb2, Carb10 and Carb13) as powerful small molecule PIM kinase inhibitors in cell free assays **(Figure 23,** kindly provided by S. Knapp**)**. We tested some of these compounds for their activity in our leukemia cell models.

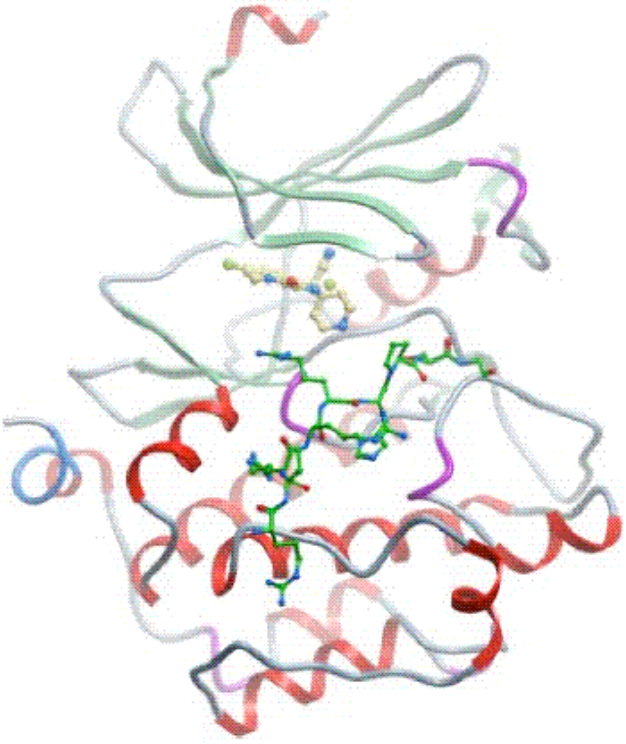

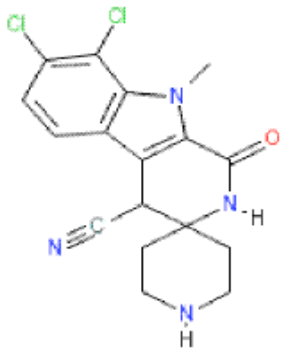

Carb13

Figure 23: Structure of PIM1 in complex with the beta-carboline Carb13 inhibitor.

Structural overview: the main secondary structure elements and the NH_2 and COOH termini of the protein are labelled. The inhibitor and the substrate peptide are shown in ball-and-stick representation (provided by S. Knapp, SGC, Oxford, UK).

In vitro cellular effect of Carb13 on Ba/F3-PIM cells, human leukemic cell lines and primary AML blasts. To investigate the potential cellular anti-leukemic activity of the carboline PIM inhibitors, the most promising compound Carb13 was tested for effects on growth and survival of the murine Ba/F3 cells transformed to IL-3 independency by over-expression of human PIMs. Exposure of the cells to different concentrations of Carb13 resulted in a dose-dependent reduction of cell survival after 48h of treatment (**Figure 24A**). Carb13 was more effective in Ba/F3-PIM1 than in Ba/F3 over-expressing human PIM2. However, in contrast to the K00135 imidazo[1,2-b]pyridazine (**Figure 17**), strong affection of parental Ba/F3 cells growing in presence of IL-3 was also observed. The reason for this strong activity in parental Ba/F3 cells is currently unclear, but could indicate some unspecific toxicity of this compound.

Cytotoxic effects of Carb13, as well as effects on clonogenic growth were furthermore tested in several human leukemia cells lines (MV4;11, RS4;11, MOLM13, SEM, K562). Treatment of the cells with different concentrations of Carb13 impaired growth of all cell lines in liquid culture with calculated IC_{50} values ranking from 2.07µM (MV4;11) to 6.49µM (K562) (**Figure 24B**). In analogy to K00135, cell lines harbouring the oncogenic FLT3-ITD mutation, like MV4;11 or MOLM13, were more sensitive than K562 cells that originate from BCR/ABL-positive blast crisis patient.

The effect of Carb13 on the growth of leukemic blasts from patients with newly diagnosed AML was also analyzed. When cultured in methylcellulose, cells from AML patients grew in small clusters (**Figure 24D**). Forty-eight hours after addition of Carb13, a strong reduction in cell survival was observed. Exposure of leukemic blasts to Carb13 in liquid culture also resulted in a significant decrease in survival: treatment with 5µM Carb13 resulted in a 50% reduction of surviving cells when compared to the control (DMSO). However, exposure of mononuclear cord

blood cells from two healthy donors to Carb13 at anti-leukemic doses affected cellular survival in a similar manner than for the AML cells (**Figure 24C**). These observations demonstrated that although Carb13 has significant anti-leukemic activity, this compound exerts strong cytotoxic effects also on normal hematopoietic cells.

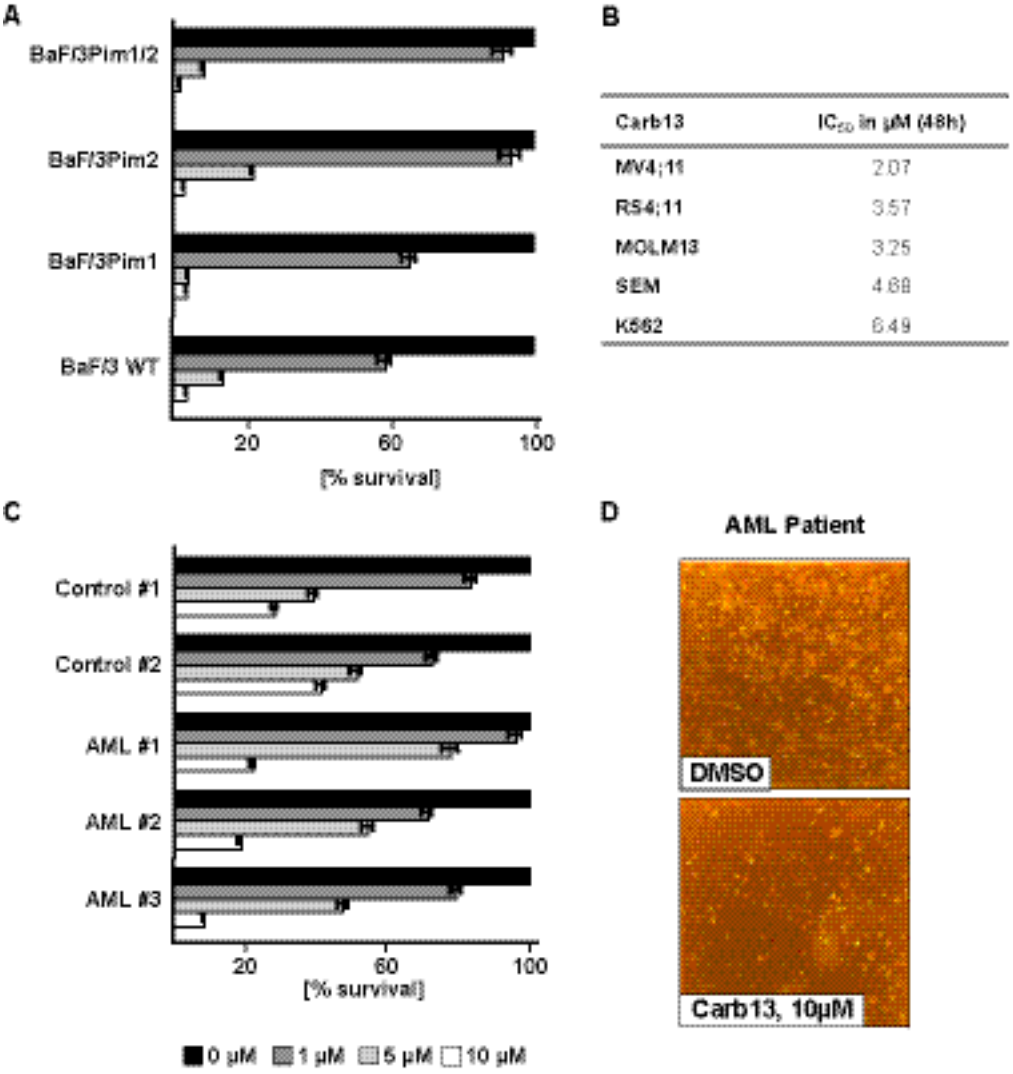

Figure 24: Evaluation of the biological activity of Carb13.

A. Ba/F3 wild-type (WT) cells and stably expressing hPIM1 and/or hPIM2 cells were exposed to increasing amounts of Carb13 and cell viability was determined 48h later (expressed as a percentage normalized to viability of cells treated with 0.1% DMSO only).

B. Carb13 IC_{50}'s were determined in different human cell lines after 48 hour-treatments.

C. Leukemic blasts from three patients and umbilical vein–derived mononuclear cells from two healthy donors were grown in liquid cultures without or with increasing amounts of the drug, and cell viability was determined 48 h later.

D. Example of leukemic blasts cultured in methylcellulose in the presence of Carb13, significantly lower density of characteristic small leukemic clusters was observed as compared with control cultures.

Effect of Carb13 on the phosphorylation of PIM1 downstream targets. In order to obtain some insights in Carb13 action on PIM kinase activity *in vivo*, we analyzed the phosphorylation status of the known PIM substrates such as BAD and 4E-BP1 by immunoblotting using phospho-specific antibodies **(Figure 25)**. As PIM1 has recently been proposed to be regulated by AKT kinase, we also included this kinase in the analysis (*Muraski, 2007*). MV4;11 cells were incubated for 30, 90 and 180 minutes with different concentrations of Carb13. During this short time period, no adverse cellular effects were observed. Whole cell lysates were prepared and separated by gel electrophoresis. Treatment of MV4;11 with Carb13 was associated with decreased phosphorylation of BAD as well as 4E-BP1 suggesting that cellular PIM1 was indeed blocked by this compound (**Figure 25)**. Rather unexpected, it was also observed that Carb13 treatment reduced phosphorylation of AKT that has never been characterized as PIM substrate.

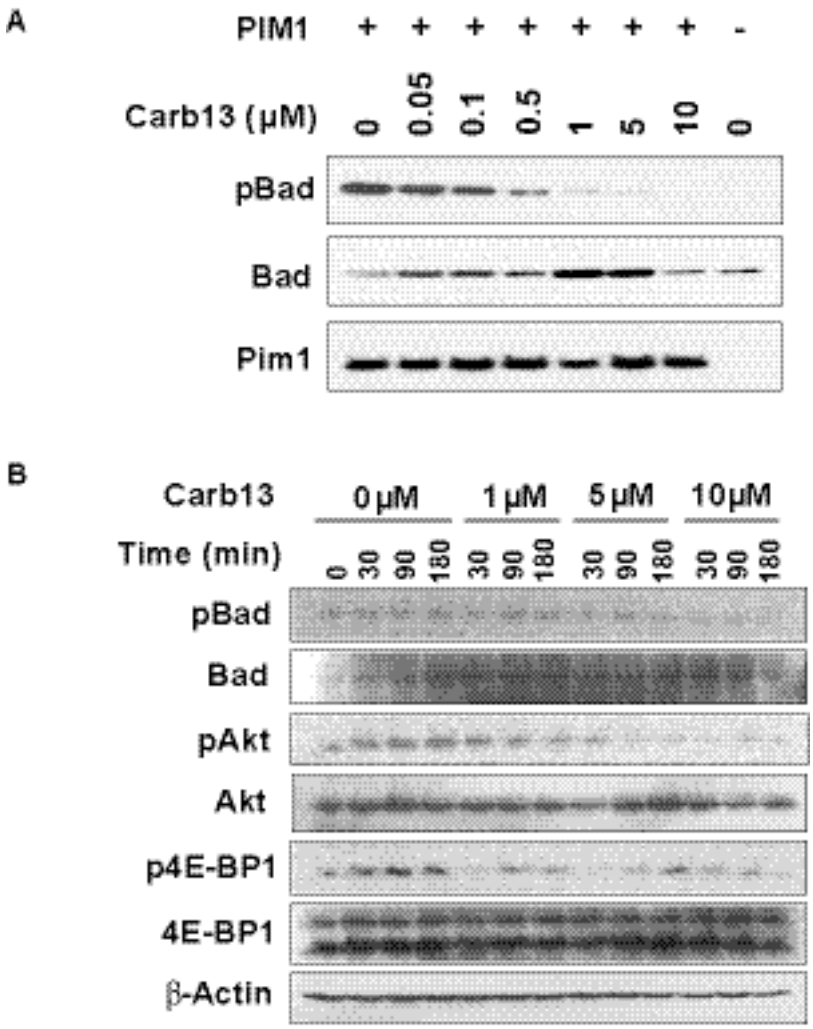

Figure 25: Effect of Carb13 on the phosphorylation of PIM1 downstream targets.

A. *In vitro* Bad phosphorylation by PIM kinase was evaluated in the presence of increasing concentrations of Carb13. Phosphorylation of BAD on Ser112 was detected by Western blotting with phospho-specific antibody.

B. MV4;11 cells were incubated with increasing concentrations of Carb13 for indicated times, harvested, and protein extracts separated by SDS-PAGE. The effect of Carb13 on PIM endogenous targets was followed by Western blotting with indicated phosphospecific antibodies.

1.3 Other potential PIM inhibitors tested

Quercetin. Quercetin, a member of the flavonoid family, is one of the most prominent dietary antioxidants. It is ubiquitously present in food including vegetables, fruits, tea and wine as well as countless food supplements and is claimed to exert beneficial health effects. This includes protection against various diseases such as osteoporosis, certain forms of cancer, pulmonary and cardiovascular diseases but also against aging (*Boots, 2008*). Especially the ability of quercetin to scavenge highly reactive species such as peroxynitrite and the hydroxyl radical is suggested to be involved in these possible beneficial health effects. Consequently, numerous studies have been performed to gather scientific evidence for these beneficial health claims as well as data regarding the exact mechanism of action and possible toxicological aspects of this flavonoid. It has been demonstrated that quercetin treatment of prostate cancer cells results in decreased cell proliferation and viability (*Boots, 2008; Aalinkeel, 2008*). Furthermore, quercetin promotes cancer cell apoptosis by down-regulating the levels of heat shock protein (Hsp) 90. Depletion of Hsp90 by quercetin results in decreased cell viability, levels of surrogate markers of Hsp90 inhibition (intracellular and secreted), induced apoptosis and activation of caspases in cancer cells but not in normal prostate epithelial cells (*Aalinkeel, 2008*)

By screening a kinase targeted compound library, Stefan Knapp and co-workers found quercetin to be a high-affinity inhibitor of PIM1 (*Bullock, 2005*). We tested quercetin on our BaF/3 cells over-expressing PIMs, as well as on BaF/3 cells over-expressing the leukemia associated TEL/JAK2 and FLT3-ITD PTK (leading to increased PIM1 and PIM2 expression) (**Figure 26**). We could observe that the survival of all BaF/3 cells decreased in a dose-dependent manner, in liquid culture, as well as in methylcellulose, as shown here for BaF/3 WT and BaF/3 PIM1. Based on the findings from Aalinkeel *et al.* as well as on those from Russo *et al.* showing that quercetin enhances CD95- and TRAIL-induced apoptosis in leukemia cell lines, these results suggested that quercetin is most likely not a PIM1 specific inhibitor: the observed effects are most probably the result of targeting other molecules such as Hsp90 (*Aalinkeel, 2008; Russo, 2007*).

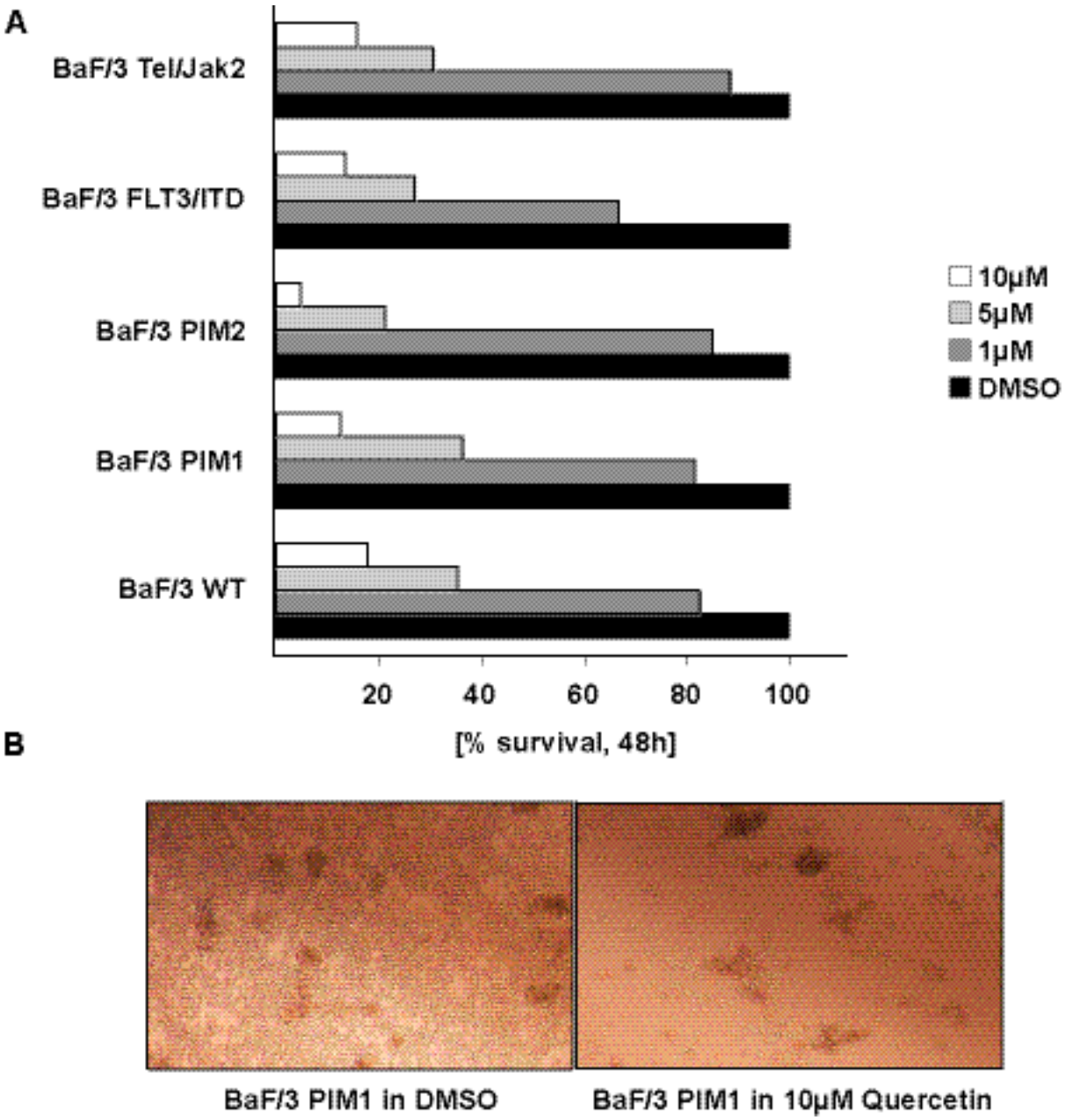

Figure 26: Evaluation of the biological activity of Quercetin.

A. Ba/F3 wild-type (WT) cells and stably expressing hPIM1, hPIM2, FLT3-ITD and Tel/JAK2 cells were exposed to increasing amounts of Quercetin and cell viability was determined 48 h later (expressed as a percentage normalized to viability of cells treated with 0.1% DMSO only).

B. Example of leukemic blasts cultured in methylcellulose in the presence of Quercetin. Significantly lower density of characteristic small leukemic clusters was observed as compared to control cultures.

New Furan compounds. The core scaffold of these compounds is furan, a heterocyclic organic compound. These compounds were discovered as potential PIM1 inhibitors by Prof. Nathanael Gray and co-workers from the Dana Farber Cancer Institute (Boston, USA). Originally, these furan scaffolds were generated to produce inhibitors for cyclin-dependent kinases (CDKS) or PI3K (*Pomel, 2006; Richardson, 2007*). Identifying them as PIM1 inhibitors was achieved by using the interaction platform provided by Ambit Biotechnology (San Diego, USA) including a panel of over 400 human kinases (www.ambit.com). The initial screen was followed by structure activity relationship (SAR) analysis to select putative PIM inhibitors with cellular activity. In analogy to the imidazo[1,2]pyridazines, these inhibitors interact with the opposite site of the PIM1 ATP binding pocket, without making significant polar contacts with the kinase hinge region.

We recieved 15 compounds that were shown to interact with PIM1 in the Ambit screen. To investigate the potential cellular anti-leukemic activity of these compounds, we tested them on the parental murine BaF/3 cell line as well as on Ba/F3 cells transformed to IL-3 independency by over-expression of human PIMs for effects on growth and survival. As a control, the cells were also treated with K00135. Exposure of the cells to different concentrations of 5 out of 15 of these compounds resulted in a dose-dependent reduction of cell survival (**Figure 27**).

<u>Figure 27:</u> Evaluation of the biological activity of the new furan compounds (pages 66-68).

Ba/F3 wild-type (WT) cells and cells stably expressing hPIM1 and hPIM2 were exposed to increasing amounts of furan compounds and cell viability was determined 24 and 48 hours later with trypan blue exclusion (expressed as a percentage normalized to viability of cells treated with 0.1% DMSO only). The most potent compounds (cvm-6-039, cvm-6-061, cvm-5-149-3, cvm-6-060-2 and cvm-6-060-3) are highlighted in red. K00135 served as a control for all the experiments.

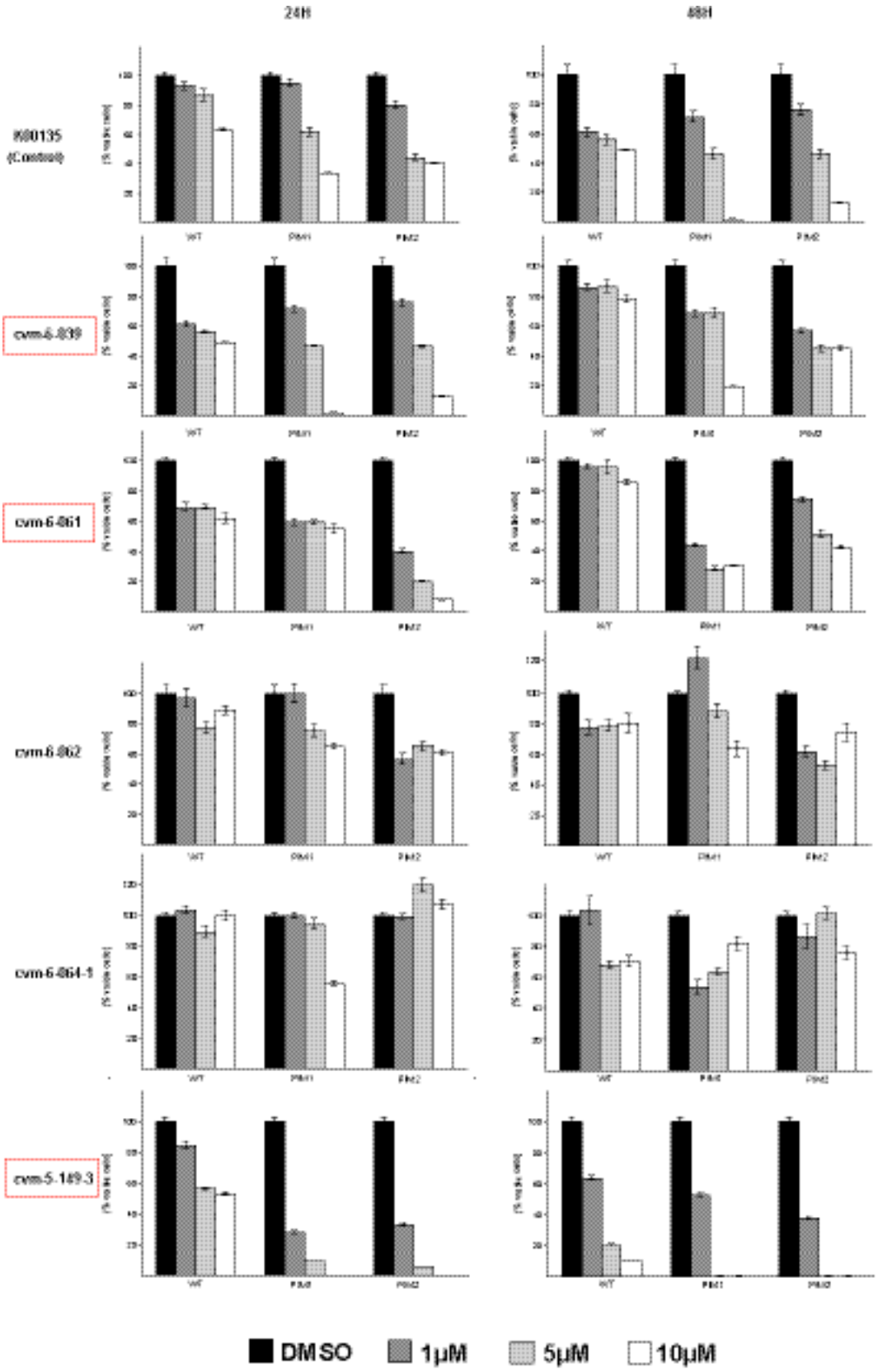
24H
48H
K80135
(Control)
cvm-6-839
cvm-6-861
cvm-6-862
cvm-6-864-1
cvm-5-189-3
WT
PM1
PM2
DMSO
1μM
5μM
10μM

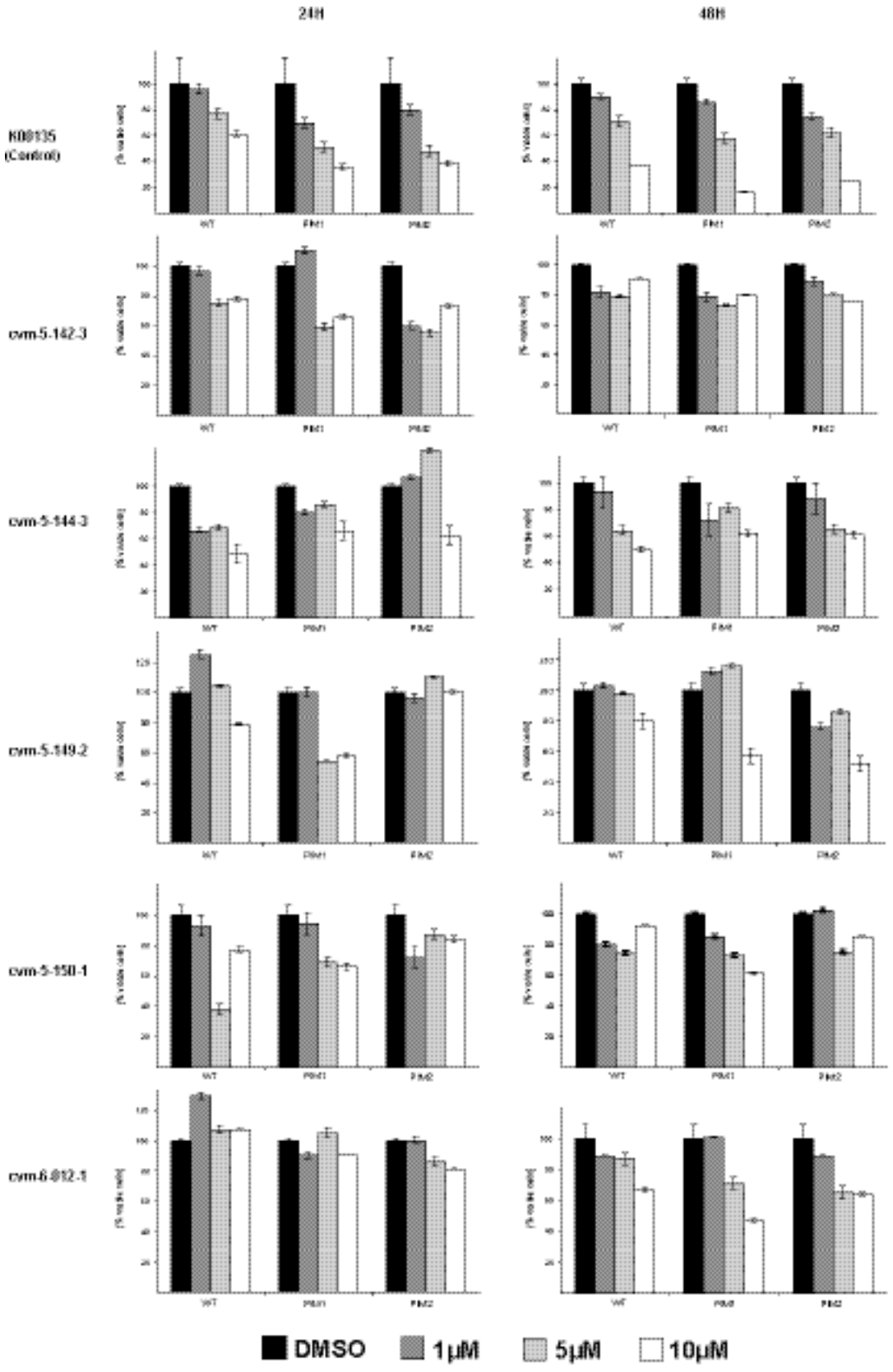
24H
48H
KB0135
(Control)
cvm-5-142-3
cvm-5-144-3
cvm-5-149-2
cvm-5-150-1
cvm-6-812-1
WT
PIM1
PIM2
DMSO
1μM
5μM
10μM

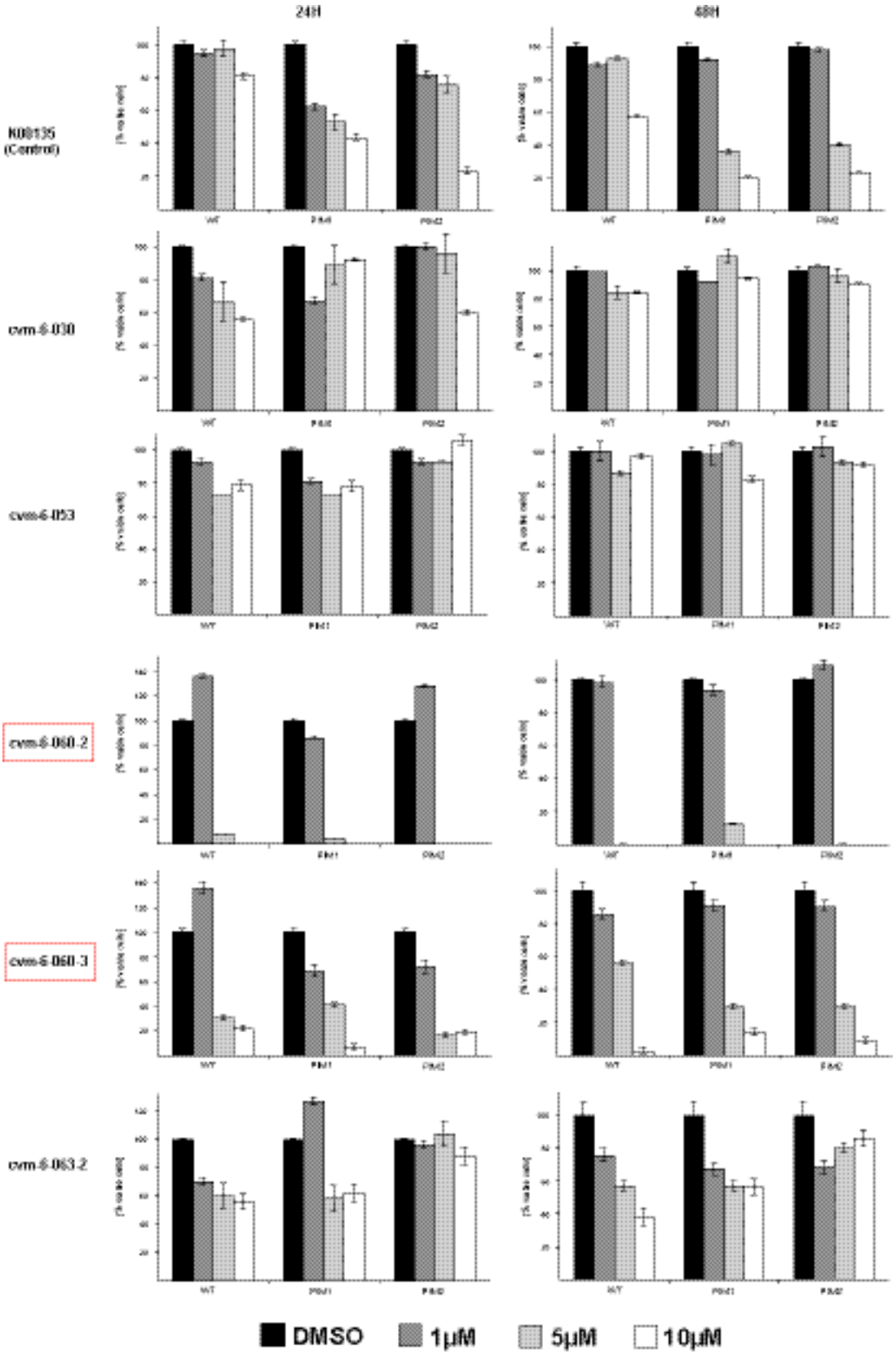
24H
48H
KI0135 (Control)
cvm-I-030
cvm-I-053
cvm-I-060.2
cvm-I-060.3
cvm-I-063.2
WT
PIM1
PIM2
DMSO
1μM
5μM
10μM

2. Discussion

Our group and others have shown that aberrant expression of PIM kinases in hematopoietic cells transformed by oncogenic protein tyrosine kinases provide a strong rationale for development of PIM kinase inhibitors as potential therapeutic targets (*Amson, 1989; Nieborowska-Skorska, 2002; Kim, 2005; Adam, 2006*). Using a combined structure functional approach in collaboration with Prof. Stefan Knapp (University of Oxford, UK) and Prof. Nathanael Gray (Dana Farber Cancer Institute, Boston, USA), we have characterized a group of small molecules that interact and block PIM kinases *in vitro* and *in vivo*. One of the imidazo[1,2]pyridazines compounds referred as K00135 significantly reduced the growth and self-renewal capacity of several human and leukemic cell lines as shown by inhibition of their clonogenic activity (**Figures 18, 19**). Furthermore, exposure of primary blasts from five AML patients to the K00135 inhibitor leads to a significant reduction in cell survival and clonogenic growth. Interestingly, exposure of mononuclear cells from human cord blood from four healthy donors to the compound was associated with minimal cytotoxic effects (**Figure 20**). These observations suggest that K00135 interacts with aberrant PIM activity found in cancer but not in normal cells. These observations go along with the finding that mice lacking all known PIM kinases are fertile and have a normal life span, suggesting that PIMs may not be essential for steady-state homeostasis, although deregulated upon malignant transformation (*Mikkers, 2004*). Biochemical analysis strongly suggests that our compound indeed blocks PIM1 function and its downstream targets such as BAD or 4E-BP1. However, a current potential drawback of the identified compound might be that significant reduction of growth and survival of human leukemia cell lines or primary samples could only be achieved at relatively high concentrations in the micromolar range.

Although almost all major pharmaceutical companies invest in generating small molecule PIM inhibitors, only a few have been published by academic labs (*Tong, 2008; Jacobs, 2005; Cheney, 2007; Holder, 2007a; Holder, 2007b*). All PIM inhibitor structures that have been published to date interact with the kinase hinge region in a classic ATP mimetic way.

Our imidazo[1,2]pyridazine PIM inhibitors result from screening of a kinase-targeted library and structure-activity relationship analysis. Related inhibitors of the pyrazolpyrimidine class were first described as specific inhibitors of the Src family of

tyrosine kinases, with several pyrazolo[3,4d]pyrimidines having low nanomolar affinity for Lck and anti-cancer activity (*Hanke, 1996*). Subsequently, similar scaffolds yielded specific inhibitors for glycogen synthase kinase 3 and members of the cyclin-dependent kinase (CDK) family (*Markwalder, 2004*).

However, all published co-crystal structures of this inhibitor class show binding to the kinase hinge region in the expected type I binding mode, meaning they target the ATP binding site in its active conformation in which the activation loop is phosphorylated. In the case of the imidazo[1,2]pyridazines, another binding mode was identified, in which the inhibitor interacts with the opposite site of the ATP binding pocket, without making significant polar contacts with the kinase hinge region. In addition, the conserved Asp-Phe-Gly (DFG) motif in the active site did not move into an “out” conformation as observed in co-crystal structures of kinases with type II inhibitor complexes. However, the described area of the binding pocket is much more diverse than the hinge region, bearing the promise that more specific inhibition may be developed on the basis of the determined crystal structure.

In a first temperature shift assay-based screen covering 50 serine/threonine kinases, Knapp and co-workers observed significant cross-reactivity of K00135 with only a few other kinases such as Cdc-like kinase 1 (CLK-1). The CLK kinase family acts as an interface between signal transduction pathways and the splicing machinery in the nucleus but a role in cancer has not been described yet (*Duncan, 1997*). With the huge number of continuously generated new scaffolds, identification of potential targets using high-throughput interaction screens becomes one of the main activities in modern drug discovery. To screen interactions of new scaffolds with the human kinome, AMBIT Biosciences (San Diego, USA) has developed a platform (referred as KINOMEscan™) to study interactions of currently >400 members of the human kinome (*Fabian, 2005; Karaman, 2008; www.ambit.com*). This assay is based on competition binding that quantitatively measures the ability of a compound to compete with an immobilized, active site directed ligand. Each assay is performed in combining three components: DNA-tagged kinase domain, immobilized ligand and a test compound. The ability of the test compound to compete with the immobilized ligand is measured via quantitative PCR of the DNA tag (*Fabian, 2005* & **Figure 28**). Although one has to keep in mind that *in vitro* interaction in this assay does not necessarily means *in vivo* inhibition, screening a large number of compounds that are either in clinical use (e.g. Imatinib-mesylate,

Gleevec) or in clinical trials (e.g. VX-680/MK0457) has nevertheless provided important insights that could help to explain cellular effects of small molecule kinase inhibitors. Based on the structural homology of certain kinases ("targets"), it is not surprising that only very few compounds are indeed selective. Interestingly, even imatinib-mesylate interacts with about 10 different kinases such as ABL, PDGFR, or KIT (**Figure 28**). Through collaboration with Prof. Nathanael Gray (Dana Farber Cancer Institute, Boston, USA) it was possible to perform a KINOMEscan™ analysis with the K00135 compound.

Interestingly, as listed in the table below, on the AMBIT platform, K00135 interacted with at least ten other kinases, some even with a higher affinity than PIM1 (unpublished). Among them, also wildtype and mutant targets (e.g. FLT3-ITD, mutant KIT) that are known drivers in leukemogenesis were found. However, one has to keep in mind the limitations of this assay that addresses binding, but not inhibition. Target affinities cannot be quantified directly since binding is reflective not only of affinity, but also abundance of the target. In addition, direct and indirect interactions that can occur in a cell cannot be distinguished.

Figure 28: The KINOMEscan platform from AMBIT Biosciences.

A. Schematic representation showing hoe KINOMEscan works (adapted from Fabian, 2005).

B. Small molecule-kinase interaction map for 38 kinase inhibitors. Kinases found to bind are marked with red circles, where larger indicate higher-affinity binding. Interactions with K_d < 3µM are shown (K_d, binding constant). Compounds with a bold edge are mentioned in this discussion part (adapted from Karaman, 2008).

A

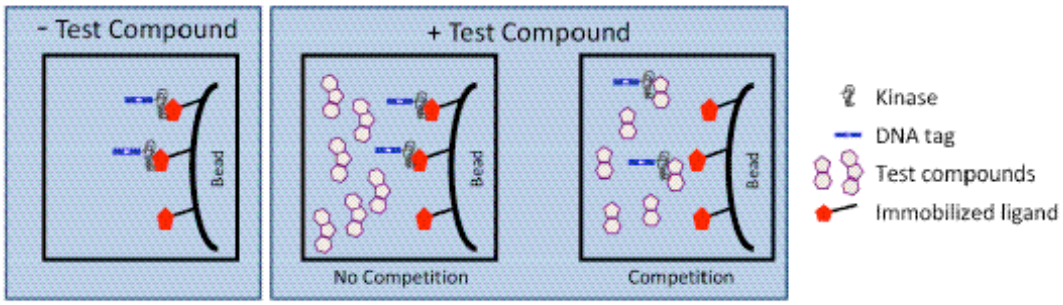
- Test Compound
+ Test Compound
Bead
Bead
Bead
No Competition
Competition
Kinase
DNA tag
Test compounds
Immobilized ligand

B


ABT-869
AMG-706
AST-487
AZD-1152HQPA
BIRB-796
BMS-387032/SNS-032
CHIR-258/TKI-258
CHIR-265/RAF-265
CI-1033
CP-690550
CP-724714
Dasatinib
EKB-569
Erlotinib
Flavopiridol
Gefitinib
GW-2580
GW-786034
Imatinib
JNJ-7706621
Lapatinib
LY-333531
MLN-518
MLN-8054
PI-103
PKC-412
PTK-787
Roscovitine/CYC-202
SB-202190
SB-203580
SB-431542
Sorafenib
Staurosporine
SU-14813
Sunitinib
VX-680/MK-0457
VX-745
ZD-6474
K_d
1 nM
10 nM
100 nM
1 µM
10 µM

K00135	Kd
AAK1	2.8
ACVR1	0.65
BIKE	0.9
CLK1	1.6
CLK2	0.45
FLT3	3.6
FLT3 D835Y	1.9
FLT3 ITD	0.45
FLT3 N841I	0.05
GAK	1.2
KIT V559D	0.55
MKNK2	0
PDGFRb	4.4
PIM1	4.2
TGFbR2	3.5

Table 1: Potential targets for K00135 found in the KINOMEscan™ assay.

Only the ones with K_d<5 are shown. As in Figure 28, the lower the K_d, the tighter the binding (K_d, binding constant).

The KINOMEscan™ analysis of K00135 might help to explain some of our observations when testing its cellular activity. Increased cytotoxicity of K00135 to MV4;11 when compared to RS4;11 might be explained by the presence of a driver FLT3-ITD mutation present in MV4;11 but not in RS4;11 leukemia cells. The same observations were made very recently for another compound: PKC-412, currently tested as FLT3 inhibitor has been shown to inhibit PIM1 in cell lines and AML cells (*Xie, 2008*). Despite the limited specificity, the biology of the K00135 recognized targets suggests that this scaffold could nevertheless be a promising lead for further optimization. Among the potential targets of K00135 are ACVR1, a TGFbeta receptor kinase, MKNK2 or PDGFRbeta, all well known for their role in malignant transformation (*Grisaru, 2007; Silva, 2008; Massague, 2008*). In conjunction with our finding that inhibition of PIM1 will also functionally impair CXCR4 signaling (see chapter II), we suggest that our imidazo[1,2]pyridazines are potent leads for targeted therapeutics against leukemic stem cells (*Juarez, 2004*). Indeed, several imidazo[1,2]pyridazines have been recently patented to be used as cancer therapeutics and one related imidazo[1,2]pyridazine compound, referred as SGI 1776, produced by SuperGen Inc. (Dublin, California, USA) shows potent anti-leukemic activity and could enter in phase I clinical trials (www.supergen.com).

Large-scale temperature-shift analysis and *in vitro* kinase assays performed in Prof. Knapp's laboratory also resulted in the identification of a new class of potential PIM kinase inhibitors: the beta-carbolines. Beta-carboline alkaloids are a heterogenous group of natural and synthetic indole alkaloids widely distributed in nature (plants, marine creatures, insects, human body). These compounds have recently gained interest due to their biological activity as neuromodulators and potential cancer drugs (*Cao, 2007*). Among 4 carbolines (AMTC, Carb2, Carb10 and Carb13), Carb13 was selected for further testing for its activity in leukemia cell models. Like K00135, Carb13 impaired growth and survival of Ba/F3 cells transformed to IL-3 independence by over-expression of human PIM1 (**Figure 24**). In contrast to K00135, Carb13 also strongly affected growth and survival of the parental Ba/F3 cells growing in the presence of IL-3. This is rather surprising, as previous siRNA-PIM knockdown experiments in Ba/F3 cells did not result in severely impaired cell survival (*Adam, 2006*). The observed effects on parental Ba/F3 cells are therefore most probably the result of interaction with other unknown targets (kinases or other molecules). Like K00135, Carb13 was also impairing proliferation of a panel of human acute leukemia cell lines, as well as primary cells from 3 patients with *de novo* acute myeloid leukemia. However, in contrast to K00135, Carb13 also strongly affected growth and survival of umbilical cord blood mononuclear cells from healthy donors. This observation together with the results observed in Ba/F3 cells strongly suggest that Carb13 has cytotoxic properties that might be independent of PIM kinases. Indeed, immunoblotting for known PIM targets and other signalling molecules showed that although Carb13 reduced phosphorylation of known PIM substrates (BAD, 4E-BP1) in MV4;11 cells, it also affected others such as the AKT kinase (**Figure 25**) that has been proposed to act upstream of PIM1 but not to be a direct substrate (*Muraski, 2007*). Although Carb13 has previously been tested in temperature-shift interaction screens against 60 human kinases to be rather specific (data not shown), our observation suggests that Carb13, like K00135, may target other kinases that are essential for cellular growth and survival. Interestingly, several carboline derivates have been recently characterized as potent inhibitors of protein kinases involved in cell survival (e.g. IkBa kinase, IKK) and/or proliferation (cyclin-dependent kinases, CDKs) (*Castro, 2003*). Despite the strong interaction and inhibition of PIM kinases by Carb13, further large-scale screening for potential targets (e.g. by using the AMBIT KINOMEscan™

platform) as well as chemical modification of the compound would be necessary to obtain a potential lead PIM inhibitor (*Fabian, 2005*). Currently, Carb13 is undergoing extensive testings as anti-cancer drug at the National Cancer Institute (NCI, Bethesda, MD, USA).

Using the KINOMEscan™ approach, Prof. Nathanael Gray and his group have identified several furan scaffolds as potential PIM1 inhibitors. These compounds harbor a similar binding mode than the imidazo[1,2]pyridazines and were originally identified as cyclin-dependent kinase inhibitors (*Pomel, 2006; Richardson, 2007*). Five (out of 15 so far characterized) showed potent cytotoxic effects when tested in our BaF/3 cells over-expressing human PIMs. Similar to Carb13, the cytotoxic effects of the 5-149-3 furan were not limited to BaF/3-PIM cells but also affected wild-type Ba/F3 cells (**Figure 27**), again suggesting that these effects might be mediated by the recognition of other targets. Indeed, a KINOMEscan™ analysis of 5-149-3 showed interactions with a large number of potential targets including AURORA, ABL, FLT3, KIT, and others. This compound is currently crystallized in complex with PIM1 by Prof. Stefan Knapp and his group.

Taken together, the imidazo[1,2]pyridazine compounds (K00135, K00486 or K00512) recognizing a limited number of kinase targets were the more promising scaffolds with potent anti-leukemic activity and limited toxicity to normal cells. Although previous studies have shown that an optimal PIM-targeted tumor therapy would include inhibition of PIM1 and PIM2 (*Mizuki, 2003; Hammerman, 2005; Adam, 2006*), thus far, there is no selective potent inhibitor for PIM2 available, suggesting that PIM2 is intrinsically more difficult to target. This finding is surprising considering the high sequence conservation of the PIM1 and PIM2 active sites. This reveals a kind of isoform selectivity suggesting that dynamic parameters like domain flexibility and plasticity of regulatory elements should be considered in structure-based inhibitor design (*Fedorov, 2007*).

As PIM kinases have been intensively characterized as proteins of relative weak inherent oncogenicity but potent in cooperation with other oncogenes such as *c-myc* (*Shirogane, 1999; Moroy, 1993*), it is likely that synergistic effects may be achieved in combination with either conventional chemotherapeutics and/or small molecules that target cooperating signaling cascades linked to survival of the malignant cells. (*Shay, 2005; Mizuno, 2001*).

The success for establishing new targeted leukemia (or cancer in general) therapies through small molecule kinase inhibitors is dependent on several general points. First, and most important, the biology of the disease that is affected by aberrantly activated kinases that are potential drug targets. Chronic myeloproliferative disorders such as CML or polycythemia vera (PV) are both driven by one or a limited number of mutated and constitutively activated kinases such as ABL, JAK2, PDGFR. Inhibition of these drivers by small molecules such as imatinib-mesylate (Gleevec) has revolutionized CML therapy (*Druker, 2002; Quintas-Cardama, 2005*). However, in contrast, acute leukemia is the product of several cooperating driver mutations affecting different pathways and therefore it is likely that selective targeting of one kinase might not necessarily be successful. This is currently best illustrated by the results of first clinical trials with very potent and selective small molecule FLT3 inhibitors targeting mutant FLT3 found in about 30% of human AML. Several studies have shown that the depth and duration of clinical responses to FLT3 inhibitor monotherapy have been modest (*Small, 2008*). Furthermore, a number of mechanisms by which blasts may acquire resistance have been proposed. Based on preclinical evidence of synergy with conventional chemotherapy, several combination trials are now underway (*Knapper, 2007*).

Based on these observations, inhibitors that would block several cooperating pathways essential for growth and/or survival of the leukemic cells would be ideal. However, dissecting of critical targets remains a major challenge of modern cancer research. Several clinical trials attempting treatment of acute leukemia with multi-kinase inhibitors (such as sorafenib or sunitinib) are currently ongoing. In spite of this, an increased number of targets recognized by a given compound is naturally linked to an increase of potentially not tolerable side-effects. Modern large-scale interaction screens such as the KINOMEscan™ from AMBIT provided important information regarding the limited selectivity of most small molecule kinase inhibitors currently in clinical trials but limited selectivity of a compound might also be an advantage: it seems that it is the combination of targets recognized by Gleevec including ABL, KIT and PDGFR that makes this drug the first choice to treat CML, gastrointestinal stromal tumors, or systemic mastocytosis driven by activating mutation of ABL, PDGFR or KIT. Interestingly, this target combination seems also to be responsible for efficacy in CML therapy (*Wong, 2004*). In addition, large-scale interaction screens also resulted in the identification of new potentially important

targets. VX680 initially developed as inhibitor of Aurora kinases could be identified as powerful inhibitor of BCR/ABL-T315I a mutant linked to Gleevec resistance (*Giles, 2007*). However, the relatively large number of recognized kinases by VX680 could also explain the strong adverse effects that were observed in first clinical trials: these were stopped due to cardiotoxicity (www.clinicaltrials.gov).

In collaboration with Prof. Stefan Knapp's laboratory we have characterized LY-333'531 (**Figure 28**), a compound initially generated as inhibitor of PKC-β as potent inhibitor of PIM1 (*Fedorov, 2007*). Our findings are further supported by the AMBIT KINOMEscan™ showing, among others, a strong interaction with PIM1. It is interesting to note that this compound has previously been in clinic as a drug (Ruboxistaurin) against long-term renal and eye complications of diabetes mellitus (*Ravera, 2007; Ryan, 2007*). Our observations of potent anti-leukemic activity of this well tolerated compound could open up some therapeutic possibilities. A derivate of LY-333'531, called LY-317'615 or Enzastaurin (Eli Lilly and Company) and also inhibiting PKC-β would also have been a potential candidate compound to inhibit PIM1 but the company declined our request to perform some tests.

Taken together, research of the last decade has provided evidence that aberrant activity of protein kinases is an important driver of a large number of human malignancies including leukemia. Much progress has been made in developing powerful small molecule inhibitors such as Gleevec, targeting constitutively activated tyrosine kinases driving CML. Further improvements for kinase inhibitor-based leukemia therapy will be dependent on identification of critical signalling pathways affected by collaborating protein kinases (e.g. FLT3-PIM1-CXCR4), and the *in vitro* and *in vivo* validation of compounds blocking the ideal number of targets with tolerable side effects.

3. Outlook

There is evidence that targeted therapy of leukemic cells harbouring an oncogenic PTK (such as FLT3-ITD or BCR/ABL) with small molecule tyrosine kinase inhibitor leads to an initial induction of PIM1 expression. Moreover, cellular hypoxia also leads to induction of PIM1 kinase expression (*Reiser-Erkan, 2008*). These observations suggest that the cells use PIM kinases to maintain survival upon external stress and raise the question whether it would be possible to enhance the cytotoxic effect of the small molecule PIM kinase inhibitors in combination with other (targeted or untargeted) cytotoxic agents. In order to experimentally address this question, we will select human leukemia cell lines harbouring either the FLT3-ITD (MV4;11, MOLM13) or BCR/ABL (K562) mutations. PIM inhibitors can then be combined to PKC412, a specific FLT3 inhibitor, or with imatinib-mesylate that efficiently blocks the ABL1 PTK. Furthermore, we will combine the PIM inhibitors with conventional anti-leukemic agents, like doxorubicin or etoposide. These agents will be applied either by (i) co-incubation, (ii) sequential incubation or (iii) pre-incubation with the cooperating compound. Previous reports testing combination of PTK inhibitor with conventional chemotherapeutic drugs have identified *synergestic* cytotoxic effects upon sequential application, *additive* effects upon co-treatment and *antagonistic* effects when treatment with the kinase inhibitor started earlier (*Jacinto, 2008*). Taken together, these *in vitro* experiments will help to select the most promising PIM inhibitor for further analysis *in vivo*.

IV. A transgenic mouse model to study the role of NUP214/ABL1 in T-cell ALL

1. Background

In T-cell acute lymphoblastic leukemia (T-ALL), several transcription factors (such as TAL1, SIL, LMO2, HOX11, HOX11L2) were shown to be deregulated by chromosomal translocations mostly involving the T-cell receptor genes (TCR), whereas activating mutations in protein tyrosine kinases have rarely been identified (*Pui, 2004; Rabbitts, 1994*). The Philadelphia translocation, resulting in the BCR/ABL1 fusion gene is typically found in chronic myeloid leukemia (CML) and precursor B-cell acute lymphoblastic leukemia (B-ALL) but very rare in T-ALL. In 2004, Graux and co-workers described an extra-chromosomal episomal amplification of ABL1 in 6% of T-ALL patients (*Graux, 2004*). Molecular analysis delineated the amplicon as a 500kb region from chromosome band 9p34, containing the oncogenes ABL1 and NUP214 (**Figure 29**). This transcript was detected in five individuals with ABL1 amplification, in 5 of 85 additional individuals with T-ALL and in 3 of 22 T-ALL cell lines (*Graux, 2004*). Like BCR/ABL1 and ETV6/ABL1 fusion proteins, NUP214/ABL1 fusions contain the SH3, SH2 and kinase domains of ABL1, and were shown to act as a constitutively activated tyrosine kinase, activating similar pathways than BCR/ABL1. This constitutively phosphorylated tyrosine kinase is also sensitive to the tyrosine kinase inhibitor imatinib (*De Keersmaecker, 2008*). As already mentioned in the introduction, constitutively active tyrosine kinases have been shown to be sufficient to induce myeloproliferative disease in mice but require the cooperative effect of other mutations to induce acute leukemia. In agreement with this, additional mutations were identified in cells expressing the NUP214/ABL1 fusion. Deletion of the tumor suppressor genes CDKN2A and CDKN2B (also called p15 and p16) were found in seven of nine cases evaluated. Screening for oncogenes known to be involved in T-ALL identified the mutually exclusive expression of HOX11 and HOX11L2 (*Graux, 2004; Ballerini, 2005; Ballerini, 2008*). Similar results were seen in T-ALL cells lines, where for example expression of

HOX11 was found in ALL-SIL. These results are consistent with a multi-step pathogenesis of T-ALL (*Graux, 2004*).

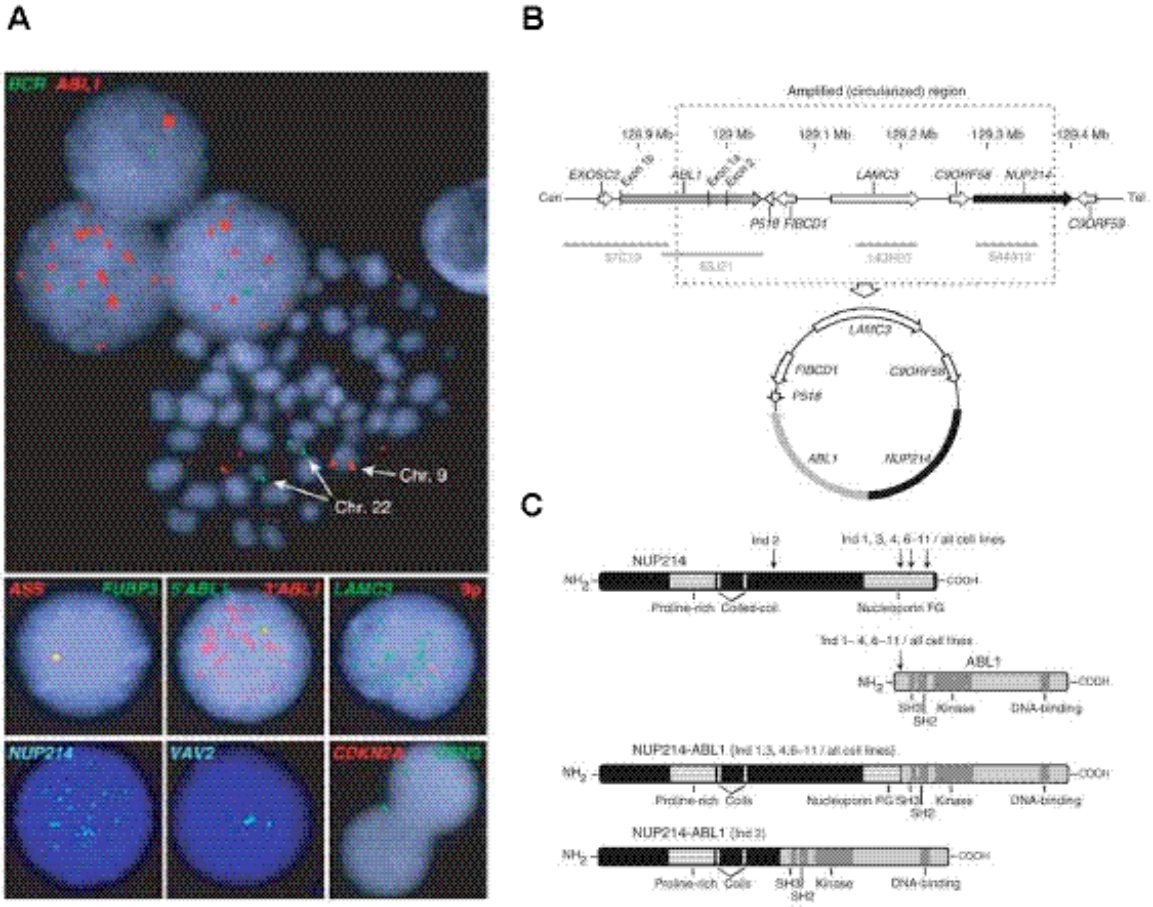

Figure 29: The NUP214/ABL1 fusion.

A. Extrachromosomal amplification of *ABL1* identified with the LSI *BCR/ABL1* probe (Vysis) in interphases and in one metaphase. Normal chromosomes 22 (*BCR*) and one normal chromosome 9 are indicated. The other chromosome 9 carries a deletion of *ASS*, *FUBP3* and *ABL1*. Nine to fifteen extra copies of *ABL1* are observed. 3' *ABL1*, *LAMC3* and *NUP214 are* amplified, whereas *ASS*, *FUBP3*, 5' *ABL1* and *VAV2* are not. *CDKN2A* shows a heterozygous deletion.

B. Detailed scheme of the amplified (circularized) region, and the proposed structure of the episome. Genes (arrows), BAC clones (gray bars), and their positions along chromosome 9 are indicated. Cen, centromeric site; Tel, telomeric site.

C. Schematic representation of the NUP214 and ABL1 proteins. Two main NUP214/ABL1 fusion proteins are generated: a shorter fusion (239kDa) present in only one individual, and longer fusions (310-333kDa) present in most individuals with T-ALL with *ABL1* amplification. This figure has been generated using figures from Graux, 2004.

2. Results

2.1 Generation of a NUP214/ABL1 transgenic mouse mode

In order to understand the role of the NUP214/ABL fusion for the pathogenesis of T-cell ALL *in vivo,* we aimed to generate a transgenic mouse model. Hereby, the NUP214/ABL1 cDNA was cloned in a conventional transgene vector bringing the fusion under the control of the Lck proximal promoter (**Figure 30A**).
Lck is a specific lymphocyte protein tyrosine kinase regulating allelic exclusion at the T-cell receptor β, used regularly for transgenes inducing hematological malignancies (*Aifantis, 2008; Condorelli, 1996*). We performed *SfiI* digestion to release the insert purified the DNA which was then injected into fertilized oocytes of C57Bl/6 mice at the Transgenic Mouse Core Facility at the Biozentrum (University of Basel). To our surprise, we had to perform several injections to obtain viable offspring enabling us to identify 2 NUP214/ABL1-positive founders. The presence of the NUP214/ABL1 transgene was assessed by PCR with a primer pair localized over the fusion breakpoint on genomic DNA (**Figure 30B**). Two transgenic mouse lines could be established.

2.2 Analysis of the NUP214/ABL1 transgene expression

As the NUP214/ABL1 fusion is under the Lck promotor, we analyzed transgene expression in the thymus of young mice of both lines. We could detect mRNA expression of the fusion in the thymus of the mice, what correlated with the use of the LCK promoter. No expression was seen in the spleen and bone marrow (**Figure 31A**). Successful attempts to generate transgenic mouse models for T-ALL were all characterized by a long latency period until the disease developed. We followed the mice once a week over a period of 18 months. However, I have not observed any signs of disease. I also analyzed the blood counts of three transgenic mice of both lines at different time points and compared it to blood counts of wild type C57Bl/6 mice but we could find no significant differences in white blood cell counts or any other parameters (**Figure 31B**). We then analyzed the distribution of T-cells in the thymus of an eighteen-month-old mouse from the first transgenic line and compared it to the thymus of wild type mouse in the same age range by FACS analysis. Again, there were no significant differences between these two mice regarding the distribution of T cells, as demonstrated by FACS analysis (**Figure 31C**).

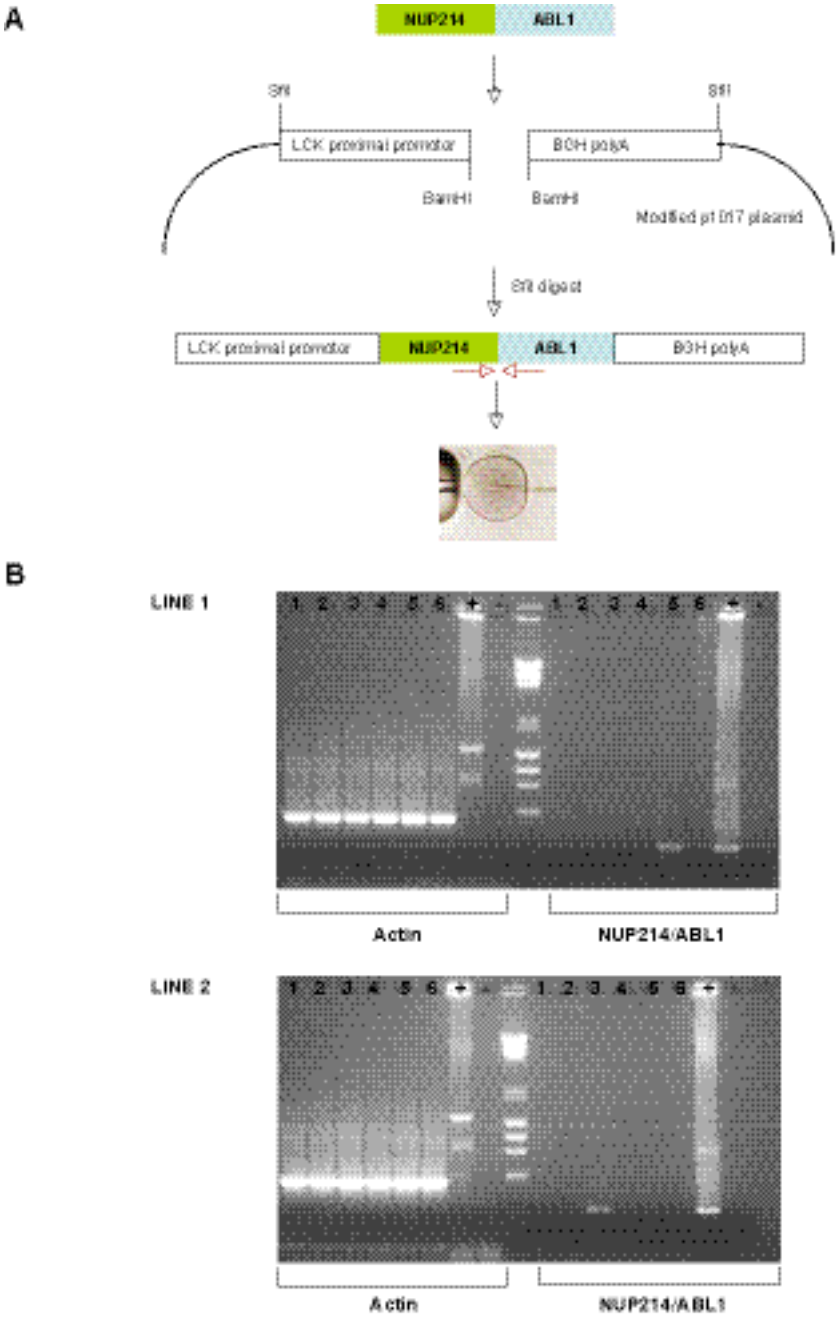

Figure 30: Generation of a NUP214/ABL1 transgenic mouse model.

A. Schematic representation of the experimental setup.

B. Detection of the NUP214/ABL1 transgene expression on isolated toe DNA with a primer pair over the breakpoint (red arrows). An actin PCR was done as control.

As no phenotype has been seen, we analyzed the copy number of NUP214/ABL1 in each line by Q-PCR. One line expresses 59 copies and the other one 86 copies of the transgene. We are still working on the Western Blot as for technical reasons, we could not detect the NUP214/ABL1 protein, even in a cell line over-expressing the fusion.

Taken together we have generated two transgenic mouse lines expressing low levels of NUP214/ABL in the T-cell lineage that did neither resulted in measurable disturbance of T-cell development nor induction of a haematological malignancy over a period of 18 months.

A

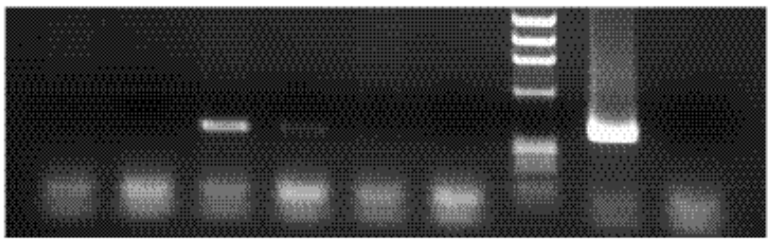

B

Mouse	Age	Analysis	WBC*10^9	RBC*10^12	HGB g/L	HCT %	MCV fL	MCH pg	MCHC g/L	MPV fl	Pla*10^9	
B6		Jackson	10.8	9.41	145	42.8	45.5	15.5	340	4.84	1146	Mean
B6		Jackson	6.21	7.09	114	31.7	42.1	12.2	289	4.1	742	Min
B6		Jackson	15.9	10.6	161	50.1	49.3	20.1	449	13.4	1624	Max
1540*B6: 2	15 months	24.4.08	7.1	9.4	140	45	48.2	14.8	307	6.6	1642	
2242*B6: 7	11 months	24.4.08	7.5	8.84	130	41	47.1	14.8	314	6.8	1350	
1540*B6: 26	12 months	24.4.08	14.3	10.84	152	50	48.8	15.2	311	6.4	1560	
2422*B6: 40	7 months	24.4.08	9	10.02	144	48	48.2	15.4	319	7	1300	
2422*B6: 50	7 weeks	24.4.08	9.1	9.1	142	44	48.8	15.6	320	6.8	1242	
1540*B6: 80	7 weeks	24.4.08	6.3	9.04	122	42	46.6	14.6	314	6.7	1360	

			WBC*10^9	Neutr %	Lymph %	Mono %	Eos %	Baso%	LUC %	
		Jackson	10.8	7.88	87.3	1.19	1.79	0.445	1.29	Mean
		Jackson	6.21	3.3	72.2	0.4	0.8	0.1	0.4	Min
		Jackson	15.9	33.8	92.9	3.1	3.5	1.7	4.2	Max
1540*B6: 2	15 months	24.4.08	7.1	20.9	71.3	3.6	2.7	0.1	1.5	
2242*B6: 7	11 months	24.4.08	7.5	4.7	84	7.2	3.4	0.1	0.5	
1540*B6: 26	12 months	24.4.08	14.3	7.6	85.6	2.8	2.1	0.5	1.4	
2422*B6: 40	7 months	24.4.08	9	6.6	88.3	2.3	2.3	0.2	0.3	
2422*B6: 50	7 weeks	24.4.08	9.1	5.2	89.1	3.2	1.6	0.1	0.8	
1540*B6: 80	7 weeks	24.4.08	6.3	9.8	77.3	8.5	1.3	0.3	2.8	

C

WT mouse		NUP214/ABL1 mouse	
CD4-CD8-	15.92%	CD4-CD8-	12.65%
CD4+CD8-	6.1%	CD4+CD8-	8.43%
CD4-CD8+	1.28%	CD4-CD8+	4.08%
CD4+CD8+	76.7%	CD4+CD8+	74.83%

Figure 31: Analysis of the NUP214/ABL1 transgene expression.

A. Detection of the NUP214/ABL1 transgene expression on thymus cDNA of three different mice: one positive founder, his negative brother and an unrelated normal B6 mouse. The band present in the RT- slot of the positive founder is believed to be the NUP214/ABL1 fusion.

B. Peripheral blood analysis of three transgenic mice of each strain (strain 1: mice 2, 26, 80; strain 2: mice 7, 40, 50) compared to wildtype B6 mice analyzed at Jackson Laboratories.

C. T-cell status analysis in a NUP214/ABL1 transgene mouse compared to a wildtype B6 mouse, both 18 months old.

3. Discussion

Approximately 15% and 25% of the newly diagnosed cases of acute lymphoblastic leukemia in childhood and adults are T-cell ALL and are generally linked with a poor prognosis. T-ALL is thought to result from malignant thymocytes that arise at defined stages of intra-thymic T-cell differentiation (*De Keersmaeker, 2005*). Several studies have shown that the NUP214/ABL1 fusion is associated in about 5-10% of human T-ALL cases (*Graux, 2004; Quintas-Cardama, 2008*). In order to study the role of the NUP214/ABL episomal amplification or single copy fusion for the pathogenesis of T-cell ALL, we have created transgenic mice expressing the NUP214/ABL1 fusion in the T-cell lineage using a T-cell specific promoter (Lck). This promoter is among the most frequently used for transgene expression in T cells, including the $p56^{lck}$ proximal promoter (*Allen, 1992*), a promoter based on the human CD2 locus control regions and promoters derived from the CD4 and CD8 genes. The $p56^{lck}$ promoter is expressed in early T cell progenitors and can be detected in DN T cells. The $p56^{lck}$ promoter is not well characterized and might be susceptible to modulations, depending on where it gets integrated into the genome (*Cantrell, 2002*). This could explain why we got only two positive founders after *in vitro* fertilization. Another possibility could be that too many copies of the transgene were lethal and that only mice expressing low levels of the fusion survived. The second possibility is more likely as over-expression of protein tyrosine kinase has been shown to be problematic for the generation of transgenic mouse models (*Cantrell, 2002*).

There are many mouse models of T-cell leukemia, but many of them do not develop leukemia, or if so, then after a long latency confirming the multi-step pathogenesis of the disease. Seo et al. created Cdt1 transgenic mice using the $p56^{lck}$ promoter and these mice showed normal T-cell development, meaning that Cdt1 over-expression under the $p56^{lck}$ promoter was not sufficient for T cells to acquire growth advantage. When they crossed these transgenic mice into $p53^{-/-}$ mice, the offspring developed thymic lymphoblastic leukemia (*Seo, 2005*). Graux et al. and others also found that

additional mutations were found in cells expressing the NUP214/ABL1 fusion. Some of these mutations involved the homeobox genes HOX11 and HOX11L2 (*Graux, 2004; Ballerini, 2005; Graux, 2008*). Homeobox genes are master regulators of transcription first identified for their function in early development and are strongly implicated in the regulation of hematopoiesis (*Aifantis, 2008*). From these, only HOX11 and HOX11L2 have been associated with T-ALL (*Su, 2006*). The HOX11 gene was originally identified because it was found to be involved in the t(10;14) translocation found in 7-10% of pediatric patients with T-ALL, and subsequently, was also found to be involved in the t(7;10) translocation. In addition, the expression of this gene is frequently up-regulated in T-ALL cells in the absence of a genetic re-arrangement. Importantly, the HOX11 gene is normally not expressed in thymocytes, but during leukemogenesis, its expression can become controlled by the regulatory regions of the TCR loci, thereby inducing aberrant expression in T cells and causing a block at the DP stage. However, over-expression of HOX11 alone is also not sufficient to induce leukemia (*Aifantis, 2008*). Retroviral infection of the NUP214/ABL1 mice with HOX11 or HOX11L2 virus would perhaps have resulted in a leukemia phenotype. Another possibility why we do not see any effect in the NUP214/ABL1 transgenic mice is that there might not be a simple linear correlation between transgene copy number and protein expression for any transgene promoter. The level of protein expression is regulated by rates of gene transcription, but not infrequently, the rate of protein translation and protein stability are of equal importance in determining steady-state protein levels. The stability and half-life of proteins is often not that relevant when they are massively over-expressed in transient transfection assays, but become crucial under more physiological conditions (*Cantrell, 2002*).

Recently, De Keersmaeker et al. found that the NUP214/ABL1 fusion is a relatively weak oncoprotein (when compared to BCR/ABL), relying on incorporation into the nuclear pore complex and interactions with other nuclear pore proteins for its kinase activation and oncogenicity. They could also explain why the NUP214/ABL1 gene is always amplified in T-ALL, as the NUP214/ABL1 protein has to compete with endogenous NUP214 for nuclear pore localization (*De Keersmaecker, 2008*). This could also explain why our

transgenic NUP214/ABL1 mice show no leukemic phenotype, even after a long latency. However, as the NUP214/ABL1 also occurs as non-amplified translocation, this observation might explain episomal amplification. It does not rule out that in other cases, this fusion needs cooperation of other alterations to induce the disease. Nevertheless, based on the findings of De Keersmeacker et al., decreasing the gene dosage of NUP214 (e.g. by crossing with NUP214+/- mice, or by siRNA) could be another possibility to induce the disease.

4. Outlook

There are many mouse models of T-cell leukemia that do not develop leukemia, or if so, then after a long latency confirming the multi-step pathogenesis of the disease. In order to obtain a leukemic phenotype from our NUP214/ABL1 transgenic lines, we planed to combine this fusion to other cooperating events known to play a role in the pathogenesis of leukemia. We thought of three different strategies:

1. Based on the lastest findings of De Keersmaecker et al., another way of inducing a leukemic phenotype in the NUP214/ABL1 transgenic mice would be to reduce the dose of endogenous NUP214 using a specific murine siRNA (*De Keersmaecker, 2008*).
2. As shown by Seo et al., crossing Cdt1 transgenic mice showing no T cell leukemia phenotype into $p53^{-/-}$ mice resulted in T-ALL (*Seo, 2005*). We could cross our mice into $p53^{-/-}$ mice or into $p15^{-/-}$ or $p16^{-/-}$ mice, as p15 and p16 tumor suppressor genes are involved in leukemo- and lymphomagenesis.
3. As HOX11 and HOX11L2 are known to be involved in T-ALL, we could perform bone marrow transplantations with HOX11- or HOX11L2-retrovirally infected NUP214/ABL1 cells. One abstract from the upcoming American Society of Hematology (ASH) meeting even suggests that HOX11L2 rearrangement and loss of p15 precede the formation of the NUP214/ABL1 fusion and subsequent amplification (*Pisecker, 2008*). This could be considered if our strategies do not result in the induction of a leukemic phenotype.

V. Material and methods

1. Material

Cell lines

293T	Human embryonal kidney
293	Human embryonal kidney
BaF/3	Mouse pro-B cell
Jurkat	Human T-cell leukemia
PC3	Human prostate carcinoma
DU145	Human prostate carcinoma
BPH1	Human benign prostate hyperplasia
LNCAP	Human prostate carcinoma
ALL-SIL	Human T-cell leukaemia
RS4;11	Human B cell precursor leukaemia
MV4;11	Human acute monocytic leukaemia
MOLM13	Human acute myeloid leukaemia
K562	human chronic myeloid leukemia in blast crisis
SEM	Human B cell precursor leukaemia

Inhibitors

Imidazo[1,2-b]pyridazines	Stefan Knapp
Beta-carbolines	Stefan Knapp
Quercetin dihydrate	Sigma
Furan compounds	Nathanael Gray

Antibodies

Mouse monoclonal α-FLAG	Sigma
Mouse monoclonal α-HA (12CA5)	Roche
Rabbit polyclonal α-HA	Santa Cruz
Mouse monoclonal α-Pim1	Santa Cruz Biotechnologies
Mouse α-Human β-Actin	Sigma
Rabbit polyclonal α-CXCR4	Abcam
Rabbit polyclonal α-NUP214	Novus Biologicals
Mouse monoclonal α-c-ABL1	Santa Cruz Biotechnologies
Alexa Fluor 488 goat α-rabbit	Molecular Probes
Alexa Fluor 555 goat α-mouse	Molecular Probes
APC-rat IgG2β,κ Isotype control	BD Biosciences
PE-rat IgG2β,κ Isotype control	BD Biosciences
FITC-rat IgG2β,κ, Isotype control	BD Biosciences
Rat α-mouse CXCR4, biotinylated	BD Biosciences
Streptavidin-APC conjugate	BD Biosciences
APC-mouse monoclonal α-human CXCR4	BD Pharmingen
PE-rat monoclonal α-mouse CXCR4	BD Pharmingen
PE anti-mouse CD4 (L3T4)	BD Pharmingen
PE anti-mouse CD45	BD Pharmingen
PE anti-mouse CD8	BD Pharmingen
FITC anti-mouse CD8	BD Pharmingen
FITC anti-mouse TCRβ	BD Pharmingen
APC anti-mouse TCRβ	BD Pharmingen
APC anti-mouse CD4	BD Pharmingen

Patient samples

Patient samples were gifts from A. Biondi (Monza) and from S. Meyer-Monard (University Hospital Basel).

Primers

NUP214 fwd	GGT CAA GCA GCC AGT ACT GG
ABL1 rev	GCT TAG AGT GTT ATC TCC ACT GGC C
NUP/ABLf-SYBR	CAG CCA ACA AAA ACC CAT TCA
NUP/ABLR-SYBR	TCC AAC GAG CGG CTT CAC
mActin fwd SYBR	CCA TAG GCT TCA CAC CTT CCT G
mActin rev SYBR	GCA CTA ACA CTA CCT TCC TCA ACC G
mJak2 fwd SYBR	CCA CGG CCC AAT ATC AAT G
mJak2 rev SYBR	CCC GCC TTC TTT AGT TTG CTA

Mice

FVB/NJ WT	M. Nawijn, The Netherlands Cancer Institute, Amsterdam Jackson Laboratories
FVB/NJ PIM1-/-	M. Nawijn, The Netherlands Cancer Institute, Amsterdam
FVB/NJ PIM2-/-	M. Nawijn, The Netherlands Cancer Institute, Amsterdam
B6	Animal facility, University Hospital Basel

2. Methods

Transient transfection of 293T cells and retrovirus production

The day before, 3.10^6 cells were plated per 10cm dish in 10mL of DMEM complete. The day of transfection, 10µg of DNA (5µg packaging plasmid IPAC6 and 5 µg plasmid of interest) were dissolved in DMEM containing no antibiotics or serum to a total volume of 300µL. 70µL of Polyfect was added, the solution was mixed and incubated for 10min at room temperature. During this time, the medium was removed from the cells and 7mL of fresh DMEM complete was added. After incubation, 1mL of DMEM complete was added to the transfection complexes; the solution was mixed by pipeting up and down twice and the total volume was immediately transferred to the cells. Plates were swirled to ensure uniform distribution of the complexes and incubated for 48h and/or 72h at 37º.

After 24h, the cell culture medium was changed. After 48h, the virus was harvested using a syringe and sterilely filtered through a 0.45µm millipore filter, aliquoted in 2mL tubes on ice and concentrated at 14000rpm, 1h at 4º. Approximately 1.8mL of supernatant was removed and the rest was carefully re-suspended, pooled together and stored on ice for cell transduction experiments.

Transduction and transplantation

Bone marrow was harvested from FVB/N [wild-type (WT)], FVB/N *PIM1*$^{-/-}$and FVB/N *PIM2*$^{-/-}$ donor mice and incubated overnight in IMDM/ 20% FCS supplemented with growth factors (10ng/ml mIL-3, 10ng/ml mIL-6, 50ng/ml mSCF). Cells were transduced in 4 rounds of spin infection (1200g, 32°C, 90min) with 4µg/ml polybrene (Sigma). Subsequently, cells were resuspended in Hanks´ balanced salt solution (Sigma-Aldrich, Irvine, UK) and injected into the tail vein of sub-lethally (750rad) or lethally irradiated (900rad) FVB/N recipient mice. All procedures were reviewed and approved by the University's supervisory animal care committee.

In vitro colony-forming assays

Bone marrow was transduced following the method described in "Transduction and transplantation of murine bone marrow". 10-20x103 EGFP-positive bone marrow cells per well were plated in triplicate in methylcellulose media containing recombinant IL3 (10ng/ml) or no cytokines (StemCell Technologies, Vancouver, Canada).

Histology

Tissue samples from PIM1$^{-/-}$, PIM2$^{-/-}$ and wild type FVB/NJ mice were fixed in 4% paraformaldehyde, paraffin-embedded and 4µM sections were stained with Haematoxiylin-Eosin (this was done at the pathology). Pictures were taken at 50 and 200 fold magnifications using a Zeiss microscope.

Flow cytometric immunphenotyping (FACS-analysis)

Single-cell suspensions of indicated tissue samples were prepared by passing tissue through 100µm nylon mesh strainers (Falcon, Becton-Dickinson, Heidelberg, Germany). Red blood cells of peripheral blood were lysed prior to analysis. Cells were pre-incubated with Fc-block and CD45-PECy5 and subsequently stained with either PE-conjugated anti CD11b (Mac-1), CD45R/B220, CD90.1 (Thy1.1), CD4 or CD8α antibodies as indicated. Dead cells were excluded by propidium iodide (PI), or 7-amino-actinomycin D (7-AAD) staining as mentioned in the text. Cell surface expression of CXCR4 was analyzed by staining with PE-conjugated anti-mouse CD184 (2B1) or APC conjugated anti-human CD184 (12G5) antibodies (Pharmingen, Becton-Dickinson). Unspecific binding was assessed by a PE- or APC-conjugated rat IgG2b isotype control. Fc-block and all antibodies were purchased from BD Pharmingen, Heidelberg, Germany.

Bone marrow cell homing

Recipient FVB/NJ mice were lethally irradiated (900rad) prior to transplantation. Donor cells from PIM1$^{-/-}$ or wild type FVB/NJ mice were re-suspended at 10^6 cells/mL in pre-warmed PBS/0.1%BSA and stained with 1µM CFSE (Molecular Probes) for 10min at 37º. The reaction was stopped by adding 5 volumes of ice-cold medium and a 5min incubation on ice. The cells were then washed three times in PBS and re-suspended in an appropriate

volume for injection. Mice received 1.10^6 CFSE-positive cells in 100µL solution via tail vain injection. Comparable staining as well as viability was determined by FACS analysis. Mice were killed 4 or 20 hours post-transplantation. Single cell suspension of bone marrow and spleen were made and the cells were stained with APC-conjugated anti-CD45 antibody and the dead cells excluded by 7AAD staining. The gates were set on CD45-positive cells and CFSE-positive cells were detected at 517nm.

Bone marrow cell migration

5.10^5 bone marrow cells from PIM1$^{-/-}$ and wild type FVB/NJ mice were allowed to migrate four hours toward a 300ng/mL SDF1α gradient using transwell chambers (5.0µm pore size, Costar). Cells found in the bottom chamber were counted and the migration index was calculated as a percentage of input cells. The same experiment was done with BaF/3 cells and Jurkat cells. Here, the migration was done toward a 10nM SDF1α gradient for four hours using the same transwell chambers. In some of the experiments, the cells were first pre-treated with 10µM K00486 for two hours.

Determination of intracellular Ca^{2+} flux

Freshly isolated bone marrow cells were loaded with 1µM Fura-2-AM (Molecular Probes) in calcium buffer (137mM NaCl, 2.7mM KCl, 1.8mM $CaCl_2$, 1mM $MgCl_2$, 5.6mM Glucose, 0.1% BSA and buffered with 20mM HEPES at pH7.4). After incubation at 37º for 10min, the cells were washed twice and re-suspended in calcium buffer to a final concentration of 2.10^6 cells/mL. Fura-2 fluorescence was monitored in an LS50B luminescence spectrophotometer (Perkin Elmer). The excitation wavelengths used were 340 and 380nm; the emission was measured at 510nm. $[Ca^{2+}]I$ was calculated from the Grynkiewicz equation. The K_d used was 224nM. R_{max} was obtained after lysis of the cells with 0.1% Triton X-100 and R_{min} was determined by addition of 10mM EDTA

Treatment of Jurkat, cells with the PIM1 inhibitor K00486

Jurkat cells were splitted the day before. For the experiment, 10^5 cells were plated in 2mL RPMI complete per well of a 24-well plate. The PIM1 inhibitor K00486 was diluted to a 5mM concentration in DMSO and 4µL were given to each well. 0.1% DMSO was used as a negative control. After different time points, cells were harvested, resuspended in 200µL PBS and incubated with the APC α-human CXCR4 antibody for 30min on ice in the dark. FACS analysis was performed on a FACSaria from BD.

CXCR4 expression after PIM inhibition in AML patient samples

Mononuclear cells from peripheral blood from AML patients with more than 90% of leukemic cells were freshly purified using Ficoll gradient. Cells were washed in PBS and seeded in 24-well plates with 10^6 cells per ml media containing RPMI and 10% FCS. Cells were treated with DMSO, 5 or 10 µM K00486. After 30 min of treatment cells were fixed in 3.75% PFA and CXCR4 surface expression was measured using APC-conjugated anti-human CD184 (12G5) antibody.

Quantitative RT-PCR analysis

mRNA expression was determined by quantitatitve real-time PCR (RT-PCR) using SYBRGreen. 1µg of total mRNA (isolated with the RNeasy kit, Qiagen, Hilden Germany) was used for cDNA synthesis (High Capacity cDNA Reverse Transcription kit, Applied Biosystems), and 50ng cDNA was applied for RT-PCR using the Power SYBR Green PCR Mastermix (Applied Biosystems) on an ABI Prism 7700 sequence detection system (Applied Biosystems). Expression levels were normalized to glyceraldehyd-3-phosphate dehydrogenase mRNA (GAPDH) using the ΔCt method. The following oligonucleotides were used as PCR primers: hPIM1-forward, 5'-cga gca tga, cga, aga gat cat-3', hPIM1-reverese, 5'-tcg aag gtt ggc cta tct ga-3' (119bp amplicon); hCXCR4-forward, 5'-atg aag gaa ccc tgt tcc cgt-3', hCXCR4-reverse, 5'-aga tga tgg agt aga tgg tgg g-3' (76bp amplicon); hGAPDH-forward, 5'-gtg gtc tcc ctg act ttc aac agc-3', hGAPDHreverse, 5'-atg agg tcc acc acc tgc ttg ctg-3' (149bp amplicon). Statistical significance was assessed by one-way ANOVA.

Regulation of CXCR4 surface expression

JURKAT cells were plated in RPMI complete at a concentration of 10^5/mL and pre-treated for one hour with 10μM K00486 or DMSO at 37ºC, as indicated. After this treatment, cells were incubated for 30 min or 60 min with 10nM SDF1α at 37ºC. Half of the cells were washed three times in PBS to remove CXCL12 and K00486 and resuspended in new medium. The rest was left in the original medium. Samples were collected right after the CXCL12 treatment and 1, 2 and 3 hours after washing. Cells were fixed in 4% PFA. Surface CXCR4 was analyzed by staining with APC-conjugated anti-human CD184 (12G5) antibody. Non-specific binding was determined by using the APC-conjugated rat IgG2b as isotype control (BD Pharmingen).

Cytospins and confocal microscopy analysis

Jurkat cells were fixed with 4% paraformaldehyde for 15min at room temperature and flattenend on a glass slide. The cells were washed twice with PBS and incubated for 10min in 1% Trition X-100. After three PBS washings, they were treated with 1mg/mL Rnase A. The Rnase was washed away by washing three times with PBS and the cells were then incubated with Image-iT FX signal enhancer (Molecular Probes) for 15min and blocked 10min in 1%BSA + 0.1% Tween in PBS. After extensive washing, cells were incubated with the primary antibody for one hour, at a 1:100 dilution in blocking solution. The cells were then washed five times with PBS and incubated for one hour with the secondary antibody (1:500, in the dark). Nucleus staining was done with propidium iodide for 10min at a concentration of 2.5μg/mL. The cells were washed again and mounted in 30μL FluorSafe Reagent (Calbiochem). Confocal microscopy was carried on a LSM 510 laser scanning microscope from Zeiss.

Phosphorylation of GST-CXCR4

PIM1 was expressed and purified as described previously (*Bullock, 2005*). GST-CXCR4 fusions were expressed in BL21 (DE3) cells with 0.5mM IPTG induction for 6 hours at 18°C. Cells were lysed using a high-pressure homogenizer, cleared by centrifugation and the lysates purified by glutathione

sepharose chromatography. Phosphorylation reactions were performed for 90 minutes at room temperature in 125µl samples containing 1µM PIM1 and 10µM GST-CXCR4 buffered in 50mM HEPES pH 7.5, 100mM NaCl, 1mM DTT, 1mM ATP, 5mM MgCl2, 1Mm MnCl2. Control samples were treated similarly in the absence of PIM1. Reactions were stopped by the addition of 0.1% formic acid and protein masses determined by ESI-LC/MS, using an Agilent LC/MSD TOF system with reversed-phase HPLC coupled to electrospray ionization and an orthogonal time-of-flight mass analyzer. Proteins were desalted prior to mass spectrometry by rapid elution off a C3 column with a gradient of 5-95% acetonitrile in water with 0.1% formic acid. Spectra were analyzed using the Agilent Protein software.

In vitro kinase assay

5µg recombinant PIM1 was incubated at 30°C for 5 min in kinase buffer [40mM Tris-HCl (pH7.4), 20mM MgCl2, 0.1mg/mL bovine serum albumin] containing 500µM ATP with or without 2mM PIM inhibitor (K00486) (51). 8µg of mentioned GST-CXCR4 construct were then added for further 10 min. The reactions were terminated by the addition of Laemmli sample buffer, and phosphorylation of CXCR4 was analyzed by Western blotting with anti-phospho-CXCR4 antibody (kindly provided by J. Rubin, St. Louis, USA).

Treatment of transformed BaF/3 cells with PIM inhibitors

BaF/3 cells were plated at a concentration of 2.10^5 cells/mL in a 24 well plate (1mL/well). PIM inhibitors were diluted to the appropriate concentrations in DMSO. A further dilution of the inhibitors in cell culture medium was performed at a ratio 2:1000 (inhibitor:medium). 1mL of this dilution was then given to each well of cells and the plates were incubated for 24h and 48h at 37º. After 24h and 48h, cells were harvested and counted using trypan blue exclusion.

Treatment of human cell lines with PIM inhibitors

Human cell lines were plated at a concentration of 2.10^5 cells/mL in a 24 well plate (1mL/well). PIM inhibitors were diluted to the appropriate

concentrations in DMSO. A further dilution of the inhibitors in cell culture medium was performed at a ratio 2:1000 (inhibitor:medium). 1mL of this dilution was then given to each well of cells and the plates were incubated for 24h and 48h at 37º. After 24h and 48h, cell proliferation and viability were assayed using 100µL of the culture and 10µL of Cell Proliferation Reagent WST-1 (Roche Diagnostics). After 4h in the cell culture incubator, plates were read with the Spectra Max 190 and data were analyzed with the Softmax Pro software.

Treatment of AML samples with PIM inhibitors

Samples were defrosted and cultured for 2h in AIM-V medium (Cambrex) supplemented with 10% FCS, 1 mmol/L L-Glutamine and 1% Pen/Strep. Cells were either used for colony forming assays, as described below, for FACS analysis (as described for human cell lines) or for viability tests. Cells were plated at a concentration of 2.10^5 cells/mL in a 24 well plate (1mL/well). PIM inhibitors were diluted to the appropriate concentrations in DMSO. A further dilution of the inhibitors in cell culture medium was performed at a ratio 2:1000 (inhibitor:medium). 1mL of this dilution was then given to each well of cells and the plates were incubated for 24h and 48h at 37º. After 24h and 48h, all the cells were harvested and re-suspended in 1mL medium. Counting was performed using trypan blue exclusion.

In vitro colony forming assay

AML sample cells (10^5) were given to 2 mL of human complete methylcellulose supplemented with PIM inhibitor and plated in 35mm Petri dishes for 10 days at 37º. Light microscopy was done to assess colony formation.

Protein extraction and Western blotting

MV4;11 cells were grown at 5 x 10^5/mL, treated with 1 to 3µM K00135 for various times, harvested, and rinsed with ice-cold PBS. Ice-cold lysis buffer [10 mM Tris-HCl (pH 7.4), 150mM NaCl, 1% Triton X-100, 0.5mM

EDTA, 10% glycerol, 10mM NaF, 1 mM Na_3VO_4, protease inhibitor cocktail] was added to the cells, incubated on ice for 20min and followed by 5min centrifugation. Proteins were precipitated from supernatant using methanol-chloroform and pellets were re-suspended in Laemmli's sample buffer, separated by SDS-PAGE, and transferred to the membranes. The membranes were blotted with primary antibodies (diluted according to the manufacturer's recommendations), followed by horseradish peroxidase–conjugated secondary antibodies, and the proteins detected by SuperSignal West Femto Maximum Sensitivity Substrate (Pierce). The same blots were stripped and re-probed with desired antibodies to confirm equal loading.

Immunoprecipitation and *in vitro* kinase assay.

Cell lysates from 2 μM K00135-treated MV4;11 cells (60 min) were prepared as described above and incubated with either no antibodies or 2μg of anti-PIM1 antibody with gentle rocking at 4°C overnight. Protein A-agarose beads (Upstate; 50μL of 50% beads slurry in 500μL of the lysate) were added and incubated for additional 2h, followed by 15s centrifugation, three washes with 300mM lysis buffer, and two additional washes with kinase buffer [40mM Tris-HCl (pH 7.4), 20mM $MgCl_2$, 0.1mg/mL bovine serum albumin]. Beads were then suspended in 50μL of kinase buffer supplemented with 500μM ATP and either no inhibitor or 2 μM K00135 and incubated at 30°C for 30min. Four micrograms of soluble BAD protein (Upstate) were then added to the reaction and incubated for additional 30 min. The reactions were terminated by addition of Laemmli sample buffer and phosphorylation of BAD was analyzed by Western blotting using anti–phospho-BAD ($Ser^{112/136}$) antibodies.

Preparation of the NUP214/ABL1 construct for injection

The p1017 NUP214/ABL1 plasmid was a gift from J. Cools. 100μg were digested with SfiI to release the NUP214/ABL1 insert, loaded on a gel, the right band was cut out and the DNA extracted with a purification kit. The injection was performed into fertilized oocytes of C57Bl/6 mice at the Transgenic Mouse Core Facility from the Biozentrum.

Genotyping of NUP214/ABL1 pups (Genomic Purification Kit, Puregene)

Toes were lysed in 300µL cell lysis solution supplemented with 5µL Proteinase K over night at 55º. The next day, 1µL of RNaseA was added, tubes were vortexed and incubated for 1h at 37º. Proteins were precipitated with 100µL of protein precipitation solution, vortexed and centrifuged for 5min, full speed. The supernatant was transferred to another tube containing 300µL 100% Isopropanol, vortexed and centrifuged again for 2min, full speed. The supernatant was discarded and the DNA pellet washed with 70% Ethanol. The pellet was air-dried, re-suspended in 50µL DNA hydration solution, incubated for 1h at 65º and left over night at room temperature.

The PCR was pipetted as follows (for 1 tube):

2.5µL	PCR reaction Buffer
1µL	dNTPs (10µM)
1µL	forward primer (15µM)
1µL	reverse primer (15µM)
1.5µL	$MgCl_2$
0.5µL	Taq polymerase
16.5µL	ddH_2O
1µL	DNA

The PCR program used was:

95º	5’		
95º	1’	}	35 cycles
60º	1’		
72º	1’15		
72º	5’		
4º	∞		

Breeding of the NUP214/ABL1 mice

The breedings were made in our mouse facility. NUP214/ABL1-positive males were bread with two wild type B6 females and NUP214/ABL1-positive females with one wild type B6 male.

Control of transgene expression in NUP214/ABL1mice

Mice were sacrificed in a CO_2 chamber. Bone marrow, spleen and thymus were isolated in order to make cell suspensions. Erythrocytes were removed with RBC Lysis Buffer. Cell pellets were resuspended in 1mL of Trizol and homogenized. RNA was isolated following the Trizol protocol and cDNA was synthetized using the *High capacity cDNA Reverse Transcription Kit* (Applied Biosystems). Amplification of the NUP214/ABL1 fragment was done following the genotyping PCR.

Blood counds

NUP214/ABL1 mice were bled into EDTA-coated tubes, the blood was diluted 1:1 in 0.9% NaCl solution and brought to the hematology lab from the Univeristy Hospital for analysis.

Thymus status

Thymi from NUP214/ABL1 and WT B6 mice were isolated and single cell suspensions were done. Cells were stained with different antibody combinations for CD4, CD8 and TCRβ and analyzed with a BD FACSAria.

NUP214/ABL1 plasmid copy number determination

Genomic DNA from one transgenic mouse of each line and from a WT B6 mouse (20ng) were used as templates for RT-PCR using the Power SYBR Green Mastermix (Applied Biosystems) on an ABI Prism 7700 sequence detection system (Applied Biosystems). The experiment was performed following the protocole from Ralph Tiedt (Tiedt, 2008).

VI. References

Aalinkeel, R. et al. The dietary bioflavonoid, quercetin, selectively induces apoptosis of prostate cancer cells by down-regulating the expression of heat shock protein 90. *Prostate* (2008).

Adam, M. et al. Targeting PIM kinases impairs survival of hematopoietic cells transformed by kinase inhibitor-sensitive and kinase inhibitor-resistant forms of Fms-like tyrosine kinase 3 and BCR/ABL. *Cancer Res* **66**, 3828-35 (2006).

Aho, T.L. et al. Pim-1 kinase promotes inactivation of the pro-apoptotic Bad protein by phosphorylating it on the Ser112 gatekeeper site. *FEBS Lett* **571**, 43-9 (2004).

Aifantis, I., et al. Molecular pathogenesis of T-cell leukaemia and lymphoma. *Nat Rev Immunol* **8**, 380-90 (2008).

Akasaka, T. et al. Nonimmunoglobulin (non-Ig)/BCL6 gene fusion in diffuse large B-cell lymphoma results in worse prognosis than Ig/BCL6. *Blood* **96**, 2907-9 (2000).

Allen, J.D. & Berns, A. Complementation tagging of cooperating oncogenes in knockout mice. *Semin Cancer Biol* **7**, 299-306 (1996).

Allen, J.D. et al. Pim-2 transgene induces lymphoid tumors, exhibiting potent synergy with c-myc. *Oncogene* **15**, 1133-41 (1997).

Allen, J.M. et al. Functional dissection of the lck proximal promoter. *Mol Cell Biol* **12**, 2758-68 (1992).

Amson, R. et al. The human protooncogene product p33pim is expressed during fetal hematopoiesis and in diverse leukemias. *Proc Natl Acad Sci U S A* **86**, 8857-61 (1989).

Bachmann, M. & Moroy, T. The serine/threonine kinase Pim-1. *Int J Biochem Cell Biol* **37**, 726-30 (2005).

Ballerini, P. et al. NUP214-ABL1 amplification in t(5;14)/HOX11L2-positive ALL present with several forms and may have a prognostic significance. *Leukemia* **19**, 468-70 (2005).

Ballerini, P et al. Impact of genotype on survival of children with T-cell acute lymphoblastic leukemia treated according to the French protocol FRALLE-93: the effect of TLX3/HOX11L2 gene expression on outcome. *Haematologica* **93**, 1658-65 (2008).

Baytel, D. et al. The human Pim-2 proto-oncogene and its testicular expression. *Biochim Biophys Acta* **1442**, 274-85 (1998).

Bergers, G. et al. Angiogenesis and apoptosis are cellular parameters of neoplastic progression in transgenic mouse models of tumorigenesis. *Int J Dev Biol* **42**, 995-1002 (1998).

Bhattacharya, N. et al. Pim-1 associates with protein complexes necessary for mitosis. *Chromosoma* **111**, 80-95 (2002).

Boots, A.W. et al. Health effects of quercetin: from antioxidant to nutraceutical. *Eur J Pharmacol* **585**, 325-37 (2008).

Borg, K.E. et al. Prolactin regulation of pim-1 expression: positive and negative promoter elements. *Endocrinology* **140**, 5659-68 (1999).

Bullock, A.N. et al. Structural basis of inhibitor specificity of the human protooncogene proviral insertion site in moloney murine leukemia virus (PIM-1) kinase. *J Med Chem* **48**, 7604-14 (2005).

Bullock, A.N., Debreczeni, J., Amos, A.L., Knapp, S. & Turk, B.E. Structure and substrate specificity of the Pim-1 kinase. *J Biol Chem* **280**, 41675-82 (2005).

Burger, J.A. & Kipps, T.J. CXCR4: a key receptor in the crosstalk between tumor cells and their microenvironment. *Blood* **107**, 1761-7 (2006).

Busillo, J.M. & Benovic, J.L. Regulation of CXCR4 signaling. *Biochim Biophys Acta* **1768**, 952-63 (2007).

Byth, K.F. et al. Imidazo[1,2-b]pyridazines: a potent and selective class of cyclin-dependent kinase inhibitors. *Bioorg Med Chem Lett* **14**, 2249-52 (2004).

Byth, K.F. et al. Imidazo[1,2-a]pyridines. Part 2: SAR and optimisation of a potent and selective class of cyclin-dependent kinase inhibitors. *Bioorg Med Chem Lett* **14**, 2245-8 (2004).

Cantrell, D.A. Transgenic analysis of thymocyte signal transduction. *Nat Rev Immunol* **2**, 20-7 (2002).

Cao, R. et al. beta-Carboline alkaloids: biochemical and pharmacological functions. *Curr Med Chem* **14**, 479-500 (2007).

Castro, A.C. et al. Novel IKK inhibitors: beta-carbolines. *Bioorg Med Chem Lett* **13**, 2419-22 (2003).

Chalandon, Y. & Schwaller, J. Targeting mutated protein tyrosine kinases and their signaling pathways in hematologic malignancies. *Haematologica* **90**, 949-68 (2005).

Chen, W.W. et al. Pim family kinases enhance tumor growth of prostate cancer cells. *Mol Cancer Res* **3**, 443-51 (2005).

Chen, X.P. et al. Pim serine/threonine kinases regulate the stability of Socs-1 protein. *Proc Natl Acad Sci U S A* **99**, 2175-80 (2002).

Cheney, I.W. et al. Identification and structure-activity relationships of substituted pyridones as inhibitors of Pim-1 kinase. *Bioorg Med Chem Lett* **17**, 1679-83 (2007).

Choudhary, C. et al. Signal transduction of oncogenic Flt3. *Int J Hematol* **82**, 93-9 (2005).

Cohen, A.M. et al. Increased expression of the hPim-2 gene in human chronic lymphocytic leukemia and non-Hodgkin lymphoma. *Leuk Lymphoma* **45**, 951-5 (2004).

Condorelli, G.L. et al. T-cell-directed TAL-1 expression induces T-cell malignancies in transgenic mice. *Cancer Res* **56**, 5113-9 (1996).

Cuypers, H.T. et al. Murine leukemia virus-induced T-cell lymphomagenesis: integration of proviruses in a distinct chromosomal region. *Cell* **37**, 141-50 (1984).

Dai, H. et al. Pim-2 upregulation: biological implications associated with disease progression and perinueral invasion in prostate cancer. *Prostate* **65**, 276-86 (2005).

Dautry, F. et al. Regulation of pim and myb mRNA accumulation by interleukin 2 and interleukin 3 in murine hematopoietic cell lines. *J Biol Chem* **263**, 17615-20 (1988).

Deininger, M et al. The development of imatinib as a therapeutic agent for chronic myeloid leukemia. *Blood* **105**, 2640-53 (2005).

De Keersmaecker, K. et al. Fusion of EML1 to ABL1 in T-cell acute lymphoblastic leukemia with cryptic t(9;14)(q34;q32). *Blood* **105**, 4849-52 (2005).

De Keersmaeker, K. et al. Genetic insights in the pathogenesis of T-cell acute lymphoblastic leukemia. *Heamatologica* **90**, 1116-27 (2005).

De Keersmaecker, K. et al. Intrinsic differences between the catalytic properties of the oncogenic NUP214-ABL1 and BCR-ABL1 fusion protein kinases. *Leukemia* (2008).

De Keersmaecker, K. et al. Kinase activation and transformation by NUP214-ABL1 is dependent on the context of the nuclear pore. *Mol Cell* **31**, 134-42 (2008).

Dhanasekaran, S.M. et al. Delineation of prognostic biomarkers in prostate cancer. *Nature* **412**, 822-6 (2001).

Didichenko, S.A. et al. IL-3 induces a Pim1-dependent antiapoptotic pathway in primary human basophils. *Blood* **112**, 3949-58 (2008).

Ding, Z. et al. L-selectin stimulation enhances functional expression of surface CXCR4 in lymphocytes: implications for cellular activation during adhesion and migration. *Blood* **101**, 4245-52 (2003).

Domen, J. et al. Impaired interleukin-3 response in Pim-1-deficient bone marrow-derived mast cells. *Blood* **82**, 1445-52 (1993).

Druker, B.J. Perspectives on the development of a molecularly targeted agent. *Cancer Cell* **1**, 31-6 (2002).

Duncan, P.I. et al. In vivo regulation of alternative pre-mRNA splicing by the Clk1 protein kinase. *Mol Cell Biol* **17**, 5996-6001 (1997).

Ellwood-Yen, K. et al. Myc-driven murine prostate cancer shares molecular features with human prostate tumors. *Cancer Cell* **4**, 223-38 (2003).

Fabian, M.A. et al. A small molecule-kinase interaction map for clinical kinase inhibitors. *Nat Biotechnol* **23**, 329-36 (2005).

Fedorov, O. et al. A systematic interaction map of validated kinase inhibitors with Ser/Thr kinases. *Proc Natl Acad Sci U S A* **104**, 20523-8 (2007).

Feldman, J.D. et al. Seizure activity induces PIM-1 expression in brain. *J Neurosci Res* **53**, 502-9 (1998).

Foulds, L. The experimental study of tumor progression: a review. *Cancer Res* **14**, 327-39 (1954).

Fox, C.J. et al. The serine/threonine kinase Pim-2 is a transcriptionally regulated apoptotic inhibitor. *Genes Dev* **17**, 1841-54 (2003).

Friedmann, M. et al. Characterization of the proto-oncogene pim-1: kinase activity and substrate recognition sequence. *Arch Biochem Biophys* **298**, 594-601 (1992).

Frohling, S. et al. Genetics of myeloid malignancies: pathogenetic and clinical implications. *J Clin Oncol* **23**, 6285-95 (2005).

Fujii, C. et al. Aberrant expression of serine/threonine kinase Pim-3 in hepatocellular carcinoma development and its role in the proliferation of human hepatoma cell lines. *Int J Cancer* **114**, 209-18 (2005).

Giles, F.J. et al. MK-0457, a novel kinase inhibitor, is active in patients with chronic myeloid leukemia or acute lymphocytic leukemia with the T315I BCR-ABL mutation. *Blood* **109**, 500-2 (2007).

Gilliland, D.G. et al. The molecular basis of leukemia. *Hematology Am Soc Hematol Educ Program*, 80-97 (2004).

Graux, C. et al. Fusion of NUP214 to ABL1 on amplified episomes in T-cell acute lymphoblastic leukemia. *Nat Genet* **36**, 1084-9 (2004).
Graux, C et al. Heterogeneous patterns of amplification of the NUP214-ABL1 fusion gene in T-cell acute lymphoblastic leukemia. *Leukemia* (2008, Epub ahead of print).

Grisaru, D. et al. Microarray expression identification of differentially expressed genes in serous epithelial ovarian cancer compared with bulk normal ovarian tissue and ovarian surface scrapings. *Oncol Rep* **18**, 1347-56 (2007).

Grisolano, J.L. et al. An activated receptor tyrosine kinase, TEL/PDGFbetaR, cooperates with AML1/ETO to induce acute myeloid leukemia in mice. *Proc Natl Acad Sci USA* **100**, 9506-9511 (2003).

Grundler, R. et al. Sensitivity toward tyrosine kinase inhibitors varies between different activating mutations of the FLT3 receptor. *Blood* **102**, 646-51 (2003).

Hammerman, P.S. et al. Pim and Akt oncogenes are independent regulators of hematopoietic cell growth and survival. *Blood* **105**, 4477-83 (2005).

Hanahan, D. & Weinberg, R.A. The hallmarks of cancer. *Cell* **100**, 57-70 (2000).

Hanke, J.H. et al. Discovery of a novel, potent, and Src family-selective tyrosine kinase inhibitor. Study of Lck- and FynT-dependent T cell activation. *J Biol Chem* **271**, 695-701 (1996).

Hantschel, O. et al. Target spectrum of the BCR-ABL inhibitors imatinib, nilotinib and dasatinib. *Leuk Lymphoma* **49**, 615-9 (2008).

Heidel, F. et al. Clinical resistance to the kinase inhibitor PKC412 in acute myeloid leukemia by mutation of Asn-676 in the FLT3 tyrosine kinase domain. *Blood* **107**, 293-300 (2006).

Hernandez, P.A. et al. Mutations in the chemokine receptor gene CXCR4 are associated with WHIM syndrome, a combined immunodeficiency disease. *Nat Genet* **34**, 70-4 (2003).

Holder, S. et al. Characterization of a potent and selective small-molecule inhibitor of the PIM1 kinase. *Mol Cancer Ther* **6**, 163-72 (2007).

Holder, S. et al. Comparative molecular field analysis of flavonoid inhibitors of the PIM-1 kinase. *Bioorg Med Chem* **15**, 6463-73 (2007).

Hoover, D. et al. Recombinant human pim-1 protein exhibits serine/threonine kinase activity. *J Biol Chem* **266**, 14018-23 (1991).

Hu, Y.L. et al. Evidence that the Pim1 kinase gene is a direct target of HOXA9. *Blood* **109**, 4732-8 (2007).

Inazawa, J. et al. Comparative genomic hybridization (CGH)-arrays pave the way for identification of novel cancer-related genes. *Cancer Sci* **95**, 559-63 (2004).

Jacinto, E. & Lorberg, A. TOR regulation of AGC kinases in yeast and mammals. *Biochem J* **410**, 19-37 (2008).

Jacobs, M.D. et al. Pim-1 ligand-bound structures reveal the mechanism of serine/threonine kinase inhibition by LY294002. *J Biol Chem* **280**, 13728-34 (2005).

Juarez, J. & Bendall, L. SDF-1 and CXCR4 in normal and malignant hematopoiesis. *Histol Histopathol* **19**, 299-309 (2004).

Juarez, J. et al. CXCR4 antagonists mobilize childhood acute lymphoblastic leukemia cells into the peripheral blood and inhibit engraftment. *Leukemia* **21**, 1249-57 (2007).

Karaman, M.W. et al. A quantitative analysis of kinase inhibitor selectivity. *Nat Biotechnol* **26**, 127-32 (2008).

Kelly, L.M. et al. FLT3 internal tandem duplication mutations associated with human acute myeloid leukemias induce myeloproliferative disease in a murine bone marrow transplantation model. *Blood* **99**, 310-318 (2002).

Kelly, L.M. et al. Genetics of myeloid leukemias. *Annu Rev Genomics Hum Genet* **3**, 179-98 (2002).

Kelly, L.M. et al. ML/RARalpha and FLT3-ITD induce an APL-like disease in a mouse model. *Proc Natl Acad Sci USA* **99,** 8283-8288 (2002).

Kim, K.T. et al. Pim-1 is up-regulated by constitutively activated FLT3 and plays a role in FLT3-mediated cell survival. *Blood* **105**, 1759-67 (2005).

Kim, K.T. et al. Constitutively activated FLT3 phosphorylates BAD partially through pim-1. *Br J Haematol* **134**, 500-9 (2006).

Kisseleva, T. et al. Signaling through the JAK/STAT pathway, recent advances and future challenges. *Gene* **285**, 1-24 (2002).

Knapper, S. et al. The effects of lestaurtinib (CEP701) and PKC412 on primary AML blasts: the induction of cytotoxicity varies with dependence on

FLT3 signaling in both FLT3-mutated and wild-type cases. *Blood* **108**, 3494-503 (2006).

Knapper, S. FLT3 inhibition in acute myeloid leukaemia. *Br J Heamatol* **138**, 687-99 (2007).

Koike, N. et al. Identification of heterochromatin protein 1 (HP1) as a phosphorylation target by Pim-1 kinase and the effect of phosphorylation on the transcriptional repression function of HP1(1). *FEBS Lett* **467**, 17-21 (2000).

Kumar, A. et al. Crystal structures of proto-oncogene kinase Pim1: a target of aberrant somatic hypermutations in diffuse large cell lymphoma. *J Mol Biol* **348**, 183-93 (2005).

Lapidot, T. et al. How do stem cells find their way home? *Blood* **106**, 1901-10 (2005).

Lataillade, J.J. et al. Stromal cell-derived factor 1 regulates primitive hematopoiesis by suppressing apoptosis and by promoting G(0)/G(1) transition in CD34(+) cells: evidence for an autocrine/paracrine mechanism. *Blood* **99**, 1117-29 (2002).

Leverson, J.D. et al. Pim-1 kinase and p100 cooperate to enhance c-Myb activity. *Mol Cell* **2**, 417-25 (1998).

Levine, R. L. et al. Role of JAK2 in the pathogenesis and therapy of myeloproliferative disorders. *Nat Rev Cancer* **7**, 673-83 (2007).

Ley, T.J. et al. DNA sequencing of a cytogenetically normal acute myeloid leukaemia genome. *Nature* **456**, 66-72 (2008).

Li, Y.Y. et al. Pim-3, a proto-oncogene with serine/threonine kinase activity, is aberrantly expressed in human pancreatic cancer and phosphorylates bad to block bad-mediated apoptosis in human pancreatic cancer cell lines. *Cancer Res* **66**, 6741-7 (2006).

Liang, H. et al. Ubiquitous expression and cell cycle regulation of the protein kinase PIM-1. *Arch Biochem Biophys* **330**, 259-65 (1996).

Lilly, M. et al. Sustained expression of the pim-1 kinase is specifically induced in myeloid cells by cytokines whose receptors are structurally related. *Oncogene* **7**, 727-32 (1992).

Liu, Y. et al. Imatinib mesylate induces quiescence in gastrointestinal stromal tumor cells through the CDH1-SKP2-p27Kip1 signaling axis. *Cancer Res* **68**, 9015-23 (2008).

Losman, J.A. et al. Protein phosphatase 2A regulates the stability of Pim protein kinases. *J Biol Chem* **278**, 4800-5 (2003).

Ma, J. et al. Negative regulation of Pim-1 protein kinase levels by the B56beta subunit of PP2A. *Oncogene* **26**, 5145-53 (2007).

Macdonald, A. et al. Pim kinases phosphorylate multiple sites on Bad and promote 14-3-3 binding and dissociation from Bcl-XL. *BMC Cell Biol* **7**, 1 (2006).

Maita, H. et al. PAP-1, a novel target protein of phosphorylation by pim-1 kinase. *Eur J Biochem* **267**, 5168-78 (2000).

Manning, G. et al. The protein kinase complement of the human genome. *Science* **298**, 1912-34 (2002).

Markwalder, J.A. et al. Synthesis and biological evaluation of 1-aryl-4,5-dihydro-1H-pyrazolo[3,4-d]pyrimidin-4-one inhibitors of cyclin-dependent kinases. *J Med Chem* **47**, 5894-911 (2004).

Massague, J. TGFbeta in Cancer. *Cell* **134**, 215-30 (2008).

Masztalerz, A. et al. Synaptotagmin 3 deficiency in T cells impairs recycling of the chemokine receptor CXCR4 and thereby inhibits CXCL12 chemokine-induced migration. *J Cell Sci* **120**, 219-28 (2007).

Matikainen, S. et al. Interferon-alpha activates multiple STAT proteins and upregulates proliferation-associated IL-2Ralpha, c-myc, and pim-1 genes in human T cells. *Blood* **93**, 1980-91 (1999).

Matsumura, I. et al. Transcriptional regulation of the cyclin D1 promoter by STAT5: its involvement in cytokine-dependent growth of hematopoietic cells. *Embo J* **18**, 1367-77 (1999).

Mikkers, H. et al. High-throughput retroviral tagging to identify components of specific signaling pathways in cancer. *Nat Genet* **32**, 153-9 (2002).

Mikkers, H. et al. Mice deficient for all PIM kinases display reduced body size and impaired responses to hematopoietic growth factors. *Mol Cell Biol* **24**, 6104-15 (2004).

Miura, O. et al. Induction of tyrosine phosphorylation of Vav and expression of Pim-1 correlates with Jak2-mediated growth signaling from the erythropoietin receptor. *Blood* **84**, 4135-41 (1994).

Mizuki, M. et al. Suppression of myeloid transcription factors and induction of STAT response genes by AML-specific Flt3 mutations. *Blood* **101**, 3164-73 (2003).

Mizuno, K. et al. Regulation of Pim-1 by Hsp90. *Biochem Biophys Res Commun* **281**, 663-9 (2001).

Mochizuki, T. et al. Physical and functional interactions between Pim-1 kinase and Cdc25A phosphatase. Implications for the Pim-1-mediated activation of the c-Myc signaling pathway. *J Biol Chem* **274**, 18659-66 (1999).

Mochizuki, H. et al. Interaction of ligand-receptor system between stromal-cell-derived factor-1 and CXC chemokine receptor 4 in human prostate cancer: a possible predictor of metastasis. *Biochem Biophys Res Commun* **320**, 656-63 (2004).

Moroy, T. et al. Expression of a Pim-1 transgene accelerates lymphoproliferation and inhibits apoptosis in lpr/lpr mice. *Proc Natl Acad Sci U S A* **90**, 10734-8 (1993).

Mui, A.L. et al. Interleukin-3, granulocyte-macrophage colony-stimulating factor, and interleukin-5 transduce signals through two forms of STAT5. *J Leukoc Biol* **57**, 799-803 (1995).

Mullighan, C.G. et al. Genome-wide analysis of genetic alterations in acute lymphoblastic leukaemia. *Nature* **446**, 758-64 (2007).

Muraski, J.A. et al. Pim-1 regulates cardiomyocyte survival downstream of Akt. *Nat Med* **13**, 1467-75 (2007).
Nakao, M. et al. Internal tandem duplication of the flt3 gene found in acute myeloid leukemia. *Leukemia* **12**, 1911-8 (1996).

Nieborowska-Skorska, M. et al. Complementary functions of the antiapoptotic protein A1 and serine/threonine kinase pim-1 in the BCR/ABL-mediated leukemogenesis. *Blood* **99**, 4531-9 (2002).

Nilsson, S.K. et al. Hemopoietic stem cell engraftment. *Exp Hematol* **34**, 123-9 (2006).

Nosaka, T. & Kitamura, T. Pim-1 expression is sufficient to induce cytokine independence in murine hematopoietic cells, but is dispensable for BCR-ABL-mediated transformation. *Exp Hematol* **30**, 697-702 (2002).

Nowell, P.C. The clonal evolution of tumor cell populations. *Science* **194**, 23-8 (1976).

Nowell, P.C. & Hungerford, D.A. Chromosome studies on normal and leukemic human leukocytes. *J. Natl. Cancer Inst.* **25,** 85-109 (1960).

Orsini, M.J. et al. Trafficking of the HIV coreceptor CXCR4. Role of arrestins and identification of residues in the c-terminal tail that mediate receptor internalization. *J Biol Chem* **274**, 31076-86 (1999).

Padma, R. & Nagarajan, L. The human PIM-1 gene product is a protein serine kinase. *Cancer Res* **51**, 2486-9 (1991).

Palaty, C.K. et al. Phosphorylation site substrate specificity determinants for the Pim-1 protooncogene-encoded protein kinase. *Biochem Cell Biol* **75**, 153-62 (1997).

Palaty, C.K. et al. Identification of the autophosphorylation sites of the Xenopus laevis Pim-1 proto-oncogene-encoded protein kinase. *J Biol Chem* **272**, 10514-21 (1997).

Pasqualucci, L. et al. Hypermutation of multiple proto-oncogenes in B-cell diffuse large-cell lymphomas. *Nature* **412**, 341-6 (2001).

Paukku, K. & Silvennoinen, O. STATs as critical mediators of signal transduction and transcription: lessons learned from STAT5. *Cytokine Growth Factor Rev* **15**, 435-55 (2004).

Pear, W.S. Signaling in leukemia: which messenger to kill? *J Clin Invest* **105**, 423-32 (2000).

Pelchen-Matthews, A. et al. Chemokine receptor trafficking and viral replication. *Immunol Rev* **168**, 33-49 (1999).

Peled, A. et al. Dependence of human stem cell engraftment and repopulation of NOD/SCID mice on CXCR4. *Science* **283**, 845-8 (1999).

Pisecker, M. et al. Sequential order of genetic events in NUP214/ABL1 positive T-cell leukemia. *ASH Abstract* 2054 (2008).

Pomel, V. et al. Furan-2-ylmethylene thiazolidinediones as novel, potent, and selective inhibitors of phosphoinositide 3-kinase gamma. *J Med Chem* **49**, 3857-71 (2006).

Pogacic, V. et al. Structural analysis identifies imidazo[1,2-b]pyridazines as PIM kinase inhibitors with in vitro antileukemic activity. *Cancer Res* **67**, 6916-24 (2007).

Pui, C.H. et al. Acute lymphoblastic leukemia. *N Engl J Med* **350**, 1535-48 (2004).

Qian, K.C. et al. Structural basis of constitutive activity and a unique nucleotide binding mode of human Pim-1 kinase. *J Biol Chem* **280**, 6130-7 (2005).

Quitas-Cardama, A. et al. Imatinib mesylate therapy may overcome the poor prognostic significance of deletions of derivative chromosome 9 in patients with chronic myelogenous leukemia. *Blood* **105**, 2281-86 (2005).

Quintas-Cardama, A. et al. Activity of tyrosine kinase inhibitors against human NUP214-ABL1-positive T cell malignancies. *Leukemia* **22**, 1117-24 (2008).

Rabbitts, T.H. Chromosomal translocations in human cancer. *Nature* **372**, 143-9 (1994).

Ravera, M. et al. Emerging therapeutic strategies in diabetic nephropathy. *J Nephrol* **20** Suppl 12, S23-32 (2007).

Reiser-Erkan, C. et al. Hypoxia-inducible proto-oncogene Pim-1 is a prognostic marker in pancreatic ductal adenocarcinoma. *Cancer Biol Ther* **7**(2008).

Richardson, C.M. et al. Discovery of a potent CDK2 inhibitor with a novel binding mode, using virtual screening and initial, structure-guided lead scoping. *Bioorg Med Chem Lett* **17**, 3880-5 (2007)

Rombouts, E.J. et al. Relation between CXCR-4 expression, Flt3 mutations, and unfavorable prognosis of adult acute myeloid leukemia. *Blood* **104**, 550-7 (2004).

Russo, M. et al. Quercetin enhances CD95- and TRAIL-induced apoptosis in leukemia cell lines. *Leukemia* **21**, 1130-3 (2007).

Ryan, G.J. New pharmacologic approaches to treating diabetic retinopathy. *Am J Health Syst Pharm* **64**, S15-21 (2007).

Schwaller, J. et al. Stat5 is essential for the myelo- and lymphoproliferative disease induced by TEL/JAK2. *Mol Cell* **6**, 693-704 (2000).

Selten, G. et al. Proviral activation of the putative oncogene Pim-1 in MuLV induced T-cell lymphomas. *Embo J* **4**, 1793-8 (1985).

Selten, G. et al. The primary structure of the putative oncogene pim-1 shows extensive homology with protein kinases. *Cell* **46**, 603-11 (1986).

Seo, J. et al. Cdt1 transgenic mice develop lymphoblastic lymphoma in the absence of p53. *Oncogene* **24**, 8176-86 (2005).

Shay, K.P. et al. Pim-1 kinase stability is regulated by heat shock proteins and the ubiquitin-proteasome pathway. *Mol Cancer Res* **3**, 170-81 (2005).

Sherbenou, D.W. et al. Applying the discovery of the Philadelphia chromosome. *J Clin Invest* **117**, 2067-74 (2007).

Shirogane, T. et al. Synergistic roles for Pim-1 and c-Myc in STAT3-mediated cell cycle progression and antiapoptosis. *Immunity* **11**, 709-19 (1999).

Silva, R.L. & Wendel, H.G. MNK, EIF4E and targeting translation for therapy. *Cell Cycle* **7**, 553-5 (2008).

Small, D. Targeting FLT3 for the treatment of leukemia. *Semin Hematol* **45**, S17-21 (2008).

Socolovsky, M. et al. Fetal anemia and apoptosis of red cell progenitors in Stat5a-/-5b-/- mice: a direct role for Stat5 in Bcl-X(L) induction. *Cell* **98**, 181-91 (1999).

Soriano, S.F. et al. Chemokines integrate JAK/STAT and G-protein pathways during chemotaxis and calcium flux responses. *Eur J Immunol* **33**, 1328-33 (2003).

Spiegel, A. et al. Unique SDF-1-induced activation of human precursor-B ALL cells as a result of altered CXCR4 expression and signaling. *Blood* **103**, 2900-7 (2004).

Spoo, A.C. et al. CXCR4 is a prognostic marker in acute myelogenous leukemia. *Blood* **109**, 786-91 (2007).

Steelman, L.S. et al. Contributions of the Raf/MEK/ERK, PI3K/PTEN/Akt/mTOR and Jak/STAT pathways to leukemia. *Leukemia* **22**, 686-707 (2008).

Steffen, B. et al. The molecular pathogenesis of acute myeloid leukemia. *Crit Rev Oncol Hematol.* **56,** 195-221 (2005).
Stirewalt, D.L. & Radich, J.P. The role of FLT3 in hematopoietic malignancies. *Nat Rev Cancer* **3**, 650-65 (2003).

Su, X. et al. Transforming potential of the T-cell acute lymphoblastic leukemia-associated homeobox genes HOXA13, TLX1, and TLX3. *Genes Chromosomes Cancer* **45**, 846-55 (2006).

Tavor, S. et al. CXCR4 regulates migration and development of human acute myelogenous leukemia stem cells in transplanted NOD/SCID mice. *Cancer Res* **64**, 2817-24 (2004).

Temple, R. et al. Microarray analysis of eosinophils reveals a number of candidate survival and apoptosis genes. *Am J Respir Cell Mol Biol* **25**, 425-33 (2001).

Tiedt, R. et al. Ratio of mutant JAK2-V617F to wild-type Jak2 determines the MPD phenotypes in transgenic mice. *Blood* **111**, 3931-40 (2008).

Tong, Y. et al. Isoxazolo[3,4-b]quinoline-3,4(1H,9H)-diones as unique, potent and selective inhibitors for Pim-1 and Pim-2 kinases: chemistry, biological activities, and molecular modeling. *Bioorg Med Chem Lett* **18**, 5206-8 (2008).

Valdman, A. et al. Pim-1 expression in prostatic intraepithelial neoplasia and human prostate cancer. *Prostate* **60**, 367-71 (2004).

Van der Lugt, N.M. et al. Proviral tagging in E mu-myc transgenic mice lacking the Pim-1 proto-oncogene leads to compensatory activation of Pim-2. *Embo J* **14**, 2536-44 (1995).

Van Limbergen, H. et al. Molecular cytogenetic and clinical findings in ETV6/ABL1-positive leukemia. *Genes Chromosomes Cancer* **30**, 274-82 (2001).

Wang, Z. et al. Pim-1: a serine/threonine kinase with a role in cell survival, proliferation, differentiation and tumorigenesis. *J Vet Sci* **2**, 167-79 (2001).

Wang, Z. et al. Phosphorylation of the cell cycle inhibitor p21Cip1/WAF1 by Pim-1 kinase. *Biochim Biophys Acta* **1593**, 45-55 (2002).

Weisberg, E. et al. Anti-leukemic effects of the novel, mutant FLT3 inhibitor, NVP-AST487: Effects on PKC412-sensitive and -resistant FLT3-expressing cells. *Blood* (2008).

Wingett, D. et al. pim-1 proto-oncogene expression in anti-CD3-mediated T cell activation is associated with protein kinase C activation and is independent of Raf-1. *J Immunol* **156**, 549-57 (1996).

Woerner, B.M. et al. Widespread CXCR4 activation in astrocytomas revealed by phospho-CXCR4-specific antibodies. *Cancer Res* **65**, 11392-9 (2005).

Wong, S. & Witte, O.N. The BCR-ABL story: bench to bedside and back. *Annu Rev Immunol* **22**, 247-306 (2004).

Xie, Y. et al. PKC412 directly inhibits the serine/threonine protein kinase PIM1 in cell lines and acute myeloid leukemia cells as a novel mechanism of inhibition of multidrug resistance. *ASH abstract 2655*, (2008).

Xu, Y. et al. Overexpression of PIM-1 is a potential biomarker in prostate carcinoma. *J Surg Oncol* **92**, 326-30 (2005).

Yip-Schneider, M.T. et al. Transcriptional induction of pim-1 protein kinase gene expression by interferon gamma and posttranscriptional effects on costimulation with steel factor. *Blood* **85**, 3494-502 (1995).

Yoshida, S. et al. Identification of heterologous translocation partner genes fused to the BCL6 gene in diffuse large B-cell lymphomas: 5'-RACE and LA - PCR analyses of biopsy samples. *Oncogene* **18**, 7994-9 (1999).

Yoshimura, A. et al. Mouse oncostatin M: an immediate early gene induced by multiple cytokines through the JAK-STAT5 pathway. *Embo J* **15**, 1055-63 (1996).

Zippo, A. et al. PIM1-dependent phosphorylation of histone H3 at serine 10 is required for MYC-dependent transcriptional activation and oncogenic transformation. *Nat Cell Biol* **9**, 932-44 (2007).